Trace Element Variation of Coarse-Grained Pyrite in the Mount Isa Copper System

Thesis submitted in accordance with the requirements of the University of Adelaide for an Honours Degree in Geology

Shauna Maguire-Olstad

November 2016

THE UNIVERSITY *of* ADELAIDE

TRACE ELEMENT VARIATIONOF COARSE-GRAINED PYRITE IN THE MOUNT ISA COPPER SYSTEM

MT.ISA COARSE-GRAINED PYRITE

ABSTRACT

The unique Mount Isa system, northwest Queensland, contains two world class deposits of copper and lead-zinc, which have a complex spatial relationship. The formation of the copper mineralization has long been debated, and occurs in a close spatial and temporal association with silica-dolomite alteration and coarse-grained pyrite (Pyrite 2). The geochemical characteristics of coarse-grained pyrite has not previously been studied and it is believed to hold valuable insight into the fluid evolution of the Mount Isa Copper System. Using LA-ICP-MS analysis, trace element variation of Pyrite 2 was investigated for numerous elements including Ag, As, Ba, Co, Cu, Mo, Ni, Pb and Zn across an explorative transect (drill hole 0406ED2), which passed through the alteration halo of the 1100 orebody. The trace element composition of Pyrite 2 was not consistent throughout the 0406ED2 transect and it does not appear to be controlled by host lithology. The analysis determined the Pyrite 2 grains formed during, or in close association with, the ore-mineral enriched hydrothermal fluid. Pyrite 2 data is consistent with the Mount Isa system having undergone multiple hydrothermal fluid events or from an evolving hydrothermal fluid. The trace element variation of Pyrite 2 is consistent with the currently established paragenesis and is indicative of the concurrent Cu, Pb and Zn mineralising system formed during protracted hydrothermal events.

KEYWORDS

Mount Isa, Pyrite, Mineralisation, Trace Element, Variation, LA-ICPMS

TABLE OF CONTENTS

LIST OF FIGURES AND TABLES

1. INTRODUCTION

Pyrite (FeS_2) is an iron sulphide mineral that occurs in abundance within the Mount Isa Copper system, Mount Isa inlier, northwest Queensland (Figure 1) (Wilde, 2011). The Mount Isa system contains both stratiform lead-zinc and copper deposits, hosted within the Urquhart Shale formation, and is enriched in pyrite in the vicinity of the ore zones (William 1998). The Mount Isa system contains two recognised styles of pyrite. Fine-grained pyrite (Pyrite 1), is typically 2-20µm (Perkins, 1996B) in size and forms as euhedral grains with characteristic 'atoll' textures (Grondijs & Schouten, 1937) and is observed as bedding parallel accumulations (O'Connell, 2016). The second recognised form is coarse-grained pyrite (Pyrite 2), which regularly forms euhedral cubic grains up to 20-200 µm in size, occurring as single grains or within veins or breccias (Perkins, 1998). Both generations of pyrite are hosted with the Urquhart Shale formation of the Mount Isa group. The coarse-grained pyrite variation is of particular interest because of its spatial relationship within the copper system and its relation to ore-formation.

To understand the relationship between the coarse-grained pyrite, and the Mount Isa Copper system, it is necessary to understand the paragenesis and timing relationship of fluid surrounding and involved in the formation of the coarse-grained pyrite. Thomas *et al* (2011) suggest that characteristic trace element patterns can be used as a proxy for fluid flow events. The Coarse-grained pyrite is poorly understood in terms of its composition and characteristics.

This project uses 6 representative drill core samples from an explorative hole, 0406ED2, for trace element analysis. This analysis aims to use petrographic observations and laser ablation analysis to record any textural or trace element variation of Pyrite 2 across a transect of the Mount Isa Copper System using samples from exploration hole 0406ED2 and determine the evolution of fluid composition at the time of formation of the coarse-grained pyrite. Understanding any variation in the Pyrite 2 compositions, will test the hypothesis that there is a trace element variation within the Pyrite 2 grains in the Isa system that can be used to further understand the mode of formation of the orebodies and paragenesis of the Mount Isa mineralised system.

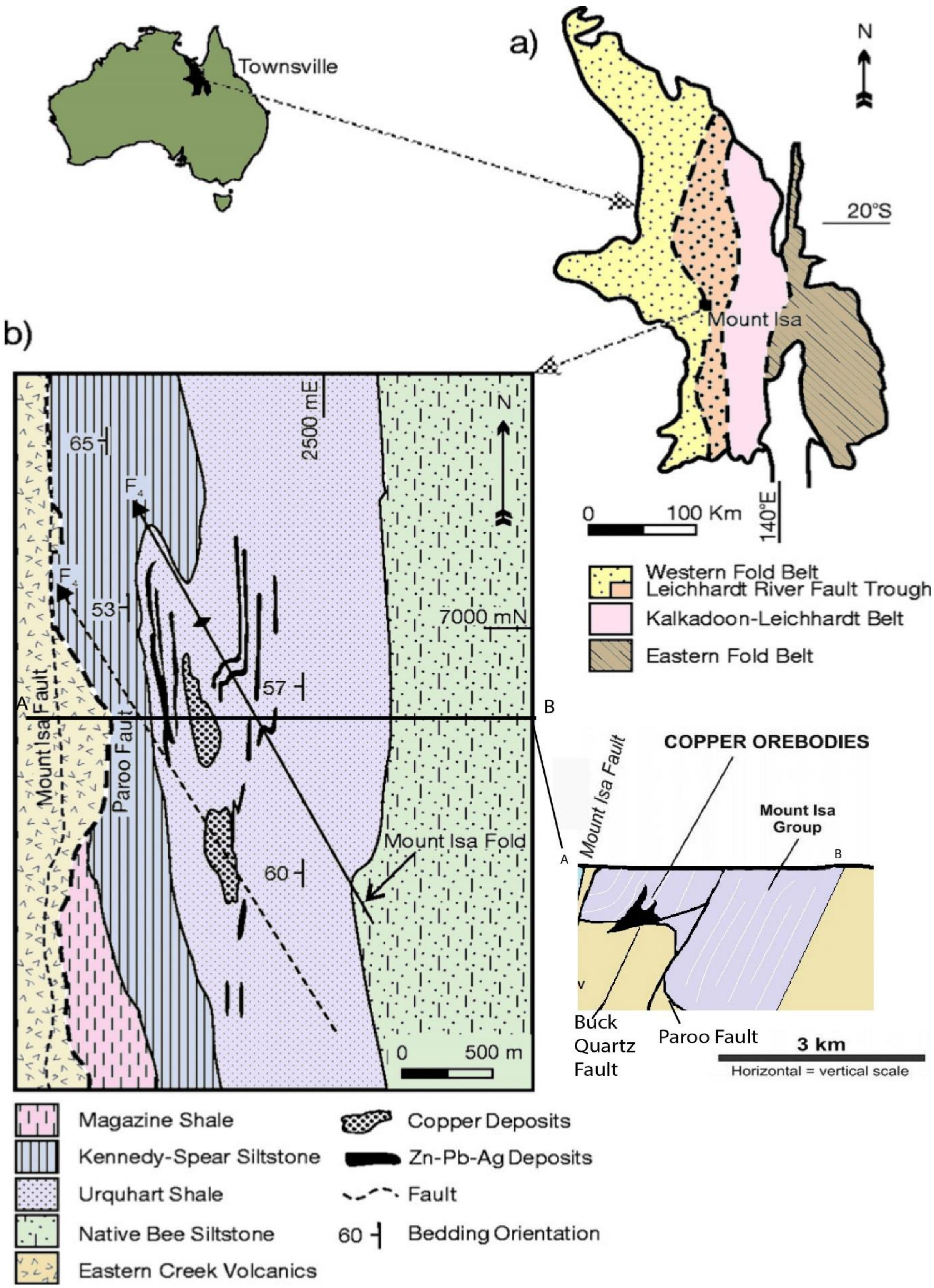

Figure 1 Location map of Mount Isa Inlier, illustrating the Western and Eastern Fold Belt, the Leichhardt River Trough, the Kalkadoon-Leichhardt Belt and the Mount Isa system. The map identifies the location of the main lithologies, ore bodies, faults and bedding

2. GEOLOGICAL SETTING/BACKGROUND

2.1 Regional Geology

Mount Isa is located within the Proterozoic aged Mount Isa Inlier, northwest Queensland. The Mount Isa Inlier has a complex tectonic evolution and deformation history and is sub-divided into 3 regions; the Western Fold Belt (WFB), Kalkadoon-Leichhardt Belt (KLB) and the Eastern Fold Belt (Wilde, 2011)(Figure 1). Each belt displays various ranges of metamorphism, deformation and mineralization. The Mount Isa deposit is located in the Leichardt-River trough, part of the Western Fold Belt (WFB)(Figure 1) (Wilde, 2006), and represents a complexly deformed Proterozoic extensional rift sequence (Warning, 1998 & Davis 2004)composed of sedimentary and bimodal (to felsic) volcanic lithologies (Wilde, 2011). The WFB sediments were deposited during three discrete episodes of basin formation (Withnall & Cranfield, 2013), consisting typically of variably carbonaceous marine sediments, in a dominantly lacustrine depositional environment (Blake, 1987) with rare incursions of high energy coastal units (Painter, 2003). The Isa Superbasin succession was deposited between 1670-1590Ma, and consists predominately of marine siliciclastic sediments. The Isa Superbasin was terminated by the Iasn Orogeny, (1620-1520Ma), which resulted in a period of thrusting and faulting, and subsequent north-south compression. This was followed by a stage of east –west shortening in the system. The detailed tectonic history and basin evolution of the Isa inlier is discussed by Painter (2003).

2.2 Local Geology

The oldest sequence within the Mount Isa area, is identified as the basement and was deformed prior to 1875Ma (Blake 1987). Unconformably overlying this are three consecutive sequences; Cover Sequence 1 (1875-1850Ma), which is composed of subaerial felsic volcanics, Cover Sequence 2 (1790-1760Ma), enriched in mafic volcanics and quartzite, and Cover Sequence 3 (1680-1670Ma), which is composed of metasediments and felsic to mafic volcanics (Geoscience Aust, 2016). The lithological units within Cover Sequence 3 are sub-divided into the upper and lower Mount Isa Groups consisting of carbonaceous, pyritic, dolomitic siltstones and shales (Painter, 2003). The upper group contains the Magazine Shale, Kennedy Spear Siltstone, and Urquhart Shale formations (discussed further in sections 2.2.1 and 2.2.2) (Perkins, 1990). The lower Isa group contains the Native Bee Siltstone (homogenous shale unit, consisting of siliceous siltstone and carbonate rich siltstone), Breakaway Shale, (grey siltstone, dark-grey shale and micaceous shale) and the Moondarra Siltstone (basal unit of Isa Superbasin, composed of grey siltstone grading into subordinate silty shale) (Painter, 2003). The units of interest for this study are the Kennedy Spear Siltstone and the Urquhart Shale formation. Mineralization occurs within the upper Mount Isa group, predominately within the Urquhart shale, but also within the Kennedy Spear Siltstone (Wilde, 2006) (Figure 2), and is terminated by the Paroo fault and underlying Eastern Creek Volcanics (Figure 1 and 2), which also belong within Cover Sequence 2. The Paroo fault is a significant structural control within the Isa system and is described in detail by Long *et al.* (2010).

Mount Isa hosts world-class deposits of both copper and lead-zinc, which have a complex spatial relationship. The mode of formation of these deposits has been continually debated since their discovery in 1923 because of their unique composition encompassing breccia-hosted copper orebodies overprinting a series of apparently strata-bound lead-zinc deposits (Perkins, 1996). Both ore systems appear to have a structural control component and are hosted within the same lithological unit, but differ in their style of mineralization (Neudert 1983). The formation of the strata-bound lead-zinc deposits has been interpreted as being a classic example of the Sedimentary Exhalative deposit style deposit (SEDEX) (Large *et al*., 2005). However, the mode of formation of the overprinting copper mineralizing system, which is not controlled by bedding is less clear (Davis, 2004 & Wilde, 2006; 2011). The copper orebodies and mineralization are hosted within, and associated with, an irregularly distributed silica-dolomite alteration sequence (or 'halo') (Van Dijk, 1991). The Silica Dolomite alteration occurs within the Urquhart Shale formation and represents the replacement of shale with dolomite and silica, and has been categorized into three stages; dolomite recrystallization and silicification, breccia veining and dolomite replacement and chalcopyrite mineralization (Van Dijk, 1991). In-depth description of the Mount Isa ore system and Silica-Dolomite alteration is described in Mathias and Clark (1975) & Perkins (1996), and Van Dijk (1991) respectively.

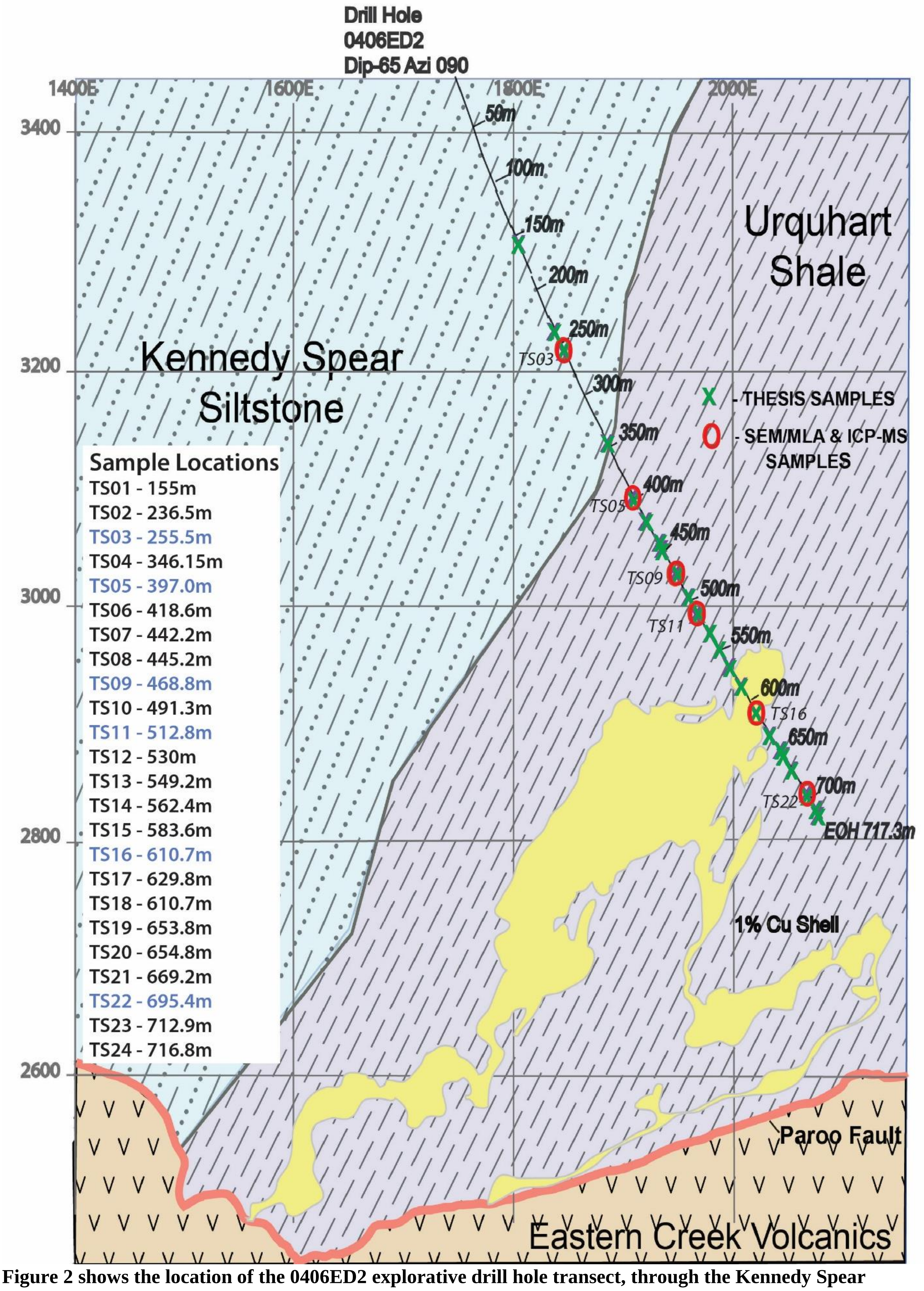

Figure 2 shows the location of the 0406ED2 explorative drill hole transect, through the Kennedy Spear Siltstone, Urquhart Shale and the 1% copper halo, with sample locations identified. The transect displays the location of each sample, with the corresponding sample location detailed in the table. The samples used for further analysis using the SEM/MLA and ICP-MS, are highlighted in blue within the table. The transect passes through the 1% copper grade halo, which surrounds the 1100 orebody, in the Mount Isa system.

2.2.1 KENNEDY SPEAR SILTSTONE

The Kennedy Spear Siltstone is typically composed of extensively folded white to light grey dolomites and dolomitic siltstones and is enriched in a quartz and carbonate. Painter (2003) identifies the Kennedy Spear Siltstone to contain interbedded parallel-laminated siltstones and homogenous mudstones and is notably barren of sulphides, with the exception of vein and breccia-hosted Pyrite 2 proximal to the ore system. The unit is considered to have a depositional environment associated with a saline mudflat (Painter, 2003). Within literature, the Kennedy Spear Siltstone has previously been sub-divided into the Kennedy Siltstone and Spear siltstone. The siltstone unit has an average depth of 480m (Wilde, 2006) and is overlain by the Magazine Shale. Pyrite 2 is present in the Kennedy Spear Siltstones as either vein-hosted coarse crystals associated with talc (after dolomite)(Figure 3a), carbonate and quartz or as large subhedral to euhedral cubic crystals, which often appear disseminated, ranging from 50µm- 5mm (width) (Figure 3b).

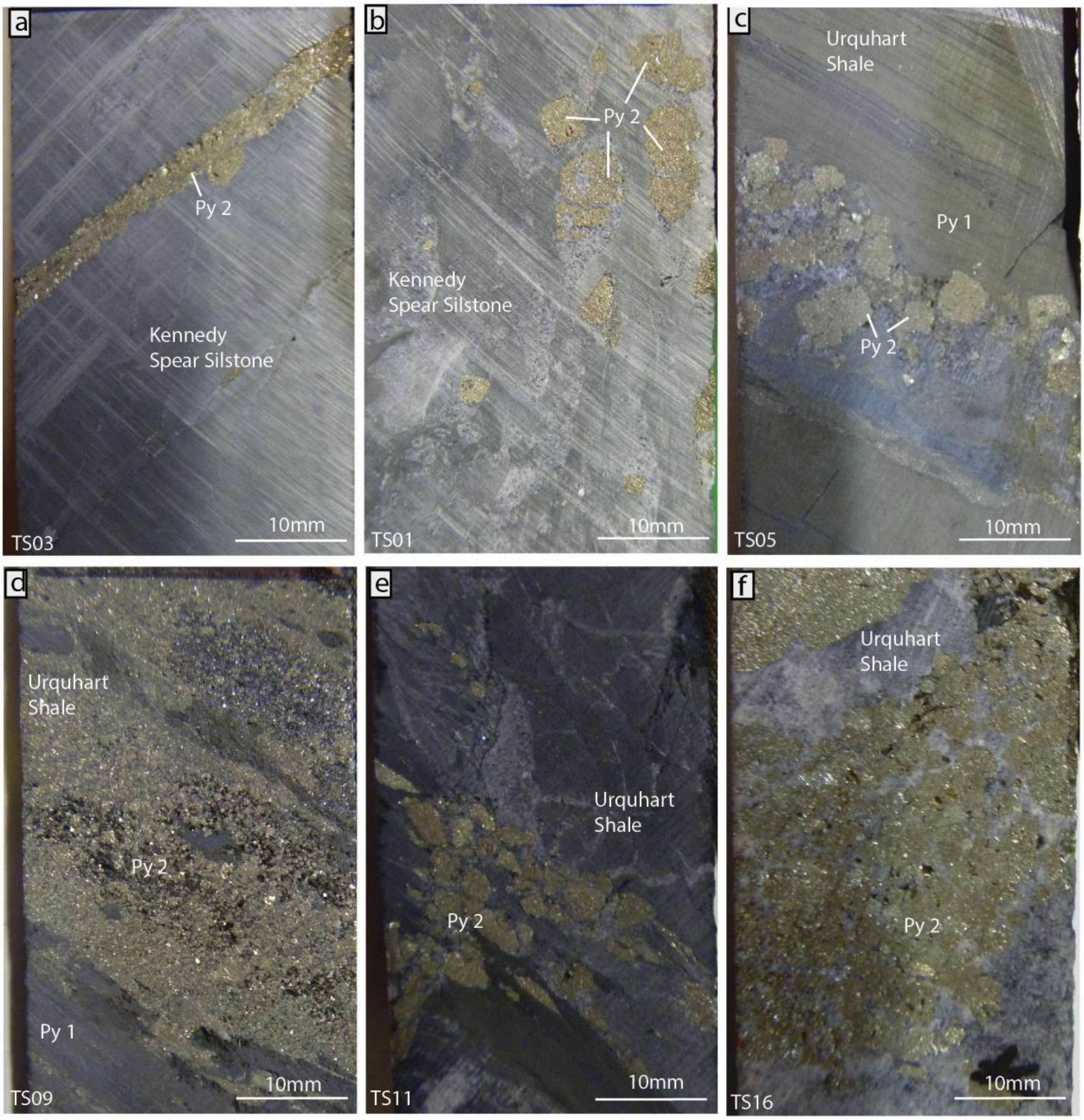

Figure 3 displays quarter core examples of the Kennedy Spear Siltstone (a-b) and Urquhart Shale (c-f) lithologies found at Mount Isa Mines from the exploration drill core transect 0406ED2. Each image indicates the lithological unit and displays a representation of the pyrite variations (Py1 and Py2) within them Images c-d show the pyritic components of the Urquhart shale, and images e-f show the shale component of the Urquhart shale, with overprinting and vein hosted Pyrite 2.

2.2.2 URQUHART SHALE

The Urquhart shale (Figure 3c-f) is stratigraphically below the Kennedy Spear Siltstone and hosts the majority of economic Cu, Pb and Zn mineralization (Painter, 2003). The shale has an average depth of 910m (Wilde, 2006) and dips in a westward direction on average of 65° (Perkins, 1998). This is relatively consistent throughout the whole unit, but varies from 57-70°, in different locations throughout the shale. The Urquhart Shale contains two main components, pyritic shale (Figure 3 c-d) and shale (Figure 3e-f). The shale component of the Urquhart unit is inter-bedded dark grey and back shale; carbonate poor, fine to medium grained siltstone and non-laminated carbonaceous fine-grained mudstone (Painter *et al.,* 1999). The pyritic component contains moderate to significant inter-beds of fine-grained pyrite (Pyrite 1), with Pyrite 2 observed over-printing as both vein-hosted and within breccia zones (Figure 3c-d) (Painter *et al.,* 1998). The Urquhart Shale, is enriched in fine and coarse-grained pyrite along with recrystallized carbonate, quartz and talc, as seen in Figure 4, which displays, Pyrite 1 and 2 generations and their relationships with other minerals in the system.

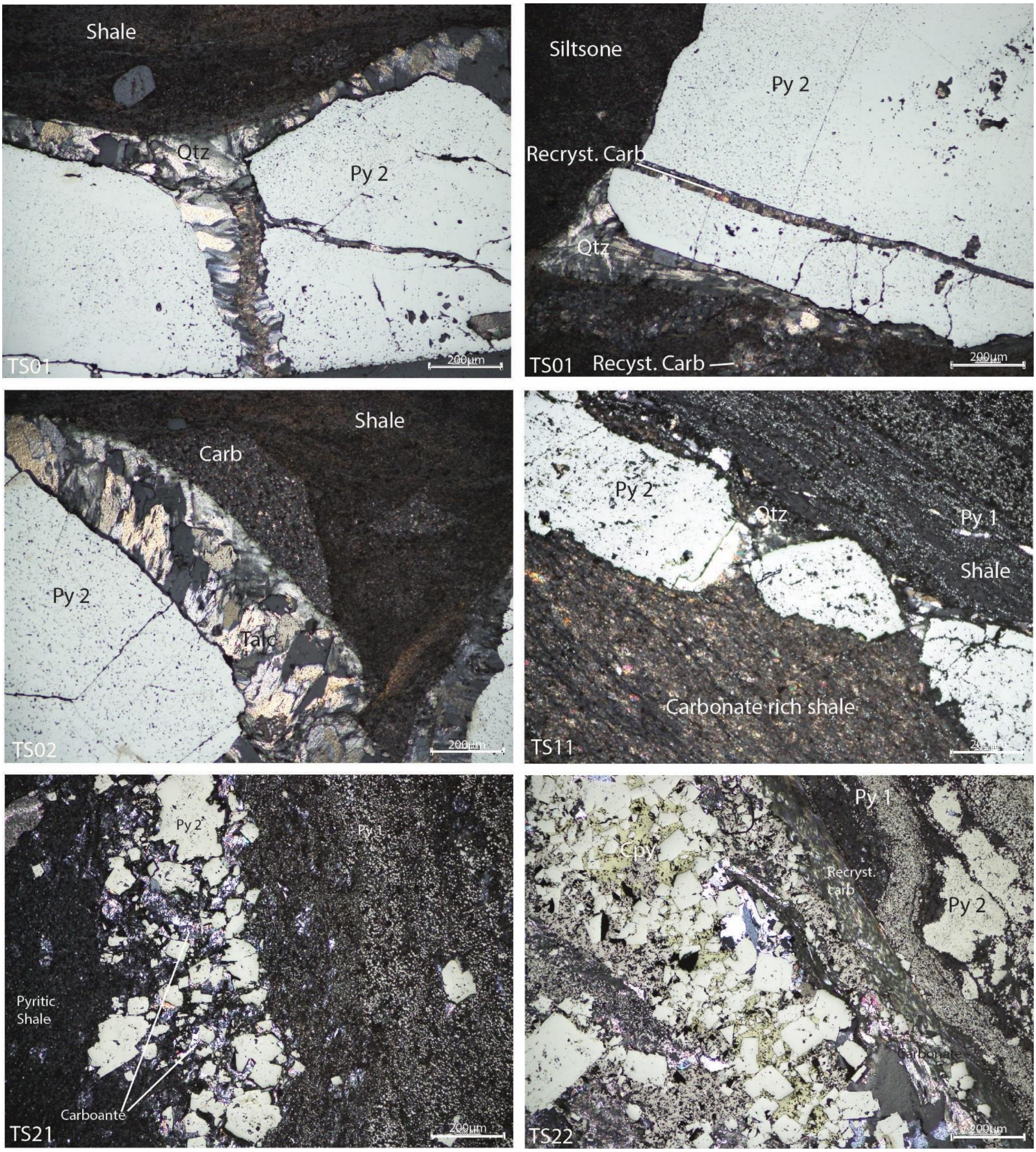

Figure 4 Displays reflected light and cross-polarized petrological images produced from the 0406ED2 explorative drill core, showing the various generations of pyrite and their relationships within the Kennedy Spear Siltstones (a, b, c), and shale and pyritic shale components of the Urquhart Shale. The images show Pyrite 1 (paragenetically early), with Pyrite 2 (paragenetically late), in several samples. The Pyrite 2 is seen overprinting, and displacing the Pyrite 1

2.2.3 PYRITE

Pyrite (FeS_2) is the dominate accessory mineral associated with the economic Mount Isa system, specifically within the Urquhart shale and the mine area (Wilde, 2006). The Pyrite within the Mount Isa System is considered by Perkins (1996), to have formed by a significant and rapid accumulation of organic matter, forming an anaerobic environment and the reduction of sulphate. This forced the mixing of hydrogen sulphide and iron (from Fe-rich detrital minerals), and the subsequent oxidation of sulphur by bacteria to form pyrite. Pyrite is a brassy yellow colour, has a black steak with a greenish tinge, is brittle and will break into thin pieces under pinpoint pressure (Painter, *et al*, 1999). Pyrite is chemically classified as a sulfide and is commonly associated with ore minerals (Williams, 1998). This is the case in Mount Isa where pyrite is found in abundance associated with the ore assemblage of galena (PbS), sphalerite ((ZnFe)S) and chalcopyrite ($CuFeS_2$) (Perkins, 1996). Mount Isa hosts two distinctively different generations of pyrite; fine-grained Pyrite (Pyrite 1) and coarse-grained pyrite (Pyrite 2) (Taylor, 2016). Pyrite 1 is inter-bedded within the Urquhart shale, and is interpreted to be sedimentary in origin (Perkins, 1996B). Pyrite 1 is typically 2-20μm and forms as euhedral grains, with cleaner core shapes and inclusion rich outer zones (Perkins, 1996). This generation of pyrite is the earliest sulphide to form as it is overprinted by all other sulphides in the system. Galena, sphalerite, pyrrhotite and chalcopyrite all display various replacement textures associated with Pyrite 1 (Figure 4). (Perkins 1996, Perkins 1998, Painter & Golding 1998, Painter 2003 and Taylor, 2016).

Pyrite 2, is a coarse-grained variation of pyrite, and is observed within the Kennedy Spear and Urquhart Shale. Previous studies have also called coarse-grained pyrite, 'Brassy Pyrite' (Warning 1990 & Perkins 1996B) and interpreted it to have formed as a result of metamorphic recrystallization of sedimentary pyrite, (Pyrite 1) (Perkins, 1996B). Currently the distinction between ‘Brassy Pyrite’ and Pyrite 2 is not clear. Pyrite 2 forms as cubic euhedral crystal grains (Figure 5) which range in size from 20μm to 200μm. Pyrite 2 can also occur in veins, as aggregates of cubic grains and has commonly been interpreted as being related to a hydrothermal mineralization event (Perkins, 1996B). Pyrite 2 is also typically associated within a quartz and carbonate enriched matrix, related to the silica-dolomite halo and copper mineralization. Pyrite 2 appears overprinting in relation to the fine-grained bedded pyrite, and other sulphide minerals present, and also occurs within brecciated textures. Pyrite 2 is also observed as bedding parallel accumulations and veins, similar to Pyrite 1 (Figure 3, 4 and 5) within the Urquhart Shale.

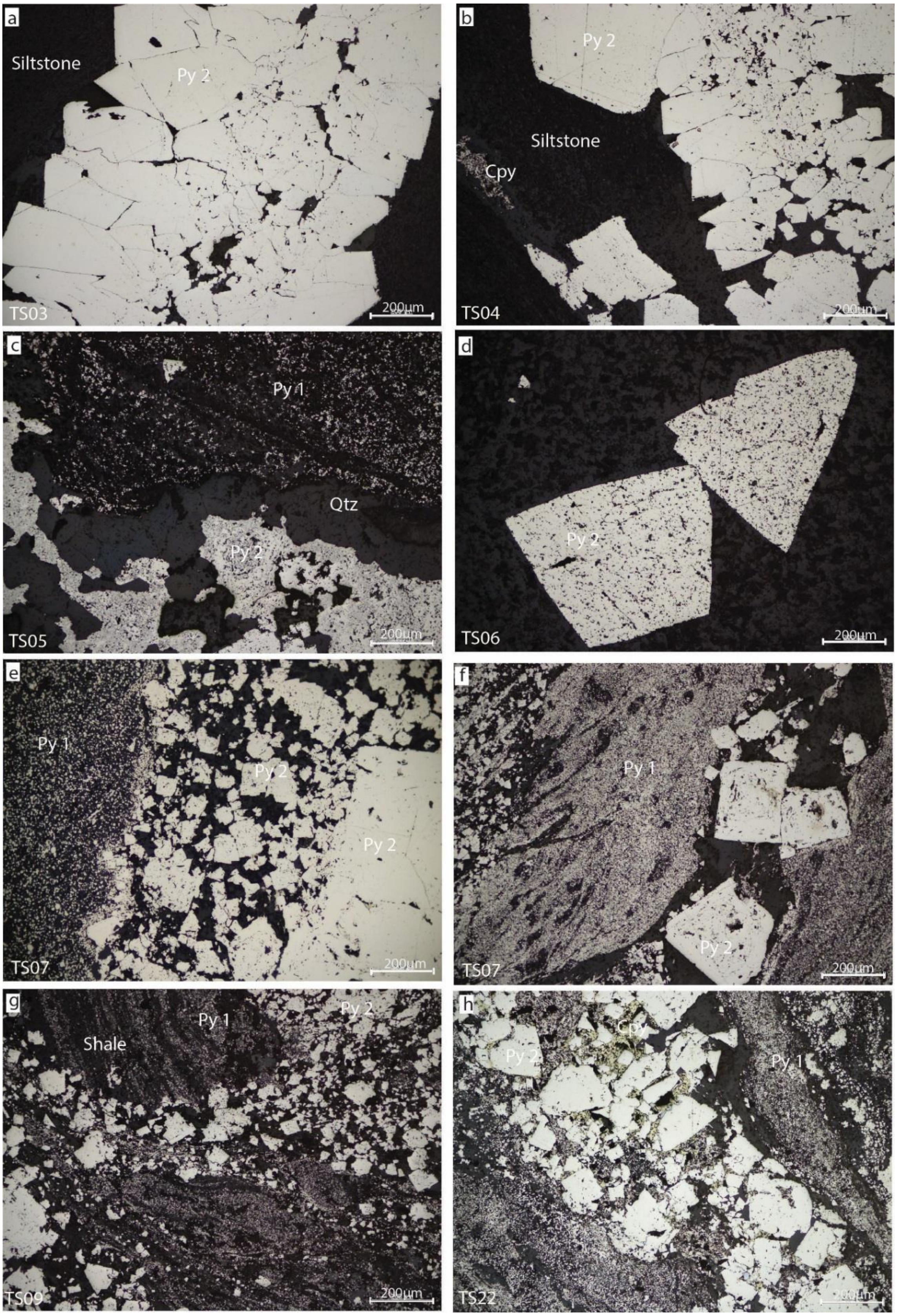

Figure 5 displays reflected light and cross-polarized petrological images produced from the 0406Ed2 explorative drill core at Mount Isa Mines. The images displaying various pyrite textural, specifically Pyrite 2 types and styles from within the mine. Images a & b, show he Pyrite 2 grains as they appear within the Kennedy Spear Siltstone, as a disseminated vein. Image c shows Pyrite 2 grain which has been altered by quartz vein. Image d, shows various shapes py pyrite 2 grains, and images e-h, display Pyrite 2 in relation and contrast to pyrite 1 and shale.

2.2.4 PARAGENESIS

The paragenesis and formation of the Mount Isa copper system has long been debated and investigated. Numerous studies, such as Perkins (1990, 1996, 1998), Blake (1987), Painter (2003), Large *et al.*, (2014) Thomas *et al.*, (2011), Wilde (2011), Wilde *et al* (2006), and Taylor (2016), have been conducted on the system to determine the paragenesis and relative timing of the formation of the system. The current paragenesis for the Mount Isa system is broken down into 5 stages (Table 1). The first stage consists of an enrichment of chlorite infill/alternation within the underlying Eastern Creek Volcanics.. The second stage identified is quartz veins with minor infill style appearance. The third paragenetic stage is the dominant Pyrite 1 stage (refer to Connell, 2016 for more detail on this paragenetic event). Stage 4 is classified as the main silica-dolomite and sulphide stage and encompasses the main copper mineralizing events (Taylor, 2016). Stage 4 is sub-divided into three phases, a, b and c. 4a is enriched in coarse-grained carbonate (Carbonate 1), quartz and Pyrite 2. Pyrite 2 in this phases forms large, cubic crystals and clusters, and also occur as cross cutting veins (Taylor, 2016 and Perkins, 1996). Phase 4b consists of Carbonate 2, chalcopyrite and pyrrhotite. During this phase, the system undergoes minor brittle refracting and re-crystallization of minerals associated with phase 4a. Phase 4c, consist of chalcopyrite precipitation in significant amounts, along with pyrrhotite galena and sphalerite. The final stage, (stage 5) of the paragenesis is enriched in chlorite, seen as veins overprinting all pervious mineral stages (Taylor, 2016).

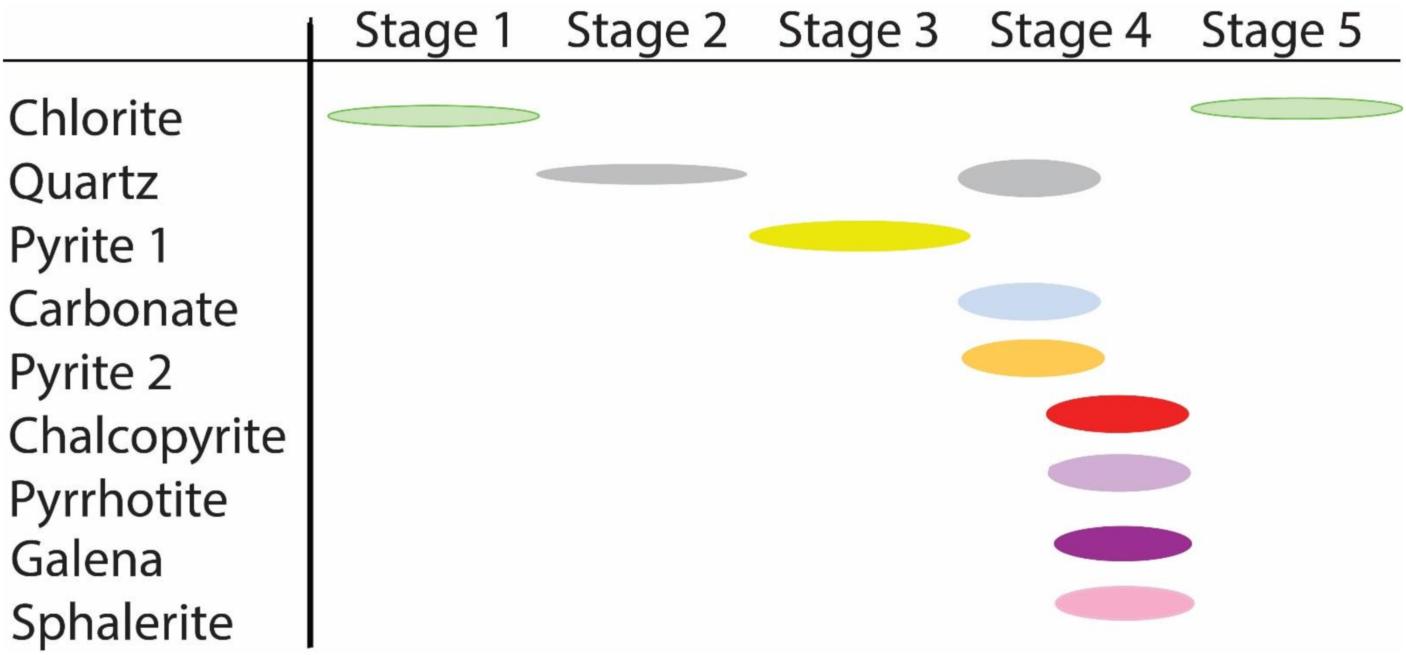

Table 1 shows the 5 stage paragenesis summary for the Mount Isa Copper System. This summary identifies the ore-bearing copper stage to occur in stage 4.

3. METHODS

3.1 Sampling

Fieldwork was completed at Mount Isa Mines, in March 2016. 24 samples were obtained from diamond drill hole 0406ED2 (717.3m from surface) as detailed in Figure 2. This resource development hole was targeted to drill through the silica-dolomite alteration halo of the 1100 orebody to establish if any additional resources were present outside the existing modelled 1% Cu resource. The core was logged with observations of structure, lithology, mineralization, alteration, veining, mineral presence and comments regarding ore textures, paragenesis, vein systems and relative deformation events. Refer to appendix A and B for detailed core and sample log, respectively, produced from the 0406ED2 transect. Appendix C, shows detailed process of selecting the 24 samples. The samples selected were to be made into polished thin sections (0406ED2_TS01-0406ED2_TS24) at approximately 20-meter intervals, to ensure that a regular and representative selection of drill core was collected. This sections were made by Ingham Petrographics (Qld).

3.2 Optical Petrology

Petrology was completed on the samples using the Olympus DP21 Camera, Olympus BX51 Microscope, and Olympus TH4-200 Light Source. Transmitted light images, in plane and crossed polarizer was used to classify the minerals within the samples. Reflected light analysis was used to detect various sulphide minerals, such as pyrite and chalcopyrite. The petrologic study was also used to identify 6 representative samples and target areas for further analysis. Detailed Petrology results for the 24 Mount Isa Samples from the 0406ED2 transect can be found in Appendix D.

3.3 SEM/MLA

Scanning Electron Microscope (SEM), FEI Quanta 600 (MLA), was used to produce thorough, and high-resolution textural analysis of the 6 representative Mount Isa samples. The analysis focused on the textural variation of the pyrite generations. A solid-state backscattered electron (BSE) detector enables mean atomic number imaging and the thin detector allows for X-ray analysis and produces images as seen in Figure 6. Mineral Liberation Analysis (MLA) was used to quantify a range of mineral characteristics, such as abundance, grain size and relationships. The BSE and MLA imaging were used to select areas of interest for further trace element analysis (Figure 6).

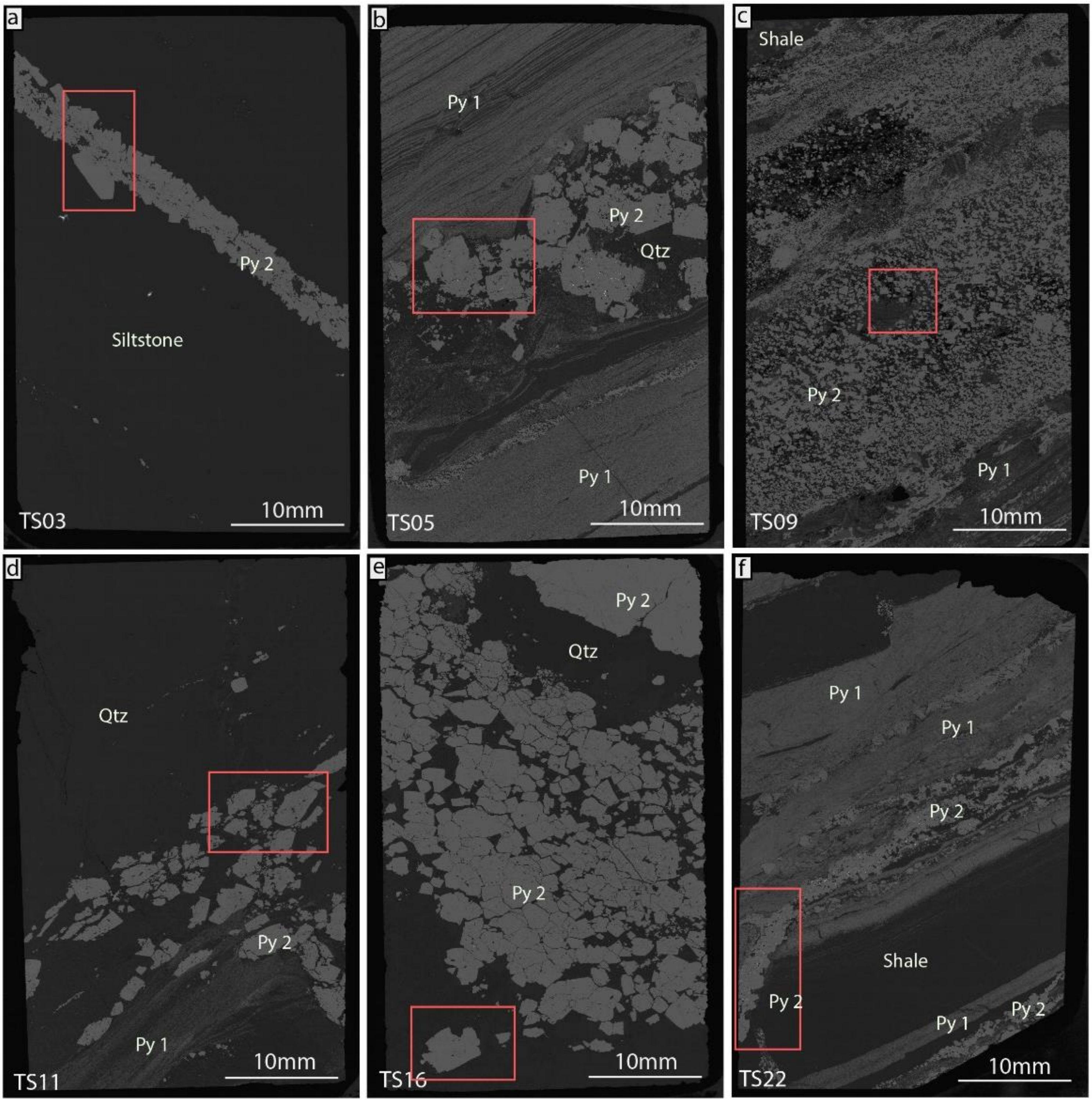

Figure 6 displays backscatter (BSE) images produced from the Quanta 600 SEM/MLA for the 6 representative Mount Isa Mine Samples (TS03, 05, 09, 11, 16, & 22 respectively), with targeted areas for further investigation identified. The samples show various style of Pyrite 2 found within the 0406ED2 transect, along with Pyrite 1 and other significant minerals and lithologies.

3.4 LA-ICP-MS

The Laser Ablation-Inductively Couple Plasma-Mass Spectrometry (LA-ICP-MS) on the RESOlution LR Laser Ablation system attached to the Agilent 7700s ICP-MS, was used for further in-depth trace element analysis on the six representative samples. The analyzed samples were compared to two standards, provided by Adelaide Microscopy, NIST_6010 and MASS_1 Sulfide. Though, both standards were used during the LA-IC-MS analysis, the MASS-1 standard was used for analytical analysis of the samples. The MASS-1 standard, was created by the U.S. Geological Survey, and is composed of a total of 25 trace elements. The standard was created through co-precipitation process, using copper, iron and zinc solutions in combination with a sodium sulfide solution. The standard is classified as a Polymetal sulfide and the micro-homogeneity of the sample was assessed using LA-ICP-MS analysis (American Geological Society). Further information on the Mass_1 standard can be found in Appendix E. For this study, the laser ablation process used, a laser spot size of 32μm, with a scan speed of 64 seconds and a laser pulse rate of 10Hz were used. These specifications were used to obtain precise and accurate results of the trace elements analyzed . The trace elements that were selected for analysis were Fe, As, Ni, Co, Mo, Pb, Ag, Cu, Zn, Mg, Pd, Rb, Ba, La, Ce and Ti. The raw data for each sample was processed using Iolite and Igor data processing software and complied into elemental concentration maps. Each sample was integrated against each standard, and the background was removed. Known element concentration (ppm) maps were created for Silver (Ag), Arsenic (As), Barium (Ba), Cobalt (Co), Copper (Cu), Molybdenum (Mo), Nickel (Ni), Lead (Pb), and Zinc (Zn) for each sample. The maps were resized, re-processed for scale purposes and the cool to warm colour scale was used to identify the elemental trends most effectively. Outlying data was coloured as black and grey if the sample contained regions that were below or above the detection limits, respectively. Scales for each sample were selected to produce the most effective elemental maps in reference to the Pyrite 2 grains within the samples.

4. OBSERVATIONS AND RESULTS

4.1 0406ED2_TS03 (255.5m)

Petrology

Sample TS 03 was collected from the Kennedy Spear Siltstone which predominantly consist of quartz and carbonate enriched siltstone with a Pyrite 2 vein ~3mm across (Figure 7a). The vein cross-cuts the sample, this is an indicative characteristic of Pyrite 2 within the Kennedy Spear Siltstone, as proposed by Perkins (1996). The vein consists of serval smaller Pyrite 2 grains, which appear cubic and euhedral on the edges of the vein and anhedral towards the centre (Figure 7c). The pyrite grains within the vein range from 20µm – 2mm in size. Minor chalcopyrite grains are seen in association within talc veins

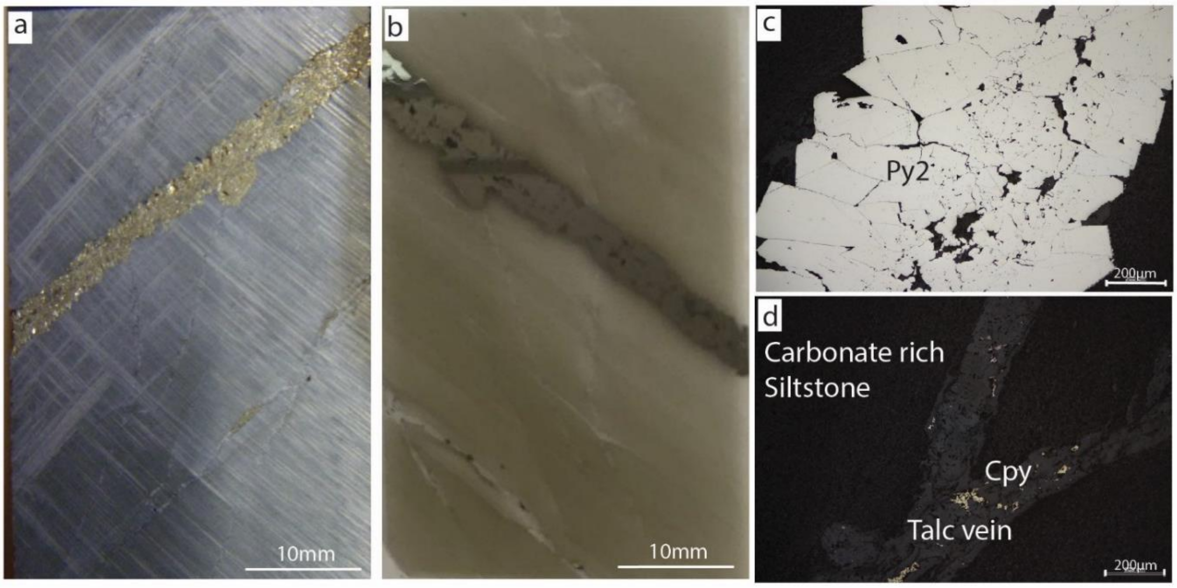

Figure 7 shows the quarter core (a), thin section (b) and petrological images (c-d) from sample TS03, displaying the pyrite 2 association with the Kennedy Spear Siltstone. Image c, displays the style of pyrite 2 grains with euhedral and subhedral pyrite grains.

within the sample. Talc in the Mount Isa system is associated with hydrothermal alteration of dolomite (Figure 7d).

SEM/MLA

SEM/MLA analysis identified that the vein infill was enriched n biotite, albite and orthoclase, with chlorite present within and surrounding the Pyrite 2 vein (Figure 8).

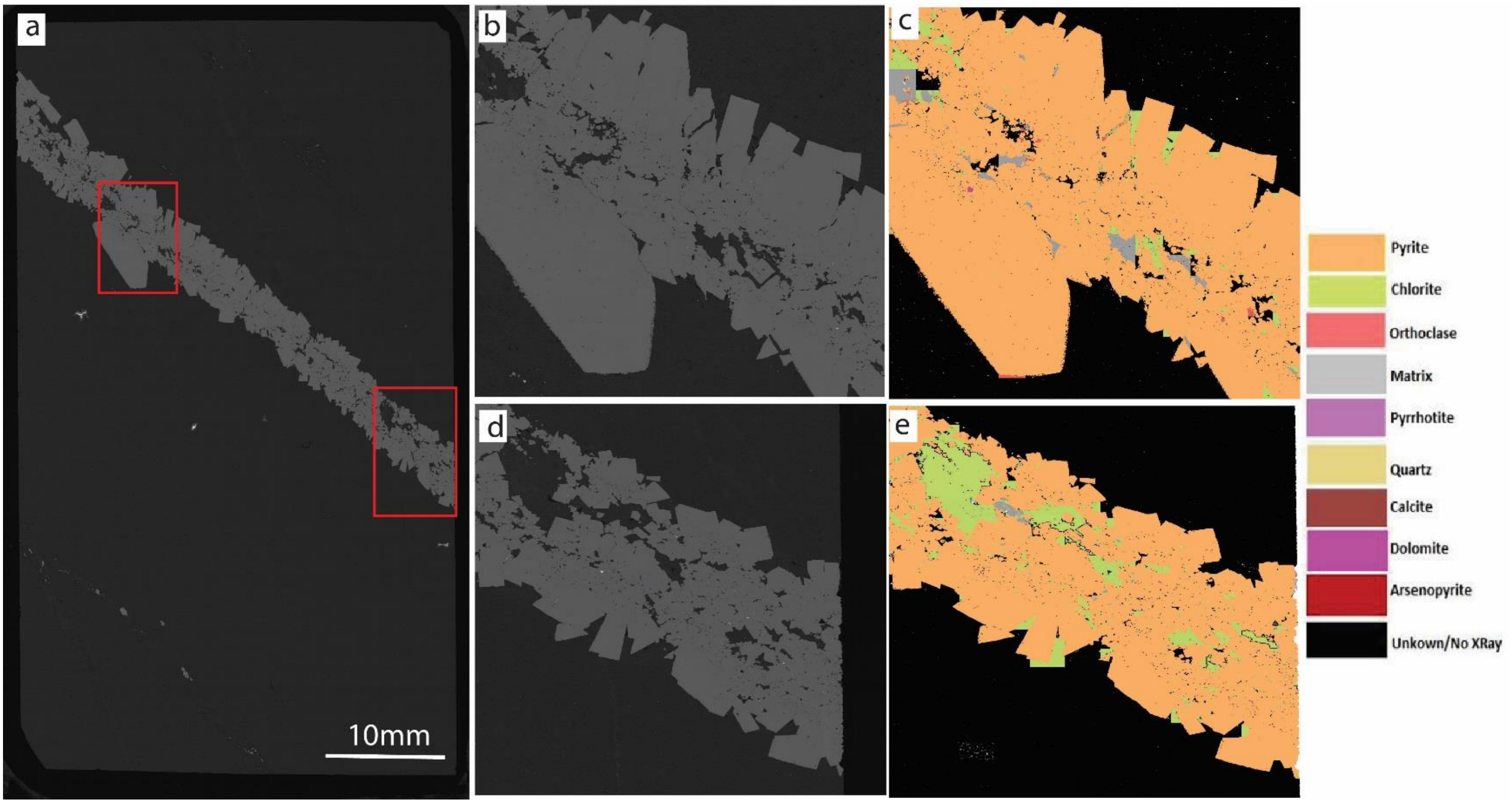

Figure 8 displays BSE images (a, b, d) for sample TS03, with corresponding MLA analysis for target areas (c, e) displayed on image a. The MLA identified the vein infill to be enriched in chlorite, and a biotite dominate matrix. The area displayed in image b and c, is the area selected for further analysis.

LA-ICP-MS

Elemental maps, (Figure 9), identified that As has the maximum concentration, of 20,000ppm (2%), within the grain. The elevated concentration is in the centre of the Pyrite 2 vein, and decreases in concertation towards the edges. The trace element variation is not homogenous or consistent throughout the sample and elemental concentrations vary considerably across the targeted area. No zoning or original pyrite cores are identified within this sample. The maps do not display individual Pyrite 2 grains, as shown in the SEM/MLA and petrological images. The larger (2mm) pyrite grain is distinguishable, but the remaining grains are not. Due to a malfunction with the ICP-MS data was not collected for Co and Ni, for some areas. However, the rest of the data for these elements is still considered fit for this study.

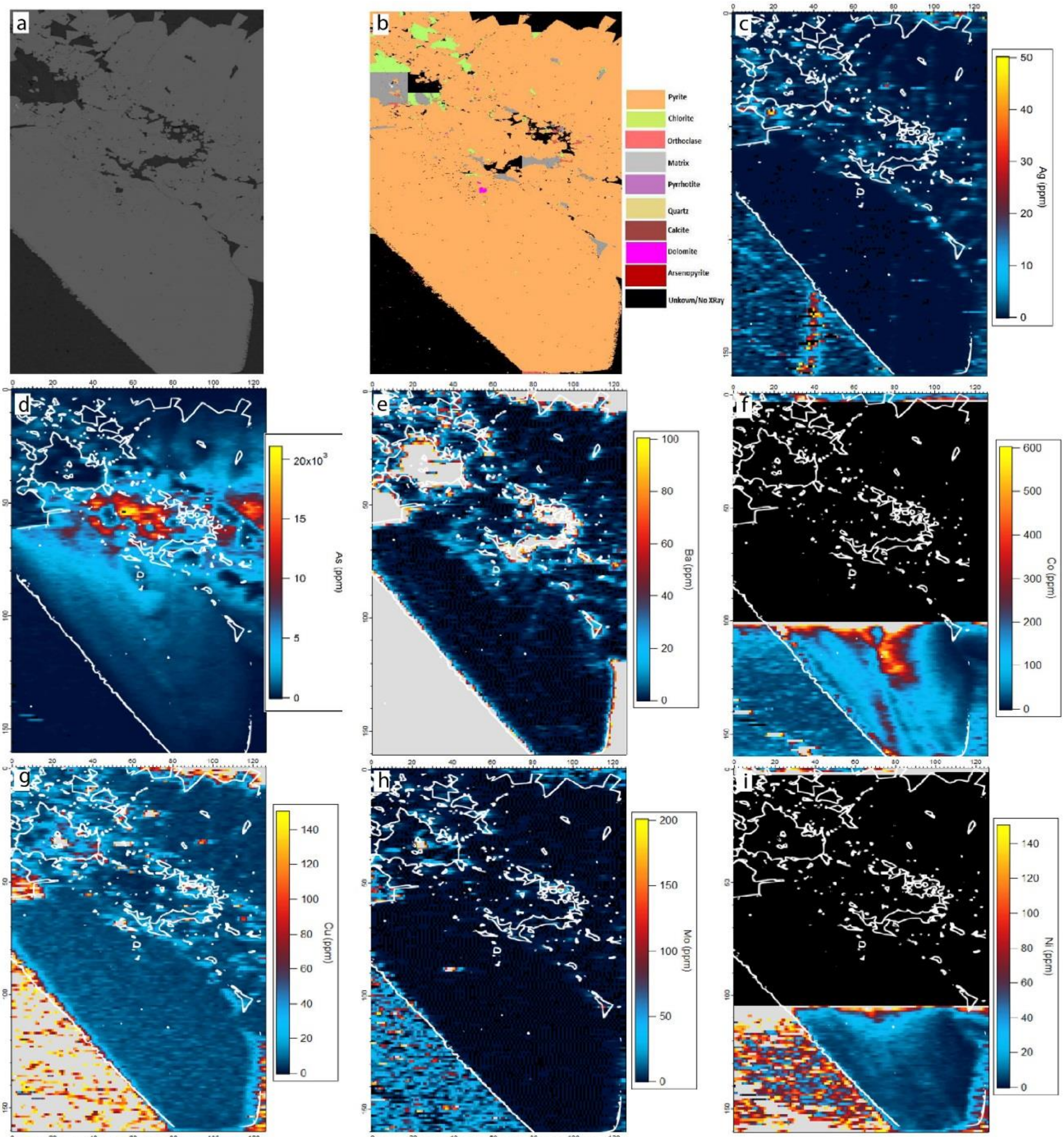

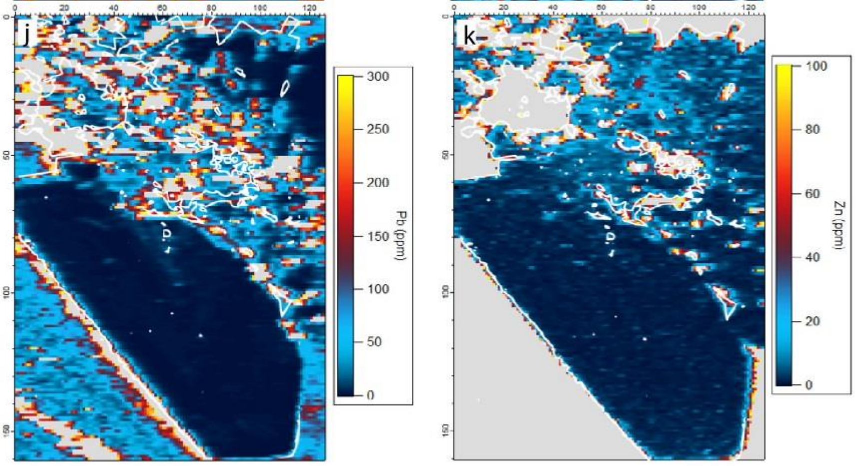

Figure 9 displays SEM BSE image (a), with corresponding MLA image (b) and ICP-MS elemental concertation (ppm) maps (c-k) for Silver (Ag), Arsenic (As), Barium (Ba), Cobalt (Co), Copper (Cu), Molybdenum (Mo), Nickel (Ni), Lead (Pb) and Zinc (Zn), respectively, form sample TS-03 (255.5m).

4.2 0406ED2_TS05 (397.7m)

Petrology

Sample TS05 was collected from pyritic shales, within the Urquhart Shale (Figure 9). The sample consists of predominately fine-grained pyrite (Pyrite 1) that is bedding parallel. Pyrite 2 grains are present within a vein, with a quartz matrix. Some of the Pyrite 2 grains are fragmented and contained numerous inclusions (figure 9c). The Pyrite 2 grains identified within this sample, are significantly larger, some spanning up to 8mm across.

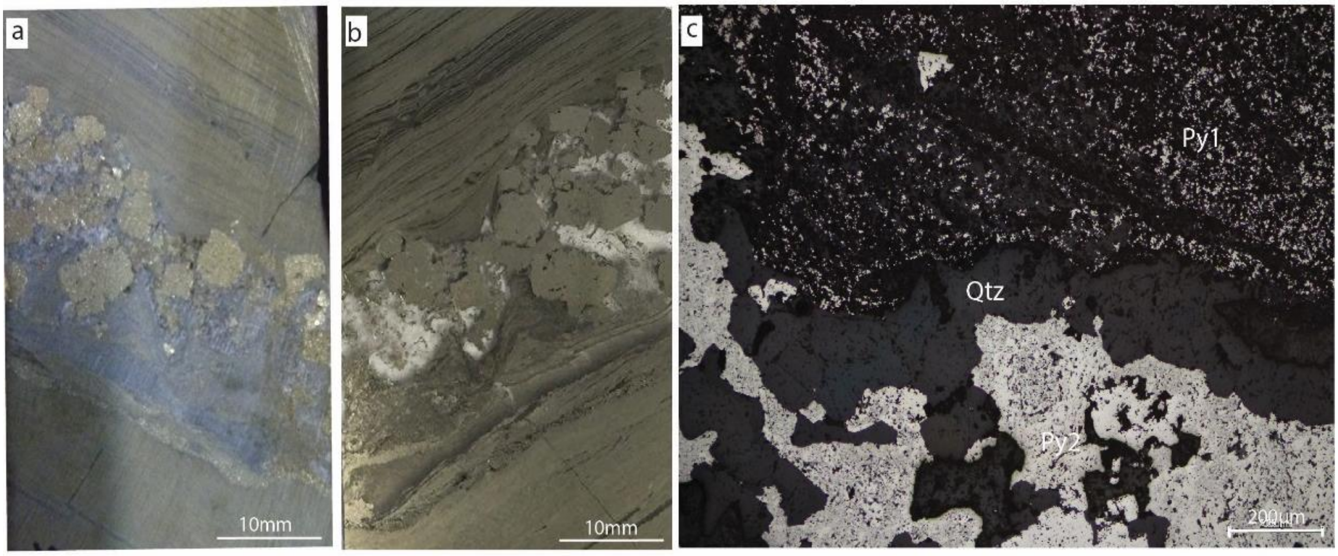

Figure 10 shows the quarter core (a), thin section (b) and petrological (c) image from sample TS05, displaying the Pyrite 2 association with the Urquhart Shale and Breccia vein, shown in image c.

SEM/MLA

SEM/MLA identified the matrix of the sample to be enriched in quartz, with chlorite appearing in close contact to edges of some Pyrite 2 crystals (Figure 11). The sample also contains minor aresnopyrite, calcite, dolomite, galena and pyrrhotite, surrounding the larger Pyrite 2 grains. Some of these minerals were also found to be inclusions within the pyrite grains.

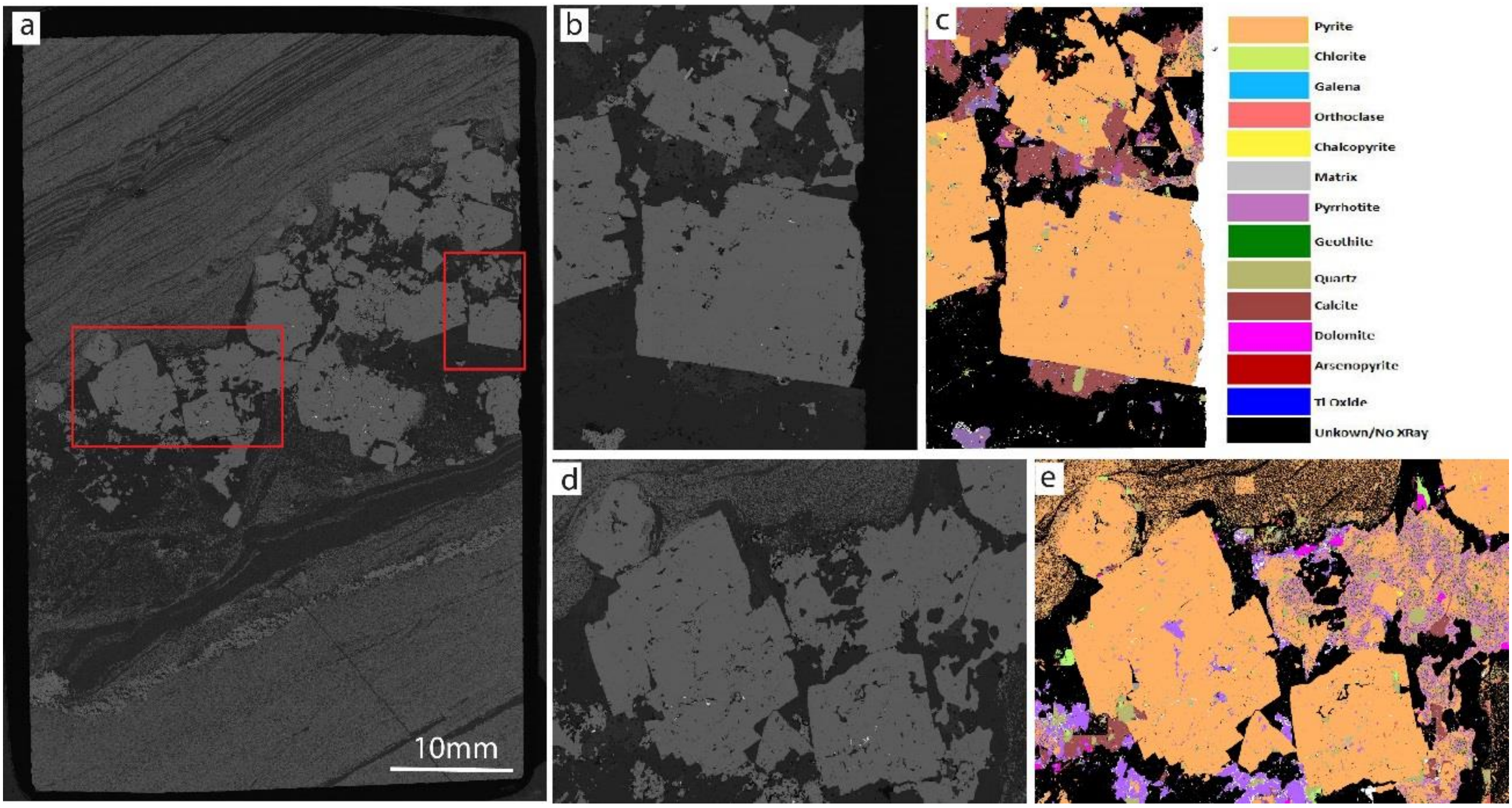

Figure 11 displays BSE images (a, b & d) for sample TS05, with corresponding MLA analysis data for the targeted areas. The MLA identified the sample to be enriched in Pyrrhotite, Aresnopyrite, and chlorite. The area displayed in image d and e, are the targeted areas selected for further analysis

LA-ICP-MS

ICP-MS produced elemental maps (Figure 11 c-k) that show As has maximum concentration of 2000ppm within the Pyrite 2 grains. The varying levels of concentration within the Pyrite 2 grains within the As map, show that variation is heterogeneous and highs occur within certain areas of grains, not homogenously throughout. This sample contains minor Ba, Co, Mo, and Zn within the Pyrite 2 grains, potentially associated with the inclusion identified in the SEM/MLA analysis. The ICP-MS sample contains minor amounts of Pyrite 1. It is noted that the elemental concentrations for Pyrite 1 and Pyrite 2 differ, such as Ba, Ag, Co, Cu, Mo Pb and Zinc showing elevated concentrations for Pyrite 1, when compared to Pyrite 2 (Figure 12).

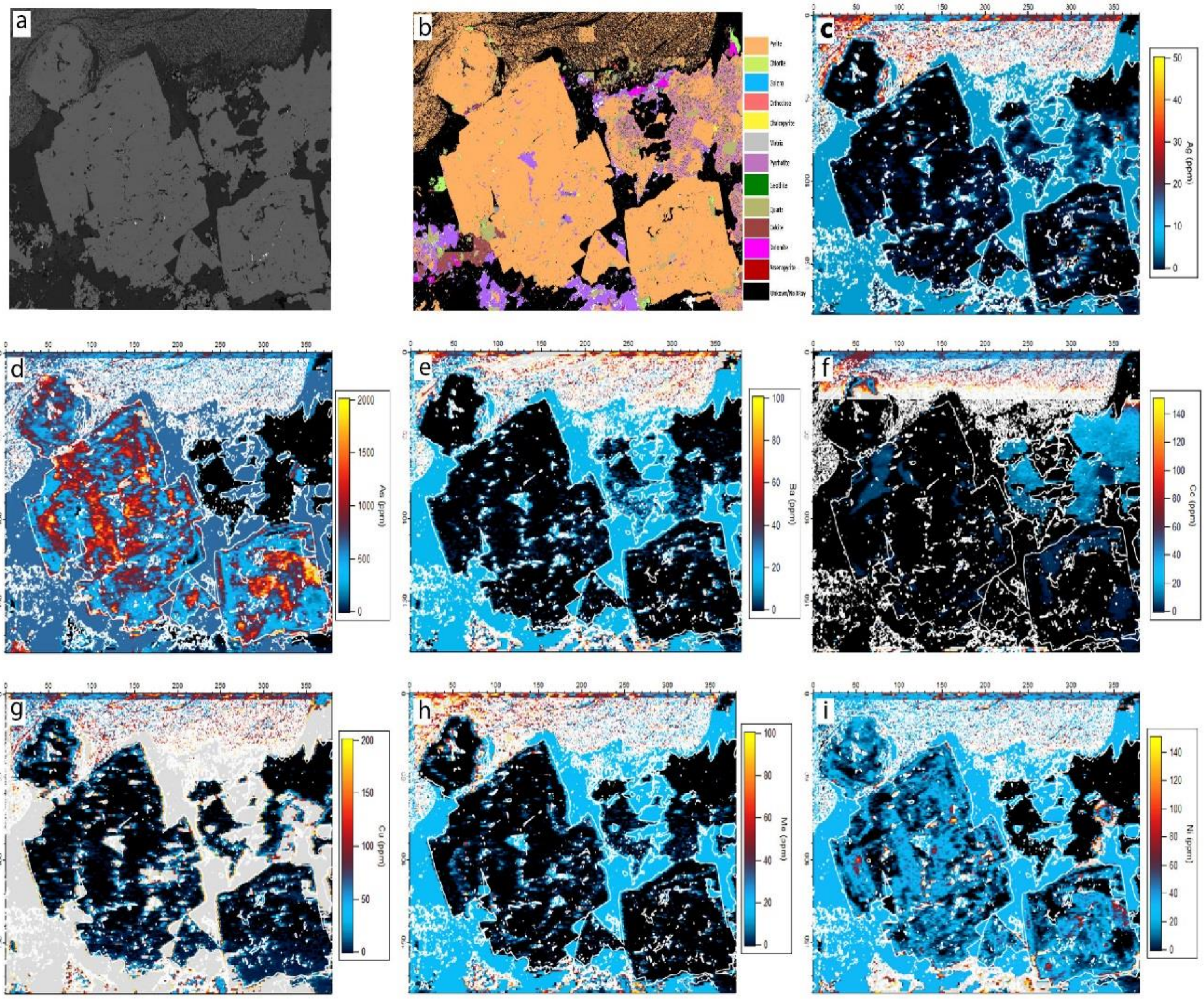

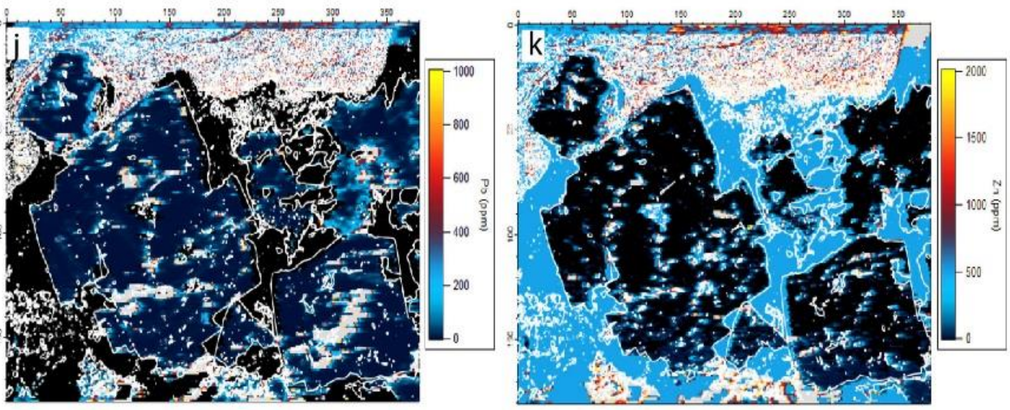

Figure 12 SEM BSE image (a), with corresponding MLA image (b) and ICP-MS elemental concertation (ppm) maps (c-k) for Silver (Ag), Arsenic (As), Barium (Ba), Cobalt (Co), Copper (Cu), Molybdenum (Mo), Nickel (Ni), Lead (Pb) and Zinc (Zn), respectively, from sample TS05

4.3 0406ED2_TS09 (468.8m)

Petrology

Sample TS09 is also hosted within a pyritic shale component of the Urquhart Shale and contains Pyrite 1 and 2 (Figure 13). This sample is dominantly composed of sulphides, with minor shale, quartz, talc and carbonate occurring inter-bedded with the Pyrite 1. The Pyrite 2 in this sample is of a smaller size, varying form 20-200μm, in comparison to sample TS05. The Pyrite 2 within TS09 appears to overprint and cross-cut the Pyrite 1 and shale (Figure 11c & 11d). The sample has areas of solely Pyrite 1 and 2, respectively, as well as areas of the pyrite generations together.

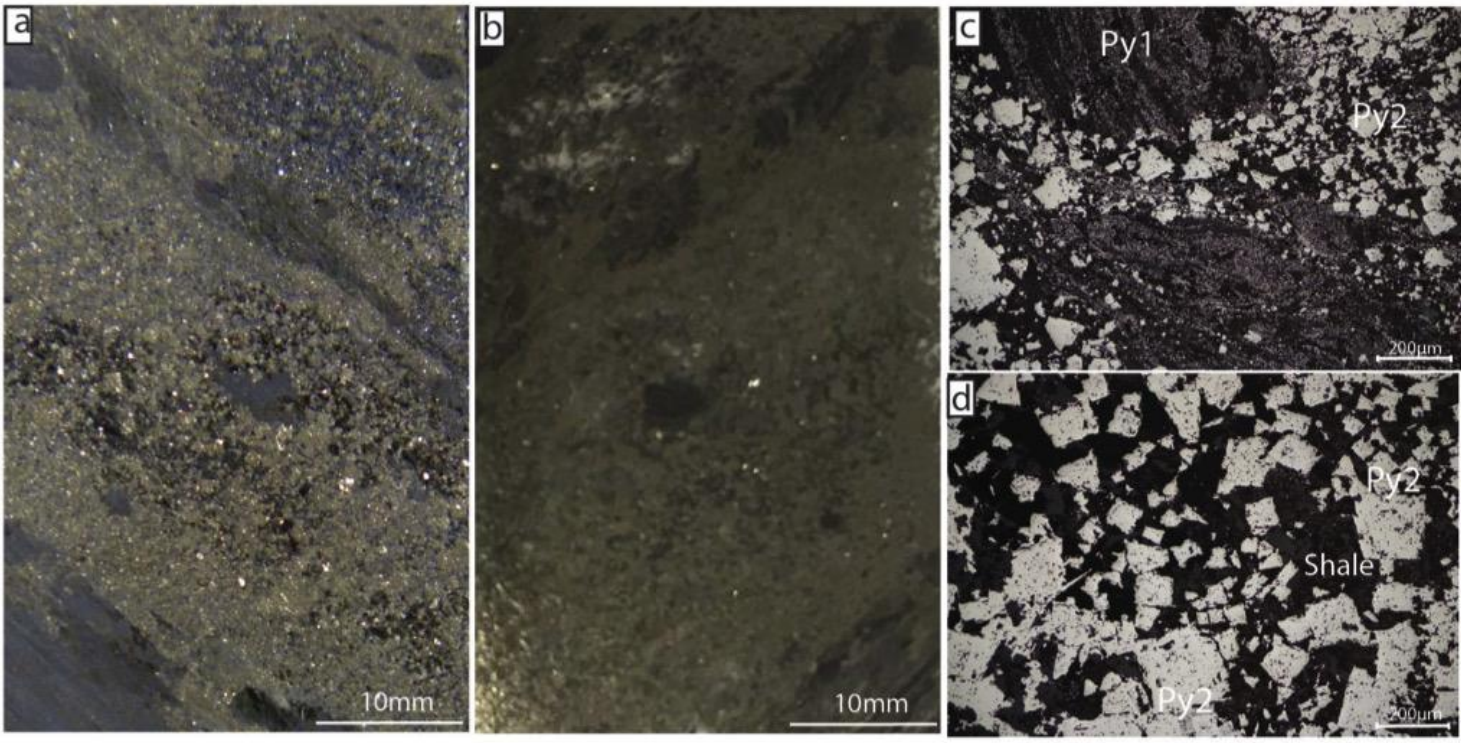

Figure 13 shows quarter core (a), thin section (b) and petrological images (c-d) from sample TS09, displaying the Pyrite 2 association with the Urquhart shale, and Pyrite 1. The Pyrite 2 within this sample, vary in size and are euhedral.

SEM/MLA

The SEM/MLA identified to have pyrrhotite surrounding the pyrite grains, along with an iron oxide mineral (goethite) and chlorite (Figure 14c). The areas containing significant amounts of pyrite 1, were not able to be analysed due to the small size of the grains and the resolution of the technique used.

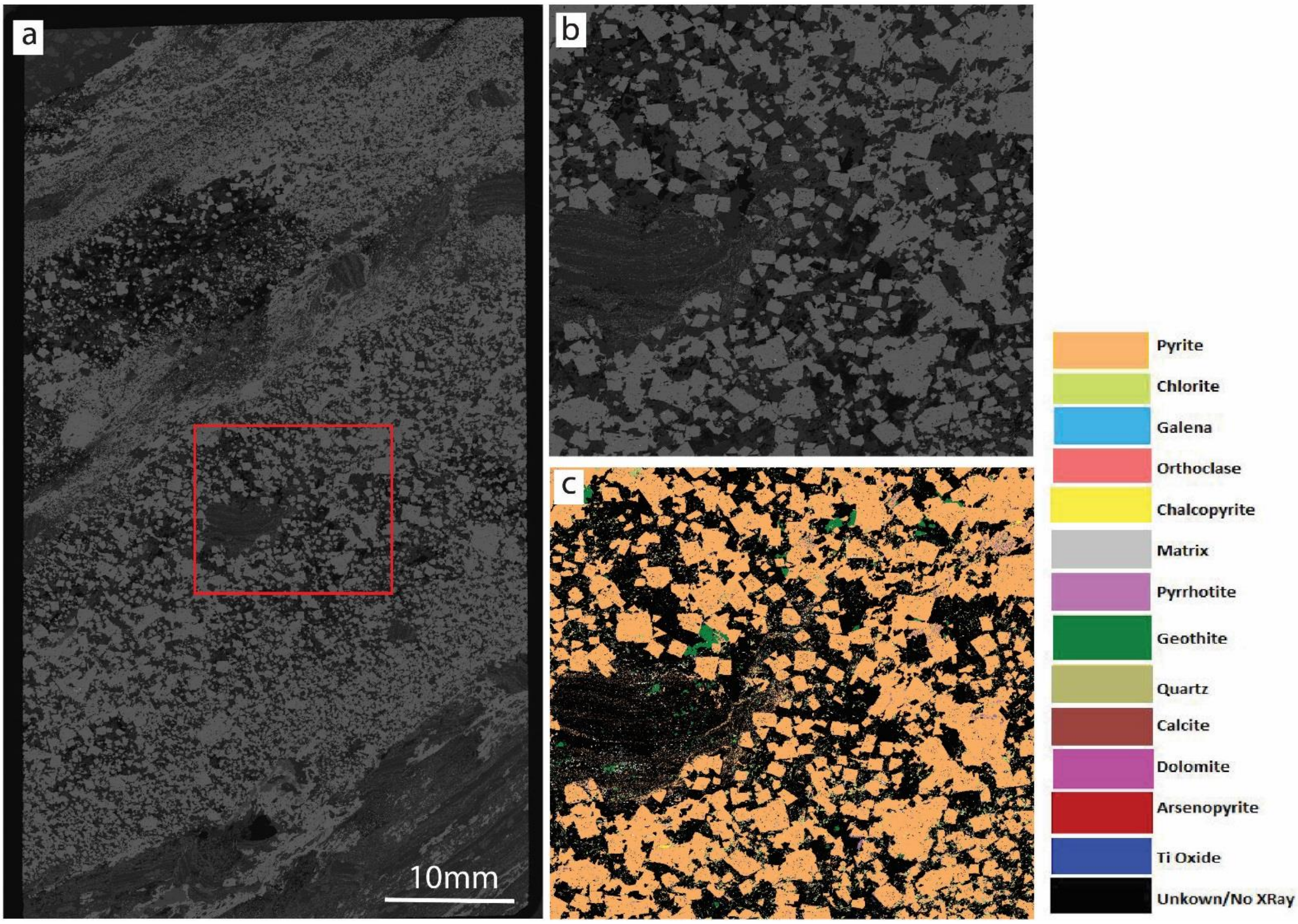

Figure 14 displays BSE images (a & b) for sample TS09, with corresponding MLA analysis for the targeted area (c) displayed on image a. The MLA identified the sample to have pyrrhotite and goethite (iron/magnesium rich mineral) in abundance. The displayed image in b & c, is the proposed target area selected for further analysis

LA-ICP-MS

LA-ICP-MS data collected for this sample produced elemental maps (Figure 15c-k), indicate that Co (Figure 15g) is the element with the maximum concentration within the

Pyrite 2 grains, with a concentration of >1000ppm. This maximum is not seen within all Pyrite 2 grains, as excepted. This suggest the Co element variation, though present is heterogeneous, and is not contained within each pyrite grain. Ag (Figure 15c), was determined to have the lowest concentration at approximately <2ppm within the Pyrite 2 grains. Again a difference between the Pyrite 1 and 2 grains can be seen within this sample (Figure 15c-f and j). The Pyrite 2 grains appear to be relatively depleted in Ag, Ba, Cu, Mo, Ni and Zn compared to the surrounding matrix, consistent with the interpretation that they predate matrix precipitation

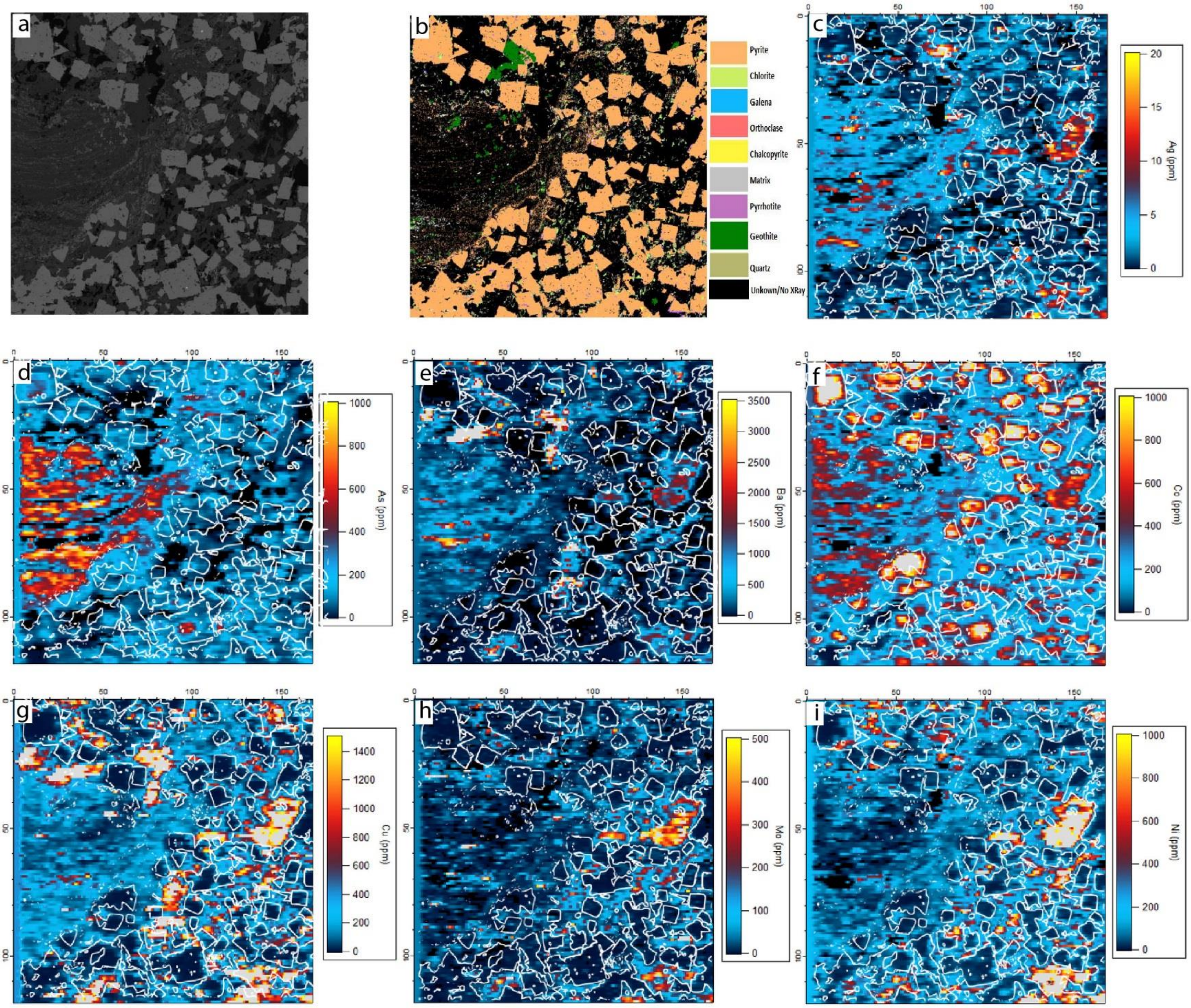

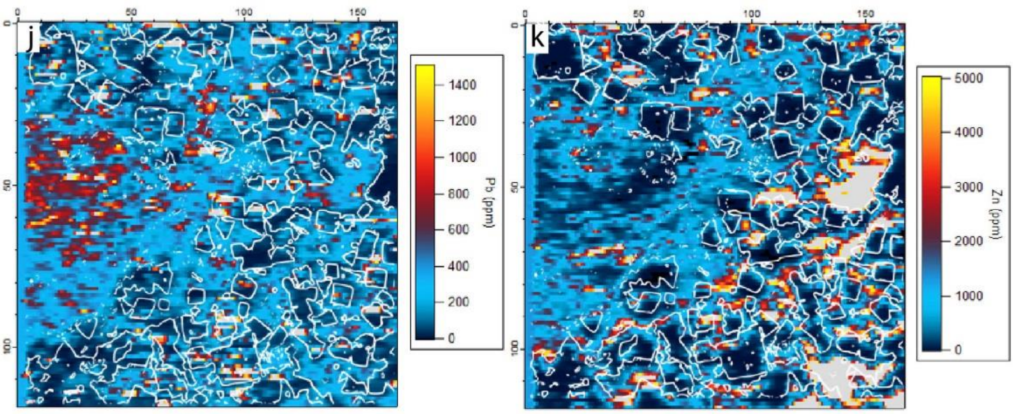

Figure 15 displays SEM BSE image (a, with corresponding MLA image (b) and ICP-MS elemental concentration (ppm) maps (c-k) for Silver (Ag), Arsenic (As), Barium (Ba), Cobalt (Co), Copper (Cu), Molybdenum (Mo), Nickel (Ni), Lead (Pb) and Zinc (Zn), respectively, from sample TS-09.

4.4 0406ED2_TS11 (512.8m)

Petrology

Sample 11, is hosted within the shale component (Figure 16a) of the Urquhart Shale in a brecciated zone. The sample contains large amounts of carbonate and quartz with carbonate veins containing Pyrite 2 and chalcopyrite as infill (Figure 16c-d). Minor Pyrite 1 is seen within the sample, associated with the shale. Pyrite 2 within the sample is surrounded by talc, quartz and carbonate (Figure 16). Chalcopyrite is associated with Pyrite 2, but occurs paragenetically later, within areas of carbonate, talc and quartz enriched shale (Figure 13c-d).

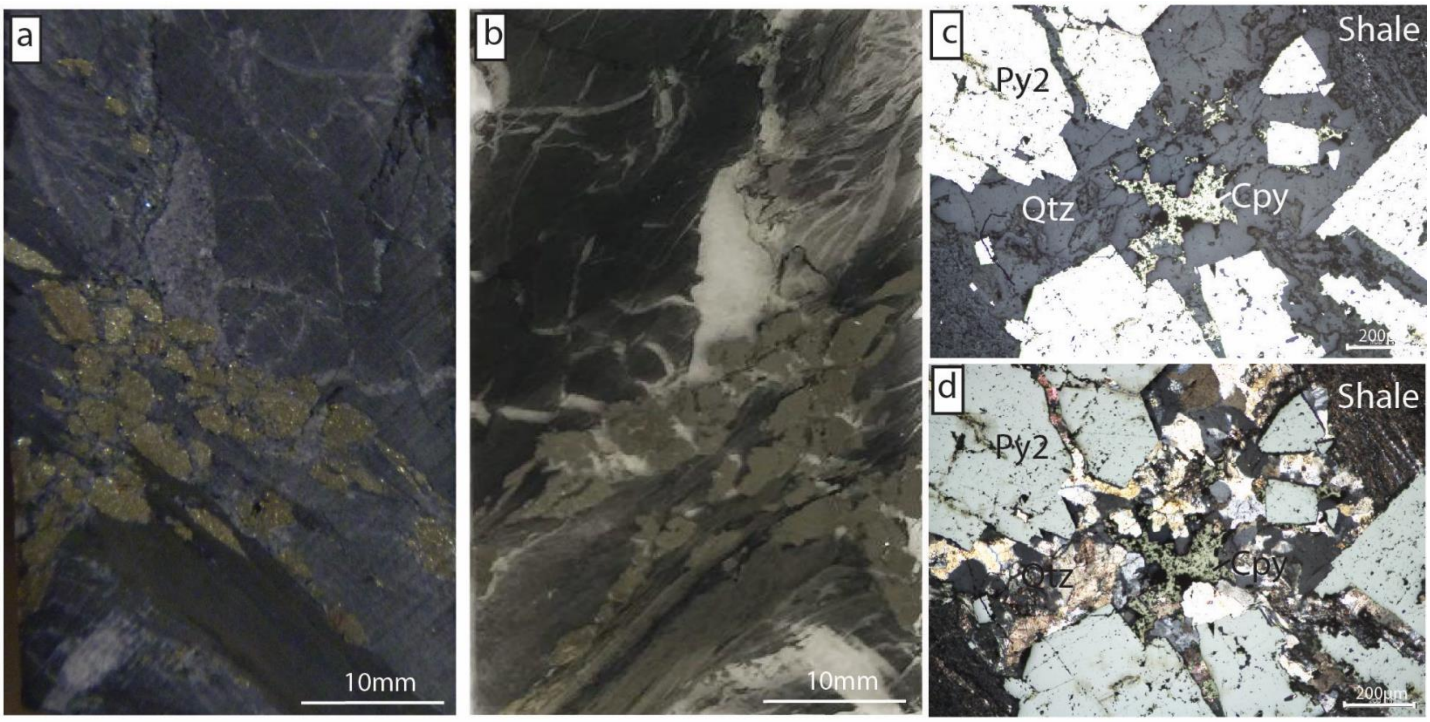

Figure 16 shows the quarter core (a), thin section (b) and petrological images (c-d) from sample TS11, displaying the pyrite 2 association with the shale component of the Urquhart shale. Image c & d, display the mineral relationship between Pyrite 2 and Chalcopyrite, which occurs paragenetically later.

SEM/MLA

SEM/MLA (Figure 17) identified the Pyrite 2 grains within the sample, to have minor inclusions of chlorite, chalcopyrite, quartz, pyrrhotite, calcite and dolomite (Figure 17c). There are veins of minerals, such as chalcopyrite, chlorite, quartz, pyrrhotite, and galena which cut several of the Pyrite 2 grains, as shown in Figure 17c on the Pyrite 2 grain located in the top left hand corner of the image.

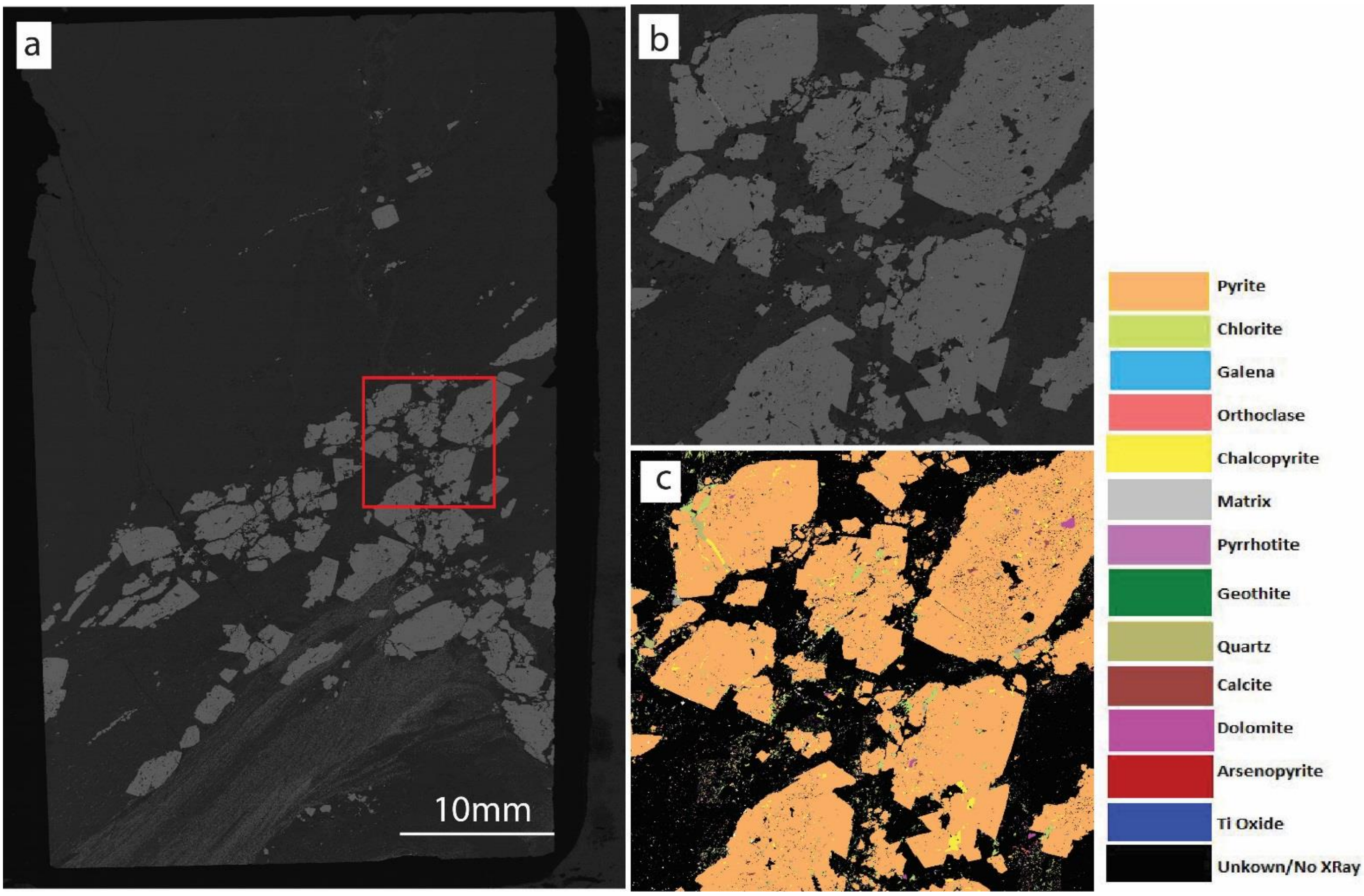

Figure 17 displays BSE images (a & b) for sample TS09, with corresponding MLA analysis for the targeted area (c) displayed on image a. The MLA identified the sample to have numerous sulphide inclusions and over-printing veins. The area displayed in image b and c is the target area selected for further analysis.

LA-ICP-MS

LA ICP-MS data for sample TS11, (Figure 18), identified Cu to be the highest concentration with >2000ppm, occurring heterogeneously throughout the pyrite 2 grains.

Within this sample, it appears that a previous pyrite cores, can be identified using the Co elemental map. The core of the grains appears relatively depleted in Co, when compared to the edges. Due to a malfunction with the ICP-MS, the elemental map for Ba (Figure 18e) has a region of error.

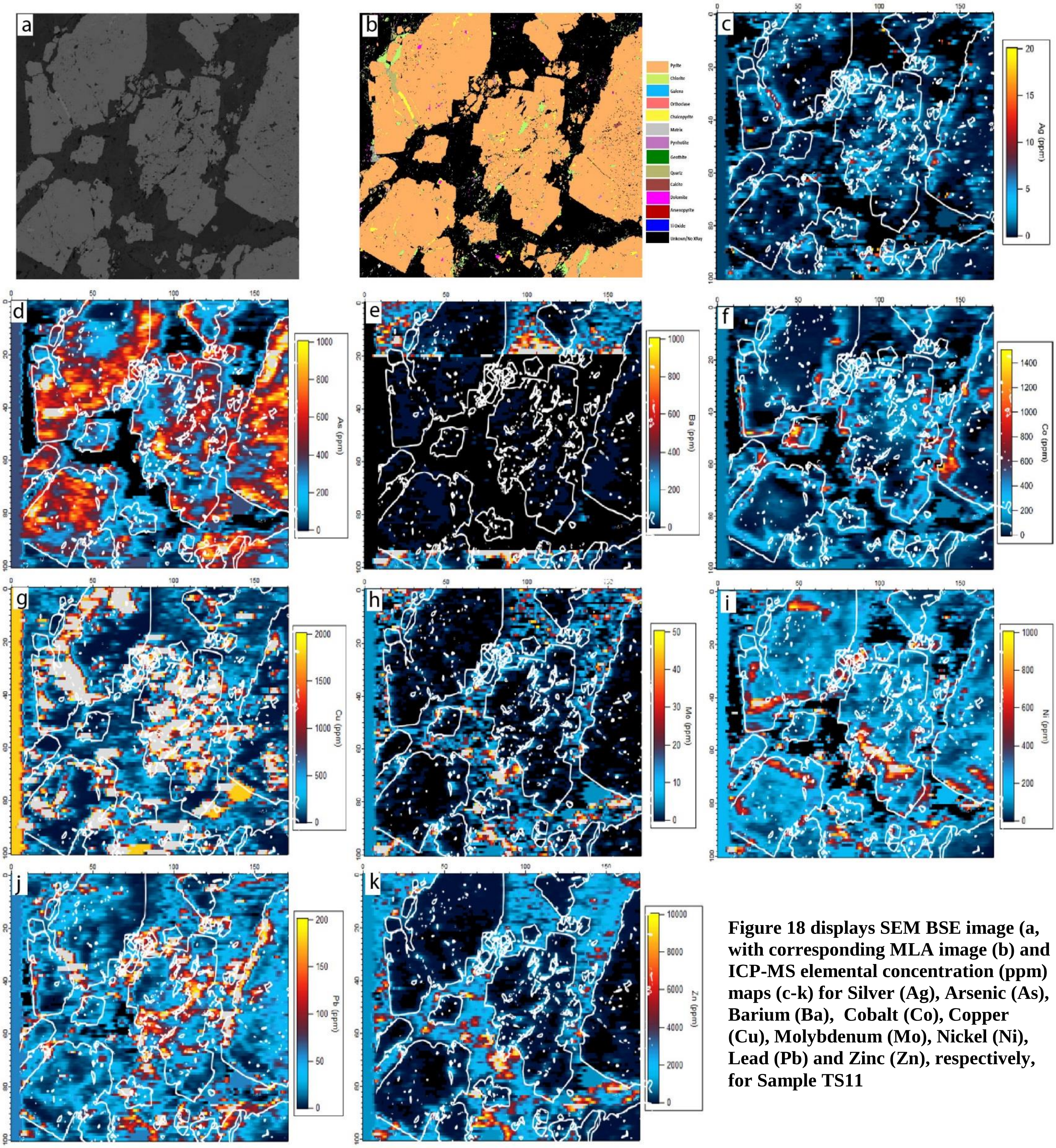

Figure 18 displays SEM BSE image (a, with corresponding MLA image (b) and ICP-MS elemental concentration (ppm) maps (c-k) for Silver (Ag), Arsenic (As), Barium (Ba), Cobalt (Co), Copper (Cu), Molybdenum (Mo), Nickel (Ni), Lead (Pb) and Zinc (Zn), respectively, for Sample TS11

4.5 0406ED2_TS16 (610.7m)

Petrology

Sample TS 16 is hosted within the intensely brecciated shale, within the Urquhart Shale (Figure 19). There are large aggregates of Pyrite 2 crystals, occurring within the sample. The Pyrite 2 occurs within a quartz vein, identified in the petrological image in Figure 19d, and rare pyrite grains broken by quartz were seen within the sample. The Pyrite 2 grains within this sample are significantly larger in comparison to other samples. With some Pyrite 2 grains spanning >200μm (Figure 19c and 19d). No internal zonation or cores were observed during petrological studies of this sample.

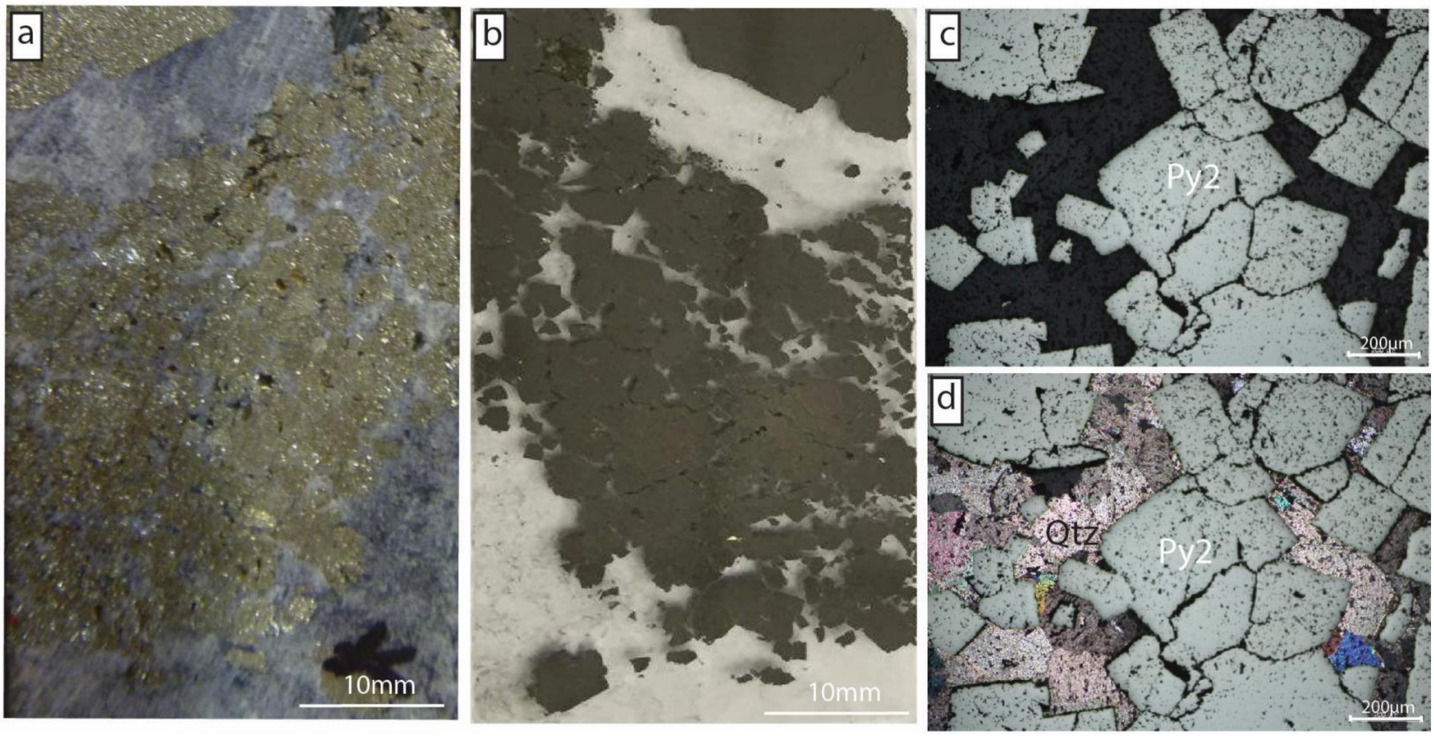

Figure 19 shows the quarter core (a), thin section (b) and petrological images (c-d) from sample TS16, displaying the pyrite 2 association with the intensely brecciated Urquhart shale. Image c & d, display euhedral and cubic Pyrite 2 grains.

SEM/MLA

The SEM/MLA analysis of this sample (Figure 20), shows a singular grain of pyrite that was found to contain quartz, galena and dolomitic inclusion. A grain of chalcopyrite was found on one of its edges, which did not appear to contain zonation or inclusion (Figure 20c).

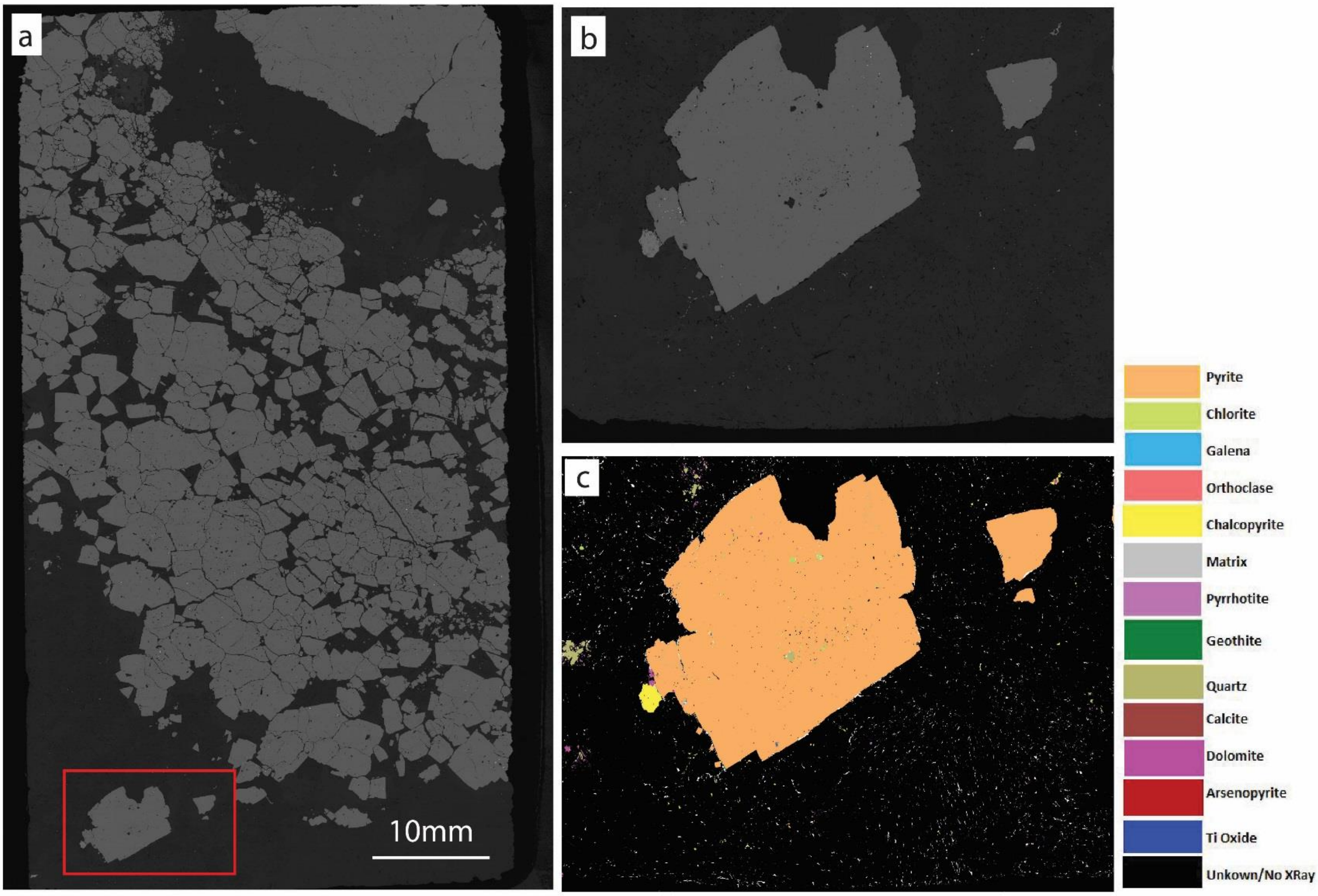

Figure 20 displays BSE images (a & b) for sample TS16, with corresponding MLA analysis for the targeted area (c) displayed on image a. The MLA identified the sample to have minor sulphide inclusions and a piece of chalcopyrite attached to the Pyrite 2 grain. The area displayed in image b and c is the target area selected for further analysis.

LA-ICP-MS

The ICP-MS data collected for this sample, (Figure 21), identifies Pb (Figure 21.j) to have the highest element concentration, with >2500ppm occurring within the Pyrite 2 grain.. The grain, though showing no previous zonation or core, shows a distinct pattern within some of the elemental maps created around the edges of the pyrite grain (Figure 21 d, f and i). This pattern shows potentially the existence of a previous pyrite core. The concentrations for elements appear heterogeneous throughout the sample. The chalcopyrite grain displays association with Ag, (>1000ppm) and Ba (50ppm) which is unlike the Pyrite 2 grain (Figure 21 c and e).

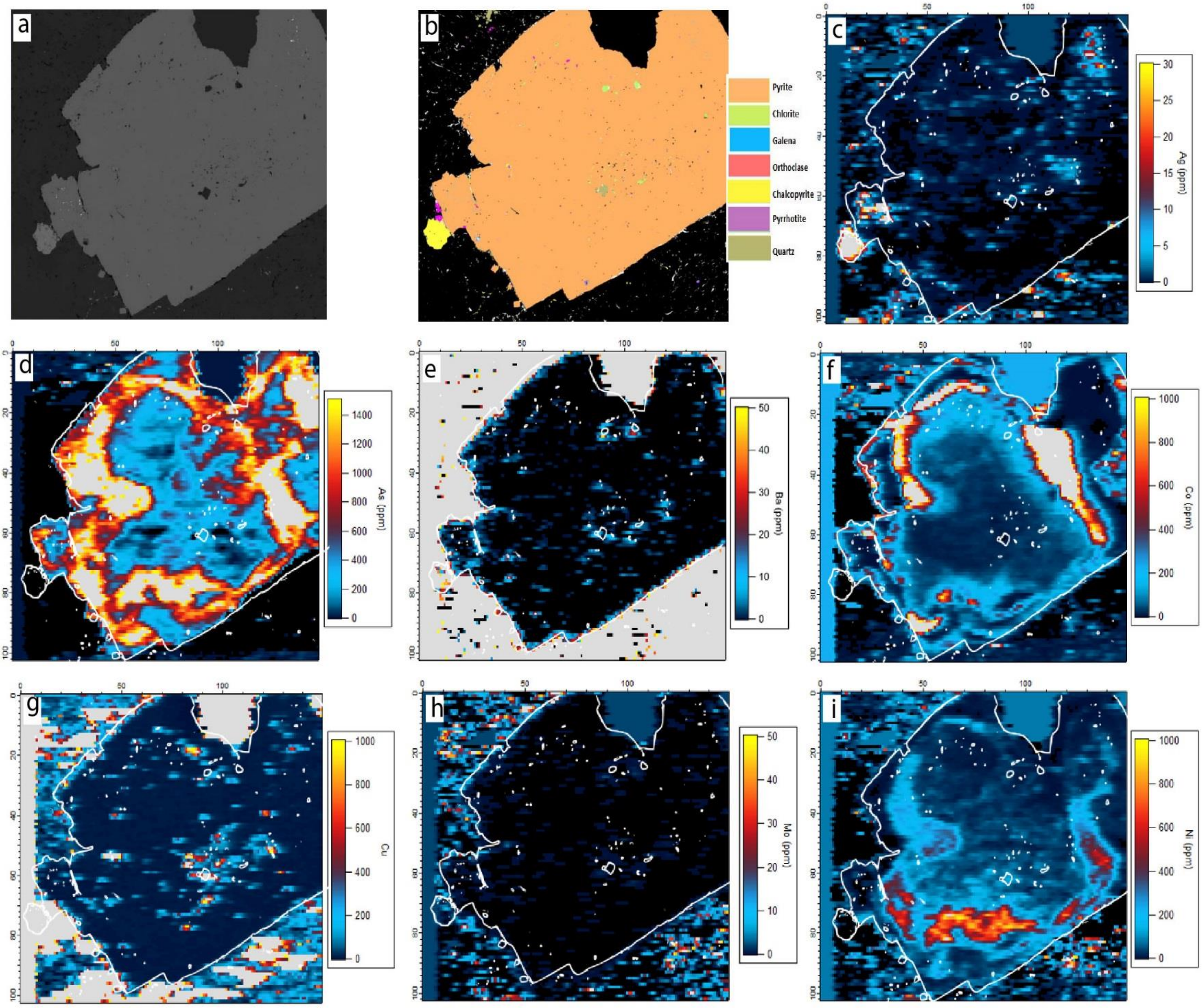

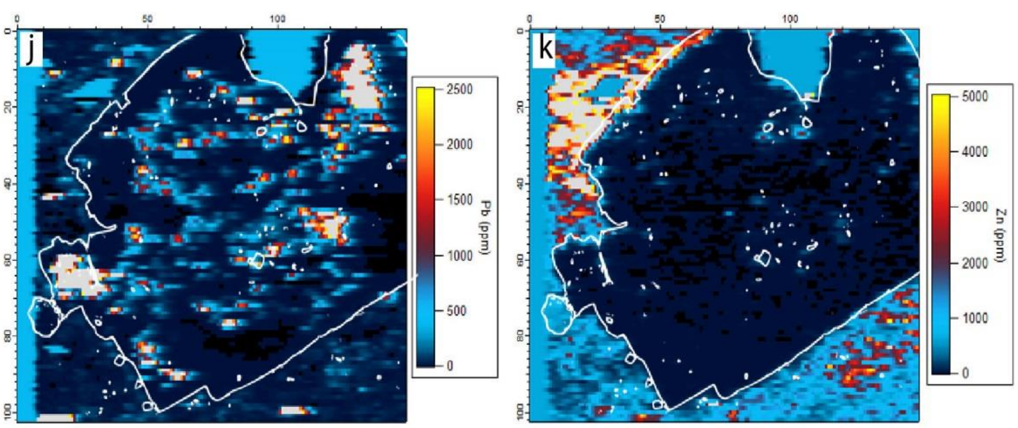

Figure 21 displays SEM BSE image (a, with corresponding MLA image (b) and ICP-MS elemental concentration (ppm) maps (c-k) for Silver (Ag), Arsenic (As), Barium (Ba), Cobalt (Co), Copper (Cu), Molybdenum (Mo), Nickel (Ni), Lead (Pb) and Zinc (Zn), respectively, for Sample TS16

4.6 0406ED2_TS22 (695.4m)

Petrology

Sample TS22 (Figure 22), is hosted within the Urquhart Shale. The sample consists of shale interbedded with Pyrite 1, and Pyrite 2 occurring as a vein, enriched in carbonate and quartz (Figure 22 c-d). The Pyrite 2 within this sample is of similar size to the Pyrite 2 grains identified within TS09.

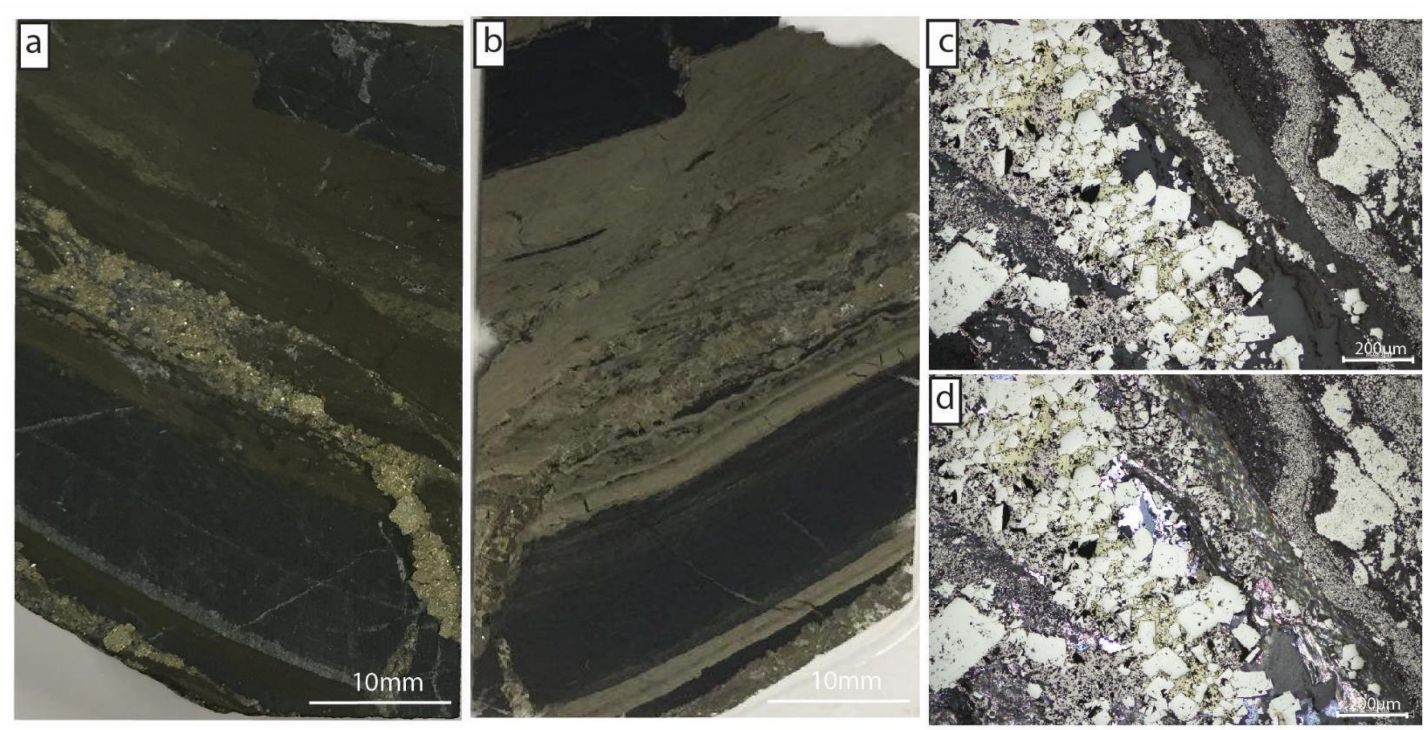

Figure 22 shows the quarter core (a), thin section (b) and petrological images (c-d) from sample TS22, displaying the pyrite 2 association with the Urquhart shale. A significant of shale is present within sample, as well as Pyrite 1 interbedded. Image c & d, display euhedral and cubic smaller grain size of Pyrite 2.

SEM/MLA

The SEM and MLA analysis on this sample, (Figure 23), identified pyrrhotite, dolomite, quartz, chlorite, chalcopyrite, galena and rutile (TiO_2), present within the sample.

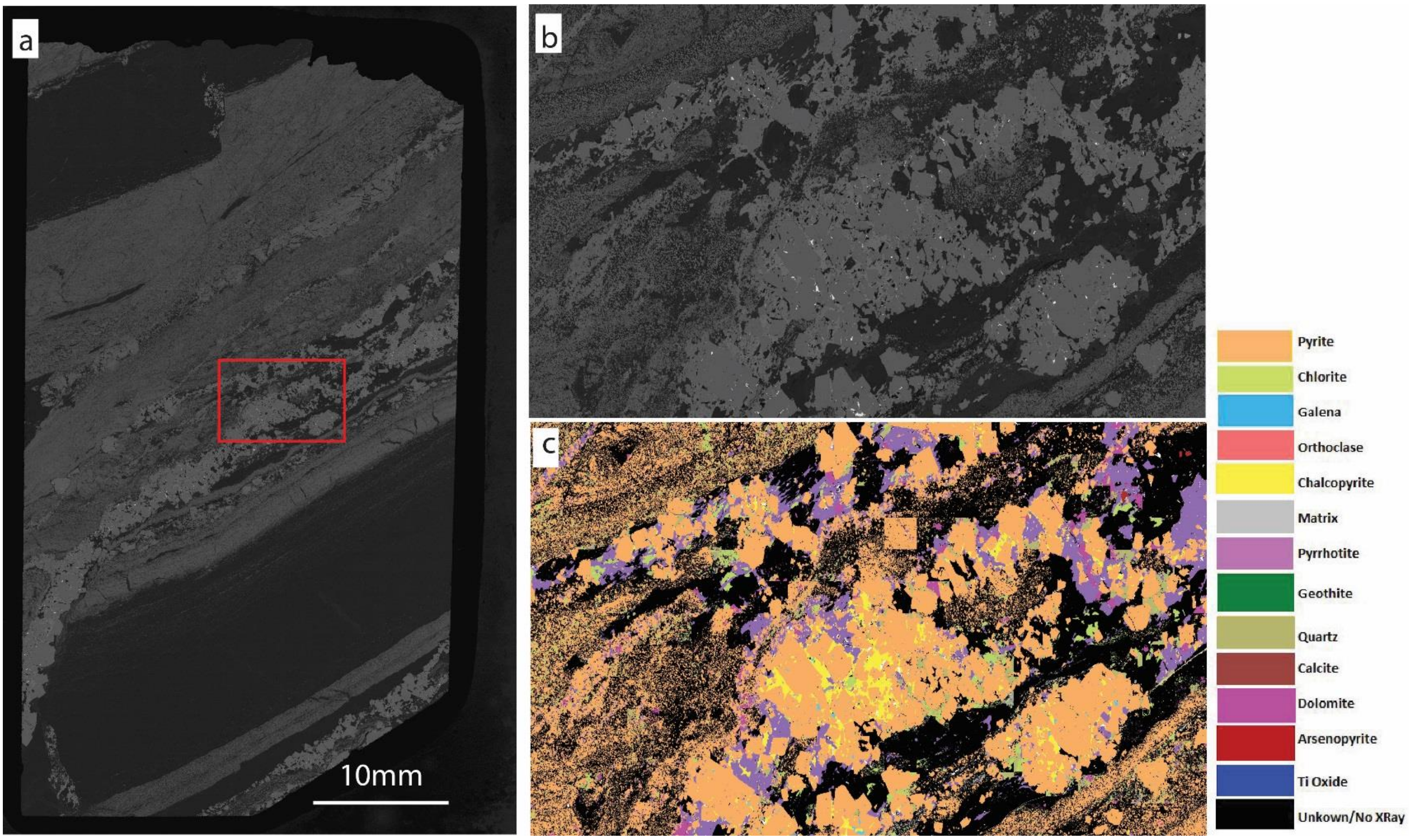

Figure 23 displays BSE images (a & b) for sample TS16, with corresponding MLA analysis for the targeted area (c) displayed on image a. The MLA identified the sample to be enriched in pyrrhotite, chalcopyrite, chlorite, aresnopyrite, and dolomite. The target area identified in image a, is not the targeted area for further analysis. Due to an error on the MLA, the area could not be processed.

LA-ICP-MS

The ICP-MS analysis (Figure 24) identified Cu to have the highest elemental concentration of approximately >300ppm, within the pyrite 2 grains. The variations of size in the Pyrite 2 grains have a different elemental trend, when compared against each other. The ICP-MS malfunctioned on the Cu elemental map, but was not disregarded dude to the high content seen throughout the rest of them map.

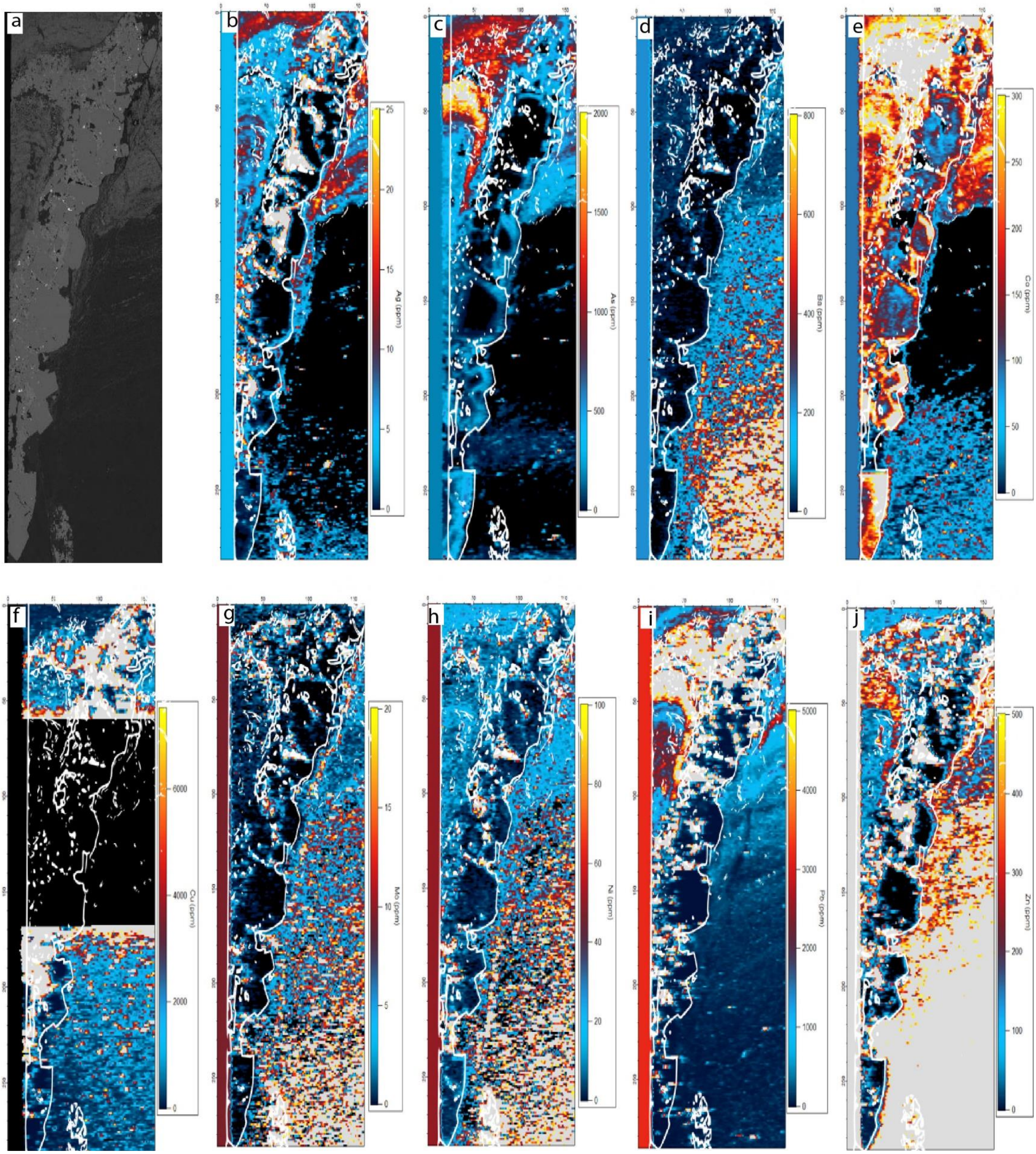

Figure 24 displays SEM BSE image (a), and ICP-MS elemental concentration (ppm) maps (b-j) for Silver (Ag), Arsenic (As), Barium (Ba), Cobalt (Co), Copper (Cu), Molybdenum (Mo), Nickel (Ni), Lead (Pb) and Zinc (Zn), respectively, for Sample TS22. The MLA image for this target area does not correspond to the image in the above result section. The identified area, is indicated on figure 6, and is located at the bottom left hand corner of sample TS22.

5. DISCUSSION

Trace element variation of silver (Ag), arsenic (As), barium (Ba), cobalt (Co), copper (Cu), molybdenum (Mo), nickel (Ni), lead (Pb), and zinc (Zn), was identified in the Pyrite 2 grains within the six representative sample analysed. The trace element variation is not consistent throughout the 0406ED2 transect, with each sample displaying different trace element abundances. This style of heterogeneous variation within the samples is indicative of hydrothermal fluid source of variable composition (Williams, 1998). This supports the interpretation that Pyrite 2, formation and precipitation is associated with a hydrothermal fluid of variable composition. A distinct trend of the elements could not accurately be defined, as each sample displayed various enrichment and depletions in the elements analysed on the micro scale.

The element variation within the Pyrite 2 grains is not apparent when analysed by optical petrology, or SEM and MLA techniques. The variation was only observed when the samples were analysed using the LA-ICP-MS. Cooke *et al* (2013) found this also to be the case, when utilizing the ICP-MS on certain pyrite grains. Elemental maps revealed a subtle chemical zoning pattern that was not visible on the backscatter images produced from the SEM, indicating that this technique may have further application within the Mount Isa system.

Thomas *et al*., (2011) conducted a comparable experiment on pyrite, which determined that generations of pyrite have characteristic trace element patterns which can be used as a proxy for fluid flow events within a system. The trace element variation determined from Pyrite 2 in this study supports a multiple fluid evolution episodes, or an evolving hydrothermal fluid, for the Mount Isa copper system.

A study conducted by Velasquez *et al*., (2014), on pyrite in Venezuela, found that pyrite cores and rims also had different trace element concentrations, such as arsenic enriched cores, with rims of the pyrite grains being depleted. The study determined that successive fluid flow episodes related to reactivation of the shear zone present within the district, caused this trace element variation investigated, such as arsenic, copper, lead and zinc within the pyrite grains during growth. Samples TS11 and TS16, shows a similar core and rim relationship in the ICP-MS elemental maps produced.

Sample TS11 (Figure 18) shows a core of Pyrite 2 grain which is relatively depleted in Co in comparison to the Co enriched rim of the grains (Figure 18f). Similarly in sample TS16 (Figure 21), a core of different composition to the rim is observed. The sample shows a depleted core of As, Co and Ni, in comparison to the enriched rim of the Pyrite 2 grain, suggesting the rim of the grain formed from a fluid that was relatively enriched in these elements (As, Co, Ni).

The core of the Pyrite 2 grains within TS16, display a relatively high concentration (ppm) of Cu, Pb and Zn, relative to the rims. The elevation in the core, suggest that the fluid present at nucleation of this pyrite grain was enriched in Cu, Pb and Zn. For sample TS16, it appears that a fluid enriched in the ore-bearing elements, (Cu- Pb-Zn) occurred at a similar time, or within the same fluid episode. This variation of elements within each sample is determined to be due to a change in the metal abundance of the hydrothermal fluid present within the system (Williams 1998), with the secondary (or more evolved fluid) hydrothermal fluid crystalizing the rim of the pyrite grain.

Studies conducted by Zhang *et al*., (2013) and Zhao *et al.*, (2011) discuss the potential of ore bearing fluids being associated with pyrite grain growths. Zhang *et al.*, (2013) suggest that a variation of pyrite within the study area, were formed during the ore-bearing fluid episode and constrained formation timing due to the rims of the pyrite grains being enriched with ore metal elements. Zhao *et al*., (2011) identifies that pyrite from the same mineralisation stage can display different trace element distributions, and that a single pyrite grain can contain different levels of trace elements, without being in association with a separate fluid.

The inconsistency of the variation throughout the 0406ED2 transect and samples is believed to be linked to pyrite's ability to accommodate trace elements in its crystal lattice (Large, 2014). Trace elements that are loosely held in the internal structure of pyrite are more readily expelled from the pyrite during recrystallization, whereas trace elements which are securely in the pyrite structure, tend to remain and become enriched during metamorphism (Large, 2014). Arsenic is found in relatively high concentrations throughout all samples, this suggests that arsenic, is either securely bonded within the pyrite structure and is not readily lost, or that the fluids which were within the system where relatively enriched in arsenic. Within the six representative samples, molybdenum, was found to be in low concentrations or not to be present, consistent with the rest of the Mount Isa system where molybdenite is a rare accessory mineral. .

Inclusions that were found within the pyrite grains can also help understand the fluid evolution of the Mount Isa copper system. Velasquez *et al*, (2014) suggests that the inclusions within the pyrite grains are considered to be trapped aliquots of the fluids circulating during growth of the pyrite grains and specifically the pyrite rims. In sample TS11 and 22 we see several inclusion and veins within and surrounding the Pyrite 2 grains. These inclusions include chlorite, galena, chalcopyrite, pyrrhotite, aresnopyrite, and dolomite. This suggests that the circulating fluid at the time of formation of the Pyrite 2 grains was enriched in lead, copper, arsenic, and iron. This supports the previously discussed idea that the Pyrite 2, formed during or in close association with the main ore stage fluid (Gregory *et al*., 2015).

Pyrite 2 is found to occur in both the Urquhart Shale and the Kennedy Spear Siltstone lithological units and is not bound to a single unit, in contrast to Pyrite 1. This is similar to the results of a study conducted by Thomas *et al*, 2011, at Bendigo. This study determined that various generations of pyrite, including hydrothermal and metamorphic-hydrothermal pyrite, were not confined to any lithology, unlike the sedimentary pyrite within the system. As seen in sample TS03, which is hosted in the Kennedy Spear Siltstone, Pyrite 2 occurs outside of the shale and across two lithologies within the Mount Isa system. The distinguishable trace element difference between the Pyrite 2 grains associated with the Kennedy Spear Siltstone, is the elevated As (20,000ppm) content, when compared to the Urquhart samples.

There are five elemental maps, TS03 – Co & Ni, TS05 – Co, TS11 – Ba and TS22 – Cu that show an area where no data was collected. This is due to the ICP-MS malfunctioning during data collection. Each of these images appears to have elevated concentrations on the edges of the unrecorded area. It is unsure if these areas of elevation are genuine or are false positives from the ICP-MS. They have been included within the samples and study, as it was not all the sample that was damaged and information was still collected from the non-damaged regions. Specifically in regards to sample TS03 (Figure 8), in which high concentrations of Co and Ni are seen to occur through the centre of the Pyrite 2 grain.

6. CONCLUSIONS

- Petrological and SEM/MLA analysis did not identify any textural or chemical zonation or variation within Pyrite 2 grains.
- LA-ICP-MS analysis identified zonation and trace element variation within the Pyrite 2 grains within the 0406ED2 transect.
- The trace element variation is not consistent throughout the 0406ED2 transect and does not appear to be controlled by host lithology.
- Geochemical data is consistent with the interpretation that Pyrite 2 grains formed during or in close association with the ore bearing fluid, as indicated by previous paragenetic studies.
- Variation in Pyrite 2 core and rim abundances of elements including Co, As, Cu, Pb and Ni, are consistent with the interpretation that the chemistry of the hydrothermal fluid varied during precipitation.
- It is believed that this variation may represent multiple hydrothermal fluid events, from an evolving hydrothermal fluid within the Mount Isa system during

the formation of Pyrite 2 and that these fluids contained different abundances of elements.

- Inclusions in the Pyrite 2 grains indicate that the fluid at time of formation was enriched in lead, copper, arsenic and iron.
- Pyrite 2 is hydrothermal in origin.

7. ACKNOWLEDGMENTS

Firstly I would like to say a huge thank you to Dr Richard Lily, for his knowledge, support and guidance throughout the year. You've been fantastic. I would also like to thank Mount Isa Mines Resource Department for funding and enabling the completion of this project, in particular everyone in MICO and Exploration Team and fieldies who helped during field work, core logging and sample collection. Your support, information and knowledge was incredible. My uttermost gratitude goes to Aoife McFadden, at Adelaide Microscopy, your expertise and ability to answer all of my annoying questions regarding data collection and processing was incredible. I cannot forget to thank Katie Howard, for all her amazing work, she has done this year, you handled all of my meltdowns and crazy moments spectacularly. This year would not have been the same without my honours cohort and my amazing amigos, Adrienne and Maria, who made every single task, field trip, late night and stressful moment manageable and fun. Thanks for making the year amazing and full of laughter and tomfoolery.

8. REFERENCES

BLAKE, D. H., 1987. Geology of the Mount Isa Inlier and environs, Queensland and Northern Territory. *Department of Resources and Energy; Queensland and Northern Territory Bureau of Mineral Resources*, Bulletin 225.

CONAGHAN, E. L., HANNAN, K. W., TOLMAN, J., 2003. Mount Isa Cu and Pb-Zn-Ag deposits, NW Queensland Australia. *CRC LEME*. 1-3.

COOK, N. J., CIOBANU, C. L., MERIA, D., SILCOCK, D., & WADE, B., 2013. Aresnopyrite-Pyrite Association in an Orogenic Gold Ore: Tracing Mineralization History from Textures and Trace Elements. *Economic Geology* **108**, 1273-1283.

DAVIS, D. P., 2004. Mine-Scale Structural Controls on the Mount Isa Zn-Pb-Ag and Cu Orebodies. *Economic Geology* **99**, 543-559.

GEOSCIENCE AUSTRALIA, 2016, 'Geology of the Mount Isa Inlier and environs Queensland and Northern Territory',

GREGORY, D. D., LARGE, R. R., HALPIN, J. A., BATURINA, E. L., LYONS T. W., WU, S., DANYUSHEVSKY, L., SACK, P. J., CHAPPAZ, A., MASLENNIKOV, V. V., & BULL, S. W., 2015. Trace Element Content of Sedimentary Pyrite in Black Shales. *Economic Geology,* **110**, 1389-1410.

GRONDIJS, H. F., & SCHOUTEN, C., 1937. A study of the Mount Isa ores. *Economic Geology* **32**, 407-450.

KOGLIN, N., FRIMMEL, H. E., MINTER, L., & BRATZ, H., 2010. Trace-element characteristics of different pyrite types in Mesoarchean to Paleoproterozoic placer deposits. *Miner Depsita*, **45**, 259-280.

LARGE, R. R., HALPIN, J. A., DANYUSHEVSKY, L. V., MASENNIKOV, V. V., BULL, S. W., LONG, J. A., GREGORY, D. D., LOUEJEVA, E., LYONS, T. W., SACK, P. J., MCGOLDRICK, P. J., &CALVER, C. R.,

2014. Trace Element content of sedimentary pyrite as a new proxy for deep-time ocean-atmosphere evolution. *Elsevier: Earth and Planetary Science*, **389,** 209-220.

LONG, R. D., BLENKINSOP, T. G., OLIVER, N. H. S., 2010. The formation of the Mount Isa copper ore-bodies, NW Queensland – a new paragenesis based on macroscopic structural elements. *Unpub*, Ph.D Thesis, James Cook University

MATHIS, B. V., CLARK, G. J. 1975. Mount Isa copper and silver-lead-zinc orebodies – Isa and Hilton mines. *Economic Geology: Australia and Papua New Guinea* **1**, 351-372.

MCGOLDRICK, P., & LARGE, R. 1998. Proterozoic stratiform sediment-hosted Zn-Pb-Ag deposits. *Journal of Australian geology & Geophysics,* **17**(4), 189-196.

CONNELL, S., 2016. Distribution of Pyrite within the Mount Isa Copper System; Geological and Structural controls. *Unpub*, Honours Thesis, University of Adelaide

PAINTER, G. M., 2003. The geochemical and Mineralogical Haloes around the Mount Isa Base Metal orebodies. *Unpub* Ph.D. Thesis, University of Queensland

PAINTER, G. M., GOLDING, S. S., HANNAN, K. W., & NEUDERT. M. K., 1999. Sedimentological, Petrographic and Sulfur Isotope Constrains on Fine-Grained Pyrite Formation at Mount Isa Mine and Environs, Northwest Queensland, Australia. *Economic Geology,* **94**, 883-912.

PERKINS, W. G., 1990. Mount Isa copper orebodies. *Geology of the Mineral Deposits of Australia and Papua New Guinea*, 935-941.

PERKINS, W.G., 1996. 'A study of the nature, timing and processes in the Mount Isa lead-zinc orebodies; their relationship to adjacent copper ore-bodies and the lead-zinc systems at McArthur River, Hilton and Mount Novit'. *Unpub*, Ph.D. Thesis, James Cook University

PERKINS, W.G., 1996. 'Timing of formation of Proterozoic Stratiform Fine-Grained Pyrite: Post-diagenetic Cleavage replacement?' *Unpub*, Ph.D. Thesis, James Cook University

PERKINS, W. G., 1998. Timing of Formation of Proterozoic Stratiform Fine-Grained Pyrite: Post Diagenetic Cleavage Replacement at Mount Isa? *Economic Geology,* **93**, 1153-1164.

ROBERTSON C. W., 1982. The Role f Pre-exiting Sulphides in copper-Ore formation at Mount Isa, Queensland. *Journal of Australian geology & Geophysics,* **7**, 119-124.

SOLOMON, P. J., 1965. Investigations into Sulfide mineralization at Mount Isa, Queensland. *Economic Geology* **60**, 737-765.

TAYLOR, R. G., 2016. Petrological and overview comments concerning 10 samples from the Mt Isa copper operations projec. *Unpub*, MICO-PCP. 1-34

THOMAS, H. V., LARGE, R. R., BULL, S. W., MASLENNIKOV, V., BERRY, R. F., FRASER, R., FROUD, S., & MOYE, R., 2011. Pyrite and Pyrrhotite textures and compositions in Sediments, Laminated Quartz Veins, and Reefs at Bendigo Gold Mine, Australia: Insights for Ore Genesis. *Economic Geology*, **106**, 1-31.

VAN DIJK, P. M., 1991. Regional Syndeformational Copper Mineralization in the Western mount Isa Block, Australia. *Economic Geology,* **86,** 278-301.

VELASQUEZ, G., BEZIAT, D., SALVI, S., SIEBENALLER, L., BORISOVA, A. Y., POKROVSKI, G. S., & PARSEVAL, P, D., 2014. Formation and Deformation of Pyrite and Implications for Gold Mineralization in the El Callao District, Venezuela. *Economic Geology*, **109**, 457-486.

WARING, C. L., HEINRICH, C. A., & WALL, V. J., 1998. Proterozoic metamorphic copper deposits. *Journal of Australian geology & Geophysics,* **17**(4), 239-246.

WILDE, A. R., 2011. Mount Isa copper orebodies: Improving predictive discovery. *Australian Journal of Earth Science,* **58**(8), 937-951

WILDE, A. R., JONES, P. A., GESSNER, K., AILLERES, L., GREGORY, M. J., & DUNCAN, R. J., 2006. A Geochemical Process Model for the Mount Isa Copper Orebodies. *Economic Geology,* **101**, 1547-1567.

WILLIAMS, P. J., 1998. An Introduction to the Metallogeny of the McArthur River-Mount Isa-Cloncurry Mineral Province. *Economic Geology*, **93**, 1120-1131.

WITHNALL, I. W, & CRANFIELD, L. C., 2013. Geological Framework. *Queensland Minerals*.

ZHANG, K., LI, H., 2014. Migration of Trace Elements in Pyrite from Orogenic Gold Deposits: Evidence from LA-ICP-MS Analyses. *Acta Geologica Sinica*, **88**(2), 841-842.

ZHANG, J., DENG, J., CHEN, H. Y., YANG, L. Q., COOKE, D., DANYUSHEVSKY, L., & GONG, Q. J., 2013. LA-ICP-MS trace element analysis of Pyrite from the Chang'an gold deposit, Sanjiang region, China: implication for ore-forming process. *Elsevier: Gondwana Research*, **26**, 557-575

ZHAO, H. X., FRIMMEL, H. E., JIANG, S. Y., & DAI, B. Z., 2011. LA-ICP-MA trace element analysis of Pyrite from the Xiaoqinling gold district, China: Implications for ore genesis. *Elsevier: Ore Geology Reviews*, **43**, 142-153.

9. APPENDIX A: CORE LOG SPREADSHEET

Appendix A, displays the detailed spreadsheet, created for the core logging process of he 0406ED2 transect, at Mount Isa mines, in March 2016.

	m	Structure	Lithology	Mineralisation	Geological Comments (Minerals, textures, paragenesis, bedding, vein systems, deformation events)	Alteration	Veining	Mineral Presence					
								Qtz	Dol	Pyrr	FG Pyr	CG Pyr	Cpy
98.4-396.6m	98.4	massive	Kennedy Spear	py/Dol	Massive unit, bedding difficult to determine, appears to be coarse, sillification varies throughout, seeing large veins/alteration	dol	sill/dol						
	121.7	massive			gradational section; more finely bedded, fault and shear zone, w/ varying sillification								
	133	massive			start seeing appearances of coarse grained sulphides								
	150	fault zone			end of gradational section. Fault/shear zone. **BOUNDARY**								
	150-153	Massive		pyr	lighter in colour, more carbonaecous rich, moderate silification (varying in some places). Seeing coarse grained pyrite; cubic following fracture and shear + veins.	dol	sill/dol						
	153-156			dol	pyrite disappeared, back to massive bedded unit								
	156-163			dol	seeing more dominate dolomitic veining	dol	dol						
	163-166				darker section of unit, soft-mod sillification, bedding still unlear								
	168				mixture of light and darker massive unit, section cut into half core								
	176-180				pyrite is back within unit (pyrite-2)edding still not distinguishable, not large pyrite crystals, but clearly pyrite 2	dol	dol						
	180-192			py/dol	small viens, minor pyrite-2 and chaclopyrite	dol	sil/dol						
	192-205				seeing more intense veining, pyrite-2 within vien, not fully infilled with Chalc	dol	sill/dol						
	205-206	fault zone			fault zone, with similar lithology as above section.	dol							

	208-225			dol	back to full core samples, soft in sillification, bedding fabric becoming more apparent (S0), lack of sulpides, dolomitic veining		dol
	225-243	slight bed		py/dol	sulphides back, pyrite-2 + Chalc, in veins and parrellel to bedding	dol	dol
	243-300	slight bed			veins intensifying an dregualrity increasing	dol	dol
	254-260	slight bed		py/pyrr/dol	Pyrrotite seen, pyrtie-2 within dolomtic veins	dol	dol
	300 - 344	bedded			seeing distinct bedding, scour and fill structures. Veins are overprinting bedding, see small clumps of sulphides in veins, rather than being major infill	dol	dol
	347-363.5	bedded			core in half core sections, less sillified, and seeing sulphides in veins becoming more apparent	dol	dol
	363.5 -370	bedded			shale becoming more noticeable within lithology. Or more bedded, potentially in sillicaified shale? Sulphides present, some following bedded foliation and over print (S2) fabric??	dol	dol
	370-396.6	laimation			lamination texture occurring, unit is not as amssive, core is fracture/breaking into smaller sections/pieces, sulphides apparent	dol	dol
	396.6 - 397.8	bedded	sulphide	Pyrite	Massive Sulphide section. Full of fine-grained pyrite (pyrtie-1), pyrite-2 within veins, pyrrohitie present in viens w/ C.G pyr **PYRTIE RIB**	py/dol	dol/py2infill
397.8-717.3	397.8 - 401.1	bedded	Urquhart Shale	pyrite-2	within bedded shales, have veins of pyrite 2, followin bedding and then some overprinting and following S2 fabric, large Pyrrotite vein (S0) fabric	py/dol	dol/py/pyr
	401.1 - 404.2	bedded		pyrtie-2	beeded pyrite 2 over pritning more frequently in both S0 and S2 direction. Seeing dolomitic veining	dol	dol
	404.2 - 407.4	bedded		py2/dol	pyrrohitie in dolomitic veins S2 fabric. High intensity of S2 overprinting veins(dol+pyr+pyrr+cpy), variation of sillification	dol	dol
	407.4 -411.	bedded		py/2dol	lovely bedding planes within shale, pyrite-1 beds w/ pyrite2+pyrr in bedding planes, as well as S2 (overprinting), late pyrr vein (no trend)	dol	dol
	411.9 - 415.9	bedded		py/pyrr	bedded shale w/ pyrite 2 parraleel to bedding throughout, see crossscuting vien with pyr-2+cpy infill, large pyrr section (15cm)	dol	dol
	415.9 - 420.1	bed/brec		py2	seeing brecciated section, within shale, bedding is still apparent, not much pyr-1, pyr-2 in bedding with cubic strucutres following foliation	pyr	silla
	420-1-424.3	brec/bed		py2	vein instensly, sillica and dol rich, not following any orientation - stockwork- Pyr-2 within, someitmes as infill, others is full vein, bedding distincitve @421.5, pyr-2 parallel in veins, cubic	dol/silla/py	sill/dol/py
	424.3 - 428.4	bedded		py/dol	see consitent shale litholgy, some vein, minor intensity, shale variation from lgith to dark, pyr+cpy in veins		

	428.4 - 432.7	bedded		py/dol	bedded chales w/. Pyr-2 parrallel to bedding occasionally. Also seeing overprinting of veins w/. Pyr-2+cpy infill, start seeing deformation - shear sense	dol/pr	dol/py						
	432.7 - 436.6	bedded		py/dol	beded shales, varying light and dark, odd layer of pyr-2-bedding parrallel +/- pyrr in some. See 4x viens 90' to bedidng, pyr-2 infill in dolmitic vein	dol/py	dol/py						
	436.6 - 440.7	bedded		py2	bedding consitent, thin beds of pyr-1 and pyr-2, see pyr-2 overprinting within dol vien - vuggey texture (created void)	py	dol/py						
	440.7 - 444.5	bedded		py2	bedded shale, w/ pyr-2 overprinting 90' to bedding. Singualr crystlas, and then with bedding folaition, pyr-1 showing signs of deformations	py	dol/py						
	444.5 - 448.5	bedded		py2/dol	larger beds of pyr-1, some pyr-2 parrallel to bedding, dolomtic veins very dolomitic evidence of displacement	py	dol/py						
	448.5 - 452.9	bedded		py2/dol	thinly laminated, fault/dhearing occuring, graphitic textures, flame structres in pyr-2, pyr-1 overprinted by cpy+pyr-2, dol veins present -thin	py/dol	dol/py						
	452.9 - 461.1	bedded		py	bedded shale >1cm-5cm, interbedded pyr-2 parallel to bedding, pyr-2 in dol veins also +/- cpy, dol veins overprinting/cross cuts beds and veins	dol	dol/py						
	461.1 - 471.5	bedded		py	pyritic bedded shale, up to 5cm wide, veining increasing in width+length+intensity, pyr-2 infill	sills/doll	dol						
	471.5 - 477.5	fault/shear		py2/gph	fault zone (graphitic) large beds (20cm)+small beds(lamination) lots of pyr-1 beds +laminations, dolomitic veins with pyr-2	py2	dol						
	477.5 -490	bedded		py2/dol	bedded shales, with interbedded pyr-2 ONLY, cubic crystals and in dolomitic veins. Large dolomitic vein (~50cm long)w/. Pyr-2 infill	py2	dol/py						
	490-502.5	bedded	Urquhart Shale		bedded shales, light great -> more carbonearous, thinly bedded, large sulphide layer (~40cm length), pyr-1 w/ pyr2 parallel, dolomitic veins cross cutting bedding(smaller)	py2/dol	dol/py2						
	502.5 - 561.5	bedded		py2	intense dolomitic veining -> stock work, consistently bedded shales, pyr-2 parallel, but majority is over printing, vugs in dol veins, increasing bed width, small fault @ 514.6	py/dol	dol						
	516.5 -522	faults/folds		py2/dol	deformation - increased bedding with not consistent orientation, folding? Stock work veining, vuggy clasts of dol, late veining of py	py/dol	dol						
	522-542.3	shearing/breccia		py2/dol	pyr-2 vug + overprinting. Seeing sheared shales- graphitic, pyr-2 following foliation some overprinting, back to normal shales, to brecciated shales w/ dol+pyr-2 veins-vugs	py/dol	dol						
	542.3 - 550.5	bedded		py	bedded sulphides - relatively consistent with shale bedding, bit of deformation, mainly pyr-2, small amounts pyr-1. dol veins, only small pyr-2 infill - chick wire texture	py	dol						

	550.5 - 554.5	bedded		py	interbedded shales and siltstones, lighter grey in colour, pyr-2+dol veining,	py	dol						
	554.5 -581	bedded		py2	interbedded shales; weakly pyritic, pyr-1+2 in foliation, small mounts of pyr-2 overprinting (cubic+blob crystals), increasing dolomitic stock work, + Cu Grade	py	dol						
	581- 600.4	brecciated		pyrite	Remnant shale bedding at beginning. Increasing breciation+Cu Grade, pyr-1 in beds, pyr-2 recrystallization in beds + over printing, increasing cpy abundance	py/dol	doll/silla						
	600.4 - 609.8	brecciated		py2	not as brecciated, more graphitic, seeing shale bedding, stock work dol veins, large amounts of overprinting pyr02, only few pyr-1 beds, high intensity deformation, increase in cpy	py	dol/silla						
	609.8 - 615.8	brecciated		cpy	recrystallised shales w/ dol+silla stock work veins, pyr-2 S2 +overprinting(cubic), increasing cpy,	py/dol	dol/silla						
	615.8 - 612.7	bedded		py2	back to shales, bedding consistent. Dol veins, stock work -overprinting w/ pyr-2, cpy in/surrounding dol vein, some pyr-1 in shale beds	py2/dol	dol						
	621.7 - 626.1	breccia		cpy	Recryst dol shales, cpy abundant/dominate, not much pyr-1or -2, stock work veins/fractures, minor pyr-2	dol	dol						
	626.1 - 637.6	Breccia		cpy	Breccia zone with some bedded shales in sections. Dominantly cpy(2-4%), which is over printing, small amounts of pyrr	py/dol/silla	dol						
	637.6 - 646.4	breccia		py/cpy	transition back to shales, darker comp, consistent bedding, see pyr-1 returning-thicker beds, pyr-2 following beds+overprinting, qtz+dol veins, Qtz following foliation	py/dol/silla	dol/silla						
	646.4 - 653.3	bedded		py	lighter shale- more carbonaceous, bedding still consistent, big decrease in cpy, thicker pyr-1 beds, pyr-2 bedded and over printed, graphitic in texture	dol	dol						
	653.3 - 659.3	bedded		py/cpy	mass sulphide section, brecciated py, massive pyr-1(~10cm), transition back to pyritic shale-reworked zone, laminated pyr-1,pyr-2 over printing+bedded +/- cpy	dol/py/cpy	dol						
	659.3 - 663.5	bed/breccia		py/cpy	dolomitic bedded shales, cpy rich, pyr-1 throughout-slightly deformed=>fault-displaced, moving into brecciated hosted section, pyr-2 some over printing, bedded		dol						
	663.5 - 667.9	bed/fault		cpy/py	bedded shales w/. Pyr-1, cpy-over printing, fault zone, 664.9-666.5, highly broken, crumbs. Large Qtz vein through fault Then back to bedded shales	silla/dol/cpy	dol/silla						
	667.9 - 678.5	bedded		cpy/py/dol	shales w/ interbedded pyr-1+-2, dolomitic shale, inter-zone of dolomitic alt within, cpy coming back-more dominant	dol	dol						
	678.5 -687	bedded		py/dol/cpy	transition zone btwn shale dominant zone to pyritic shale zone, dol veins, pyr-1 bedded, pyr-2 bedded+overprint. Minor faulting in sections ~>10cm width	dol	dol						
	687- 715.2	bedded		pyrtitic	pyr-1 dominated shale, pyr-2 in bedded folliation+overprint, sections of recrystallised dol shales, deformation -folding, large fault zone (~2m, 692-694)	dol	dol/sillia						

					sections of shale dominated ->dolomitic veins, large qtz veins (706.8-707.3m), faulting-graphitic, overprinting of dol veins throughout								
	715.2 - 717.3	bedded		pyritic	bedded pyrites w/ pyrrotite+sphalerite, no dolomitic veins, only pyr-1								

9.2 APPENDIX B: SAMPLE LOG SPREADSHEET

Appendix B, displays the detailed spreadsheet used and created for the 24 samples collected from the 0406ED2 transect, at Mount Isa Mines, in March 2016.

Sample no#	m	tray	Structure	Lithology	Mineralisation	Geological Comments (minerals, textures, paragenesis, bedding, vein systems, D-events)	Veining	Mineral Presence					
								Qtz	Dol	Pyrr	Py1	Py2	Cpy
1	155	45	siltstone		py	py2 within siltstone. Cubic shaped crystals, overprinting. Don't see pyr-1.	py2						
2	236.5	72	siltstone		py/cpy	py2+cpy is infill in dol vein. Py2-over-printing as S2 fabric	py2/cpy						
3	255.5	78	siltstone		py	py2 vein in S2 direction, over-printing, +/- pyrr, is vein, but no dol	py2						
4	346.2	106	siltstone	Kennedy Spear	py	py2 vein in S0 fabric (bedding foliation	py2						
5	397	122	Bedded sulp.	mass sulphide	py	massive bedded sulphide unit, within is py2 vein as cubic crystals, following py1 foliation/bedding	py2						
6	418.6	129	silt/bedded	transition	py	py2 as infill in dol vein, maybe recrystallised pyr-1 into py2 that is parallel to bedding, see cubic crystals-stock work veining	py2/dol						
7	442.2	135	bed/folded		py	py2 veins, parallel to bedding, in pyr-1 beds within shale. Deformation occurring - folding	py2						
8	445.2	136	bedded		py	py1+2 interbedded within shale, seeing some dol veins	py2						
9	468.8	141	bedded	Urquhart Shale	py/cpy/dol	py1+2 within shale. Py2 occurring parallel + overprinting +/- cpy - seeing vugs within py2	py2/dol/cpy						
10	491.3	147	bedded		py	inter-bedded py1+2 within pyritic enriched shales; py2 parallel	py2						
11	512.8	152	bedded		py/dol	py1+2 within stock work zone - dol, py2 cubic - not following bedding	pyr-2/dol						

12	530	156	bedded		py	p2 parallel and overprinting bedding. No cpy present py2 seen as cubic, sometimes singular crystals	py2						
13	549.2	161	bed/fault		py	py1 beds, py2+cpy overprinting. Within bedded sulphide zone, beds slightly deformed-fault/shearing? Stock work veins	py2/cpy						
14	562.4	165	bedded		py/dol	py1+2 bedded within shale. Py2 also overprinting. Potentially py2 replacing py1, +/-cpy, near shear zone	py2/dol						
15	583.6	170	bed/brec		py/dol	py1 bedded, with py2 +/-cpy within semi brecciated zone	py2/cpy/dol						
16	610.7	177	recryst.shale		py/dol	py2 in recrystallised shale, in breccia zone, don't see py1. (transition halo)	py2/dol						
17	629.8	182	brec/shale		py/dol	py1 thin bed, py2 scattered throughout, breccia zone, cpy within zone	py2/dol						
18	650	186	bed/brec	shale/brecc	py/dol	Py1/2/cpy. Contact between brecciated and shale	py2/dol						
19	653.8	187	breccia		py/dol	Brecciated mass sulphide zone in shale unit. Pyr-1/2 bedded/deformed. +/-cpy	py2/dol						
20	654.8	188	sulphide		py	massive sulphide zone, abundant pyr-1 bedded, w/ pyr-2 in foliation + over printing	py2						
21	669.2	191	bed/breccia		py/dol	py1 with py2 within shale	py2						
22	695.4	198	sulphide		py/cpy	mass bedded sulphide zone, py1/2 with interbedded shale	py2						
23	712.9	202	bed/sulph	mass sulphide	py/dol	End of massive sulphide section, py1/2bedded/brecciated slightly. Py2 also overprinting	py2						
24	716.8	203	bedded	Urquhart Shale	py/pyrr/sphal	EOH. Pyritic bedded shales, py1/2 bedded parallel, py2 also over printing	py2/pyrr						

9.3 APPENDIX C: 0406ED2 SAMPLE COLLECTION

Appendix C, displays the 24 samples selected from 0406ED2 transect, in full (where applicable), half and quarter core form, prior to thin section construction.

Drill core ID: 0406ED2
Length: 717.3M

Sample No #	Sample Photos	Sample description
1	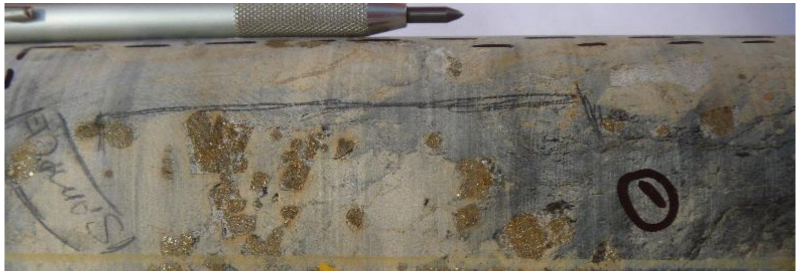 Full core 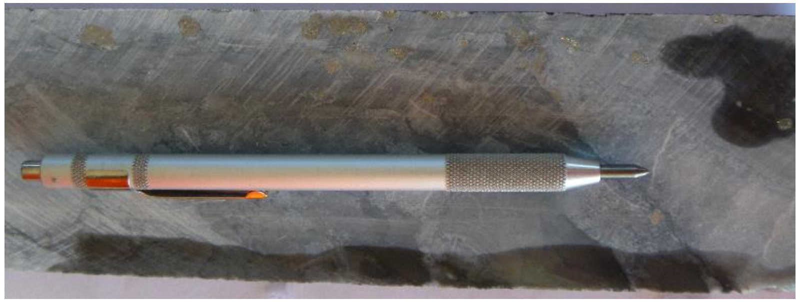 Half core	Shows Coarse grained pyrite in Kennedy Spear lithology. Notable we do not see fine-grained pyrite in this section. See cubic shaped crystals of Pyrite, overprinting. (Tray 45, @ 155m)

	Quarter core 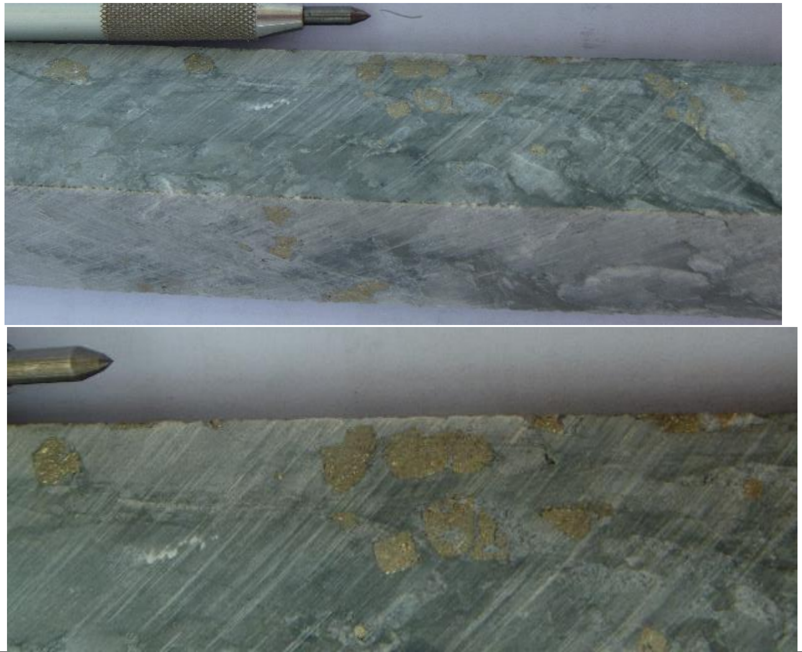	
2	 Full Core	Coarse –grained Pyrite and Chalcopyrite infill in dolomitic vein, within Kennedy Spear lithology. Coarse-grained pyrite is (S_2) overprinting lithogies

	Half Core 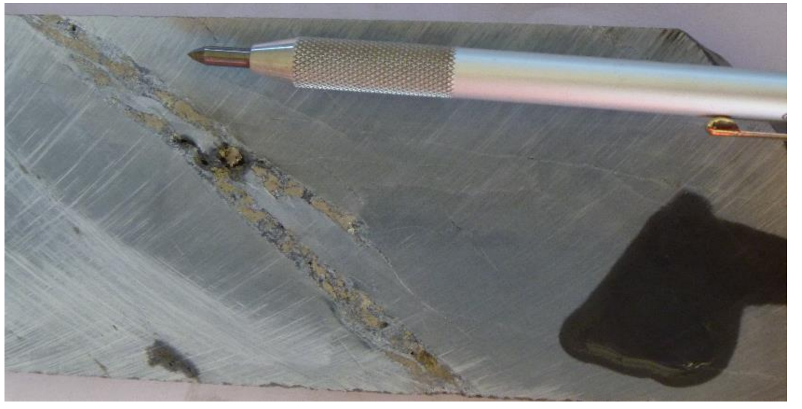 Quarter Core 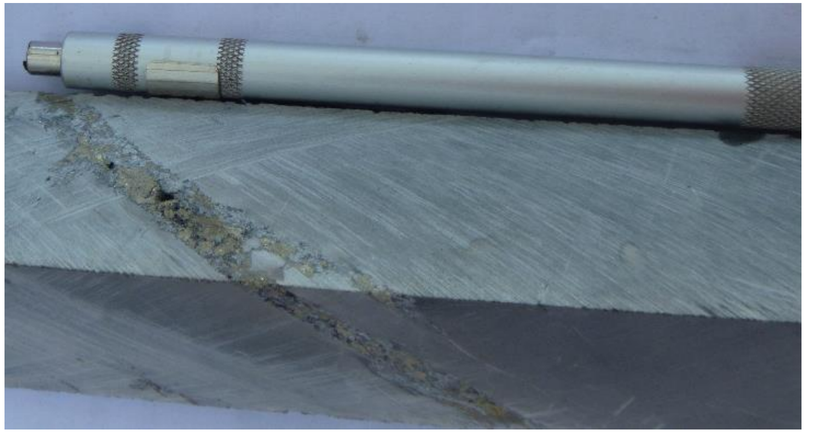	and parallel to bedding (S_0) (Tray 72 @ 236.5,)

	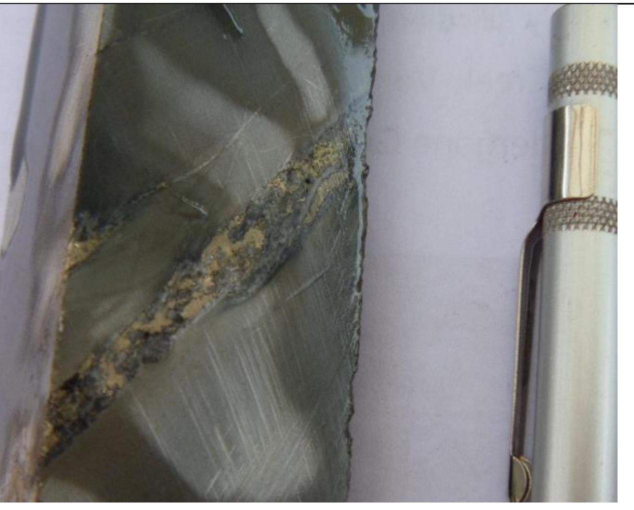	
3	 Full core Half core	Coarse-grained Pyrite vein in S_2 direction, again overprinting lithology of Kennedy Spear, potentially Pyrrohtite as well (Tray 78 @ 255.5m)

	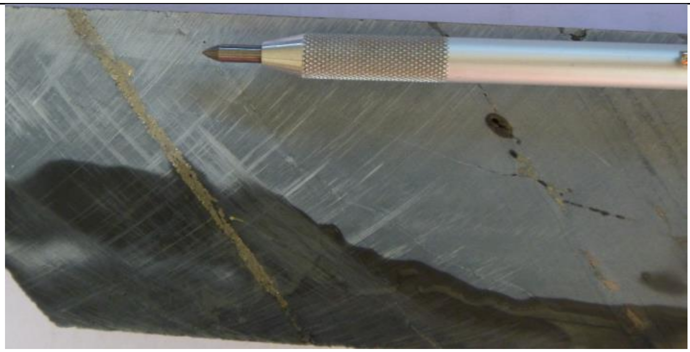 Quarter Core 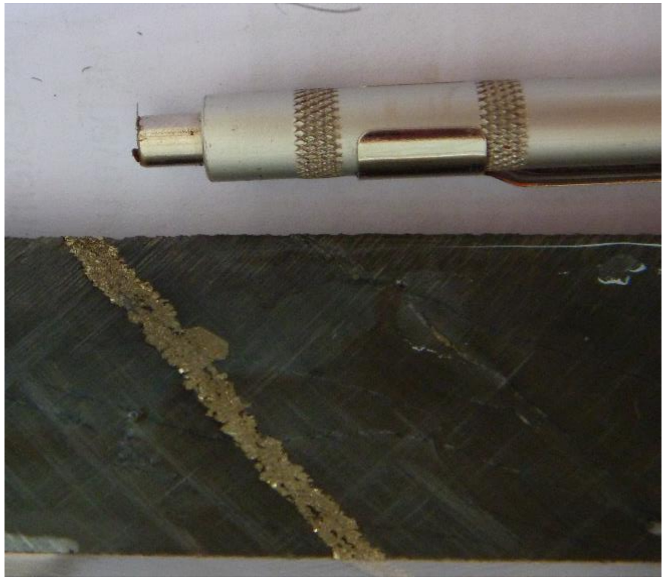	

4	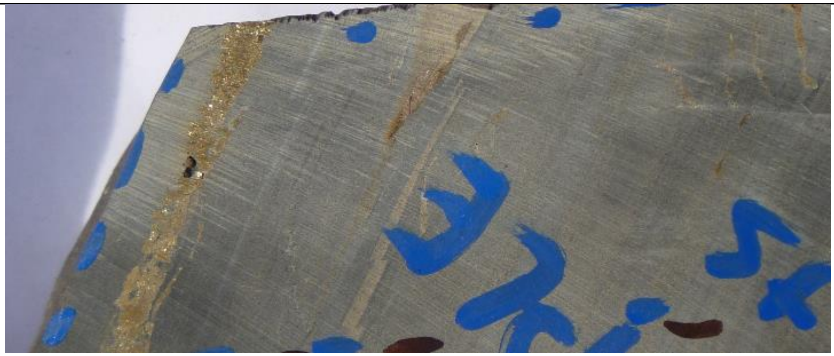 Half Core Quarter Core 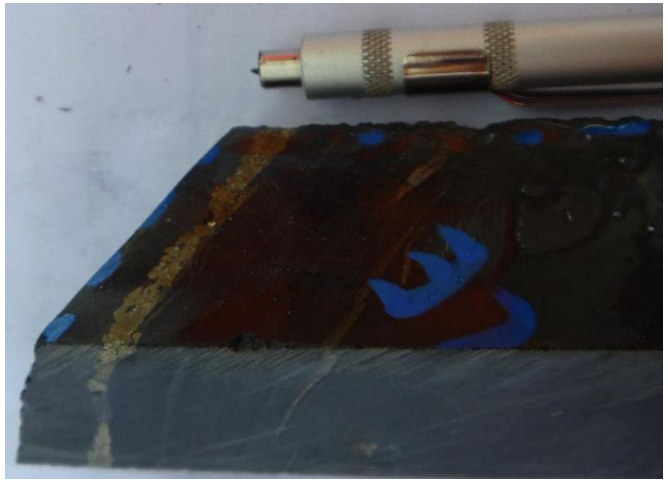	Large Coarse-Grained Pyrite vein, following bedded foliation (S_0). (Tray 106 @363.15m)

5	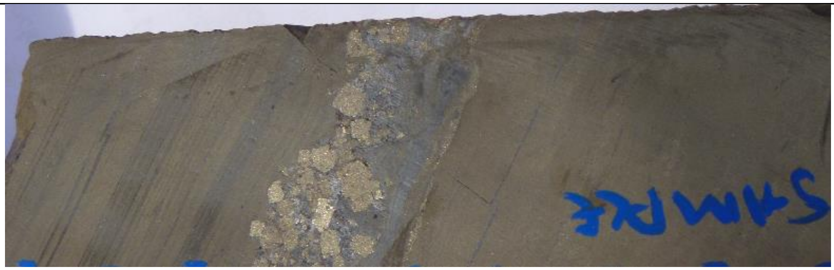 Half core Quarter Core 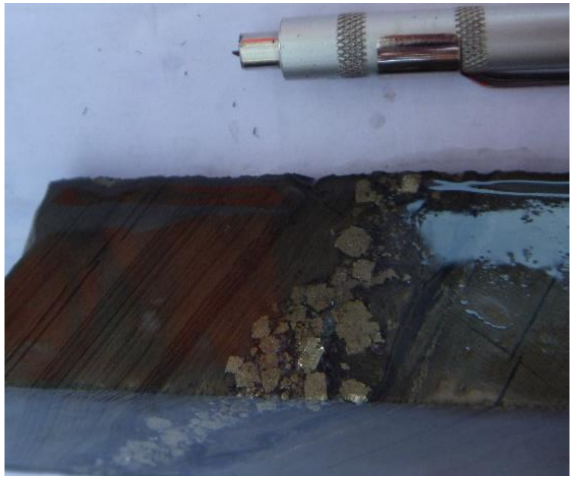	Sample from within mass bedded pyritic Shale. Dominantly Fine-grained Pyrite, with Coarse-grained Pyrite vein, displaying cubic crystal shapes. (Tray 122 @ 397m)

	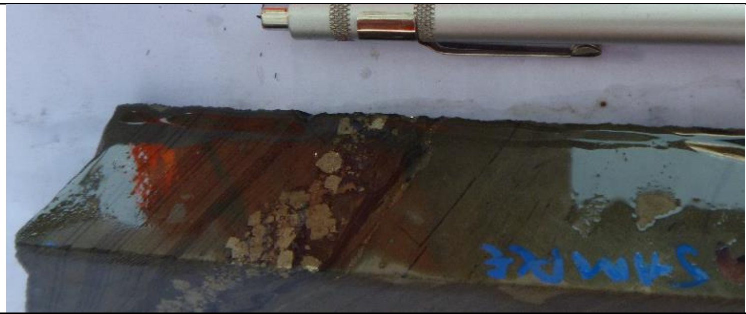	
6	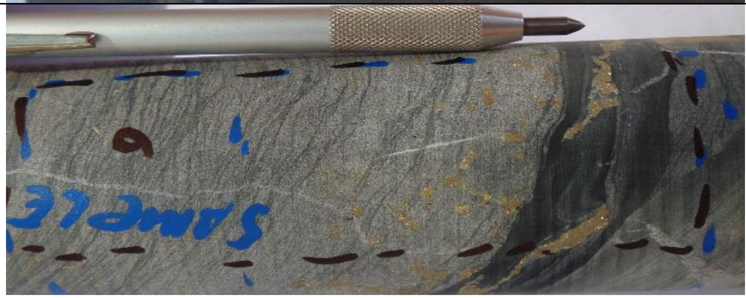 Full Core Half core: 	Coarse grained pyrite, as in fill in a dolomitic vein and also, potentially recrystallized pyrite parallel to bedding foliation, again see larger, cubic crystals (Tray 129, @ 418.6m)

	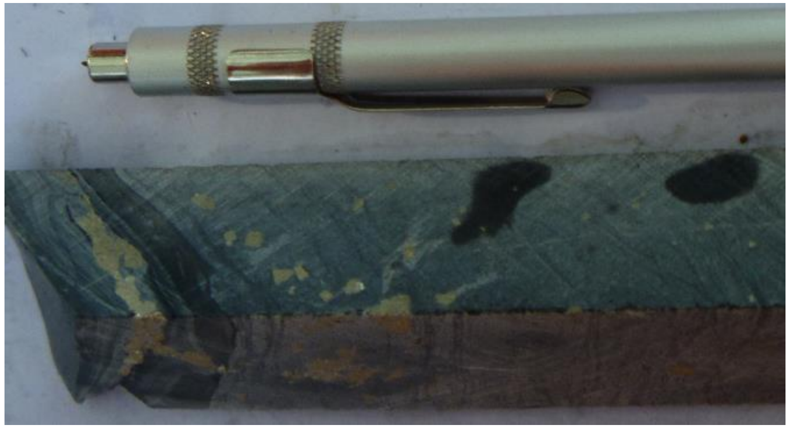	
7	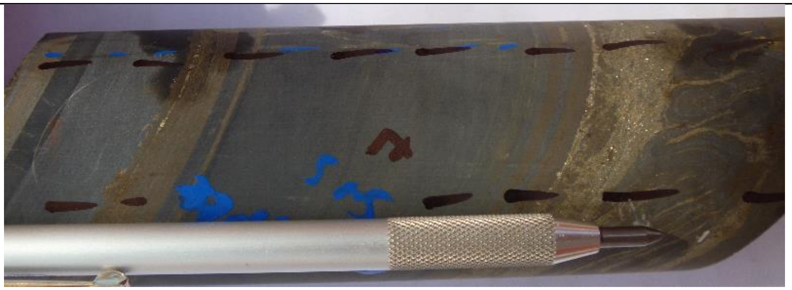 Full core Half core (wet+dry)	Fine and Coarse Grain Pyrite interlayered, which has been physically altered – deformation within Urqurhadt Shale (Tray 135 @ 442.2m)

	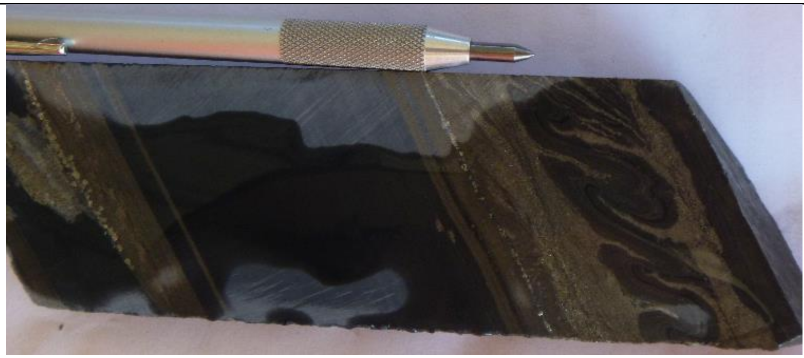 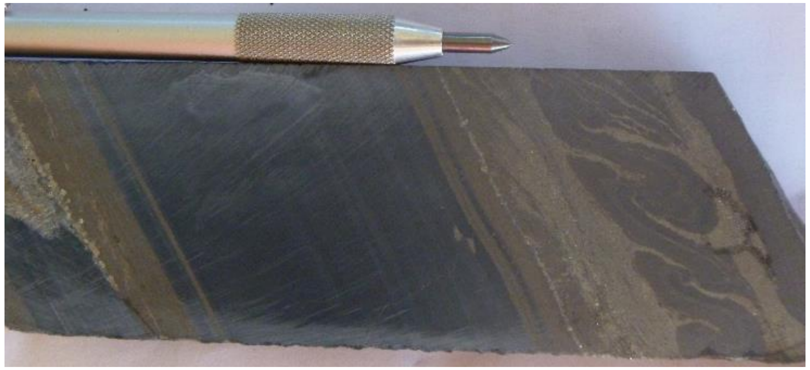 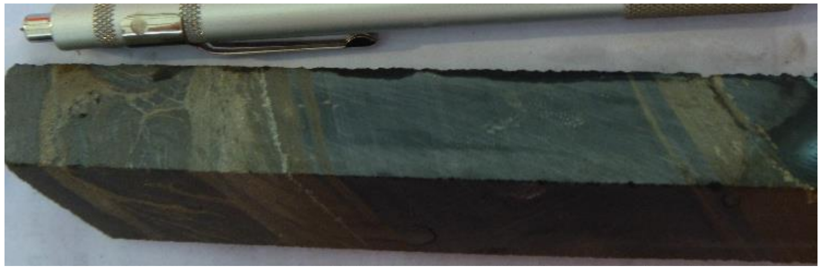	

<table>
<tr><td>8</td><td>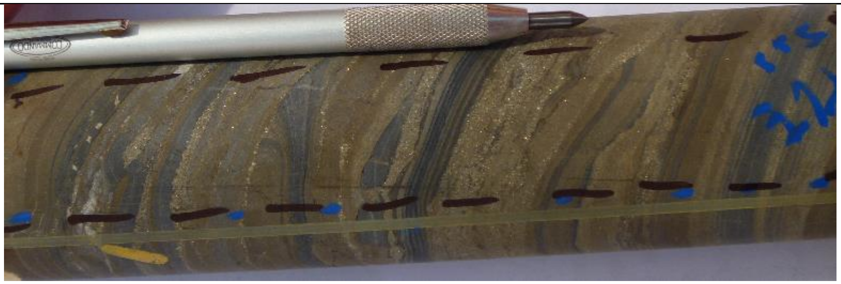
Full core

Half core


</td><td>Fine and Coarse grained pyrite inter-bedded within Urqurhadt shale. Seeing some deformation of bedding. (Tray 136 @ 445.2m)</td></tr>
</table>

9	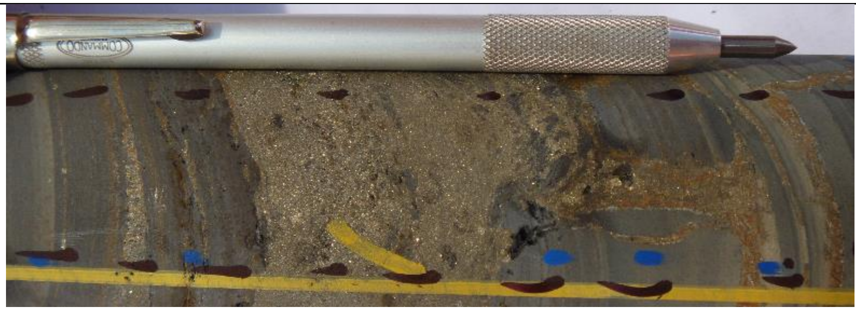 Full core Half core (wet + dry) 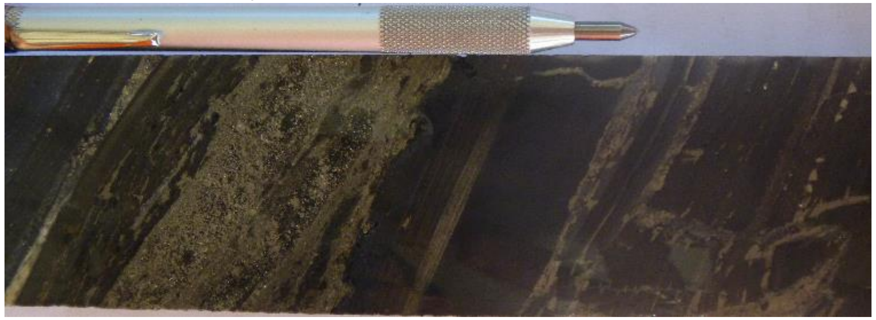 	Fine and coarse grained pyrite within shale. See Coarse grained pyrite parallel to and over printing bedding. (Tray 141, @ 416.8)

	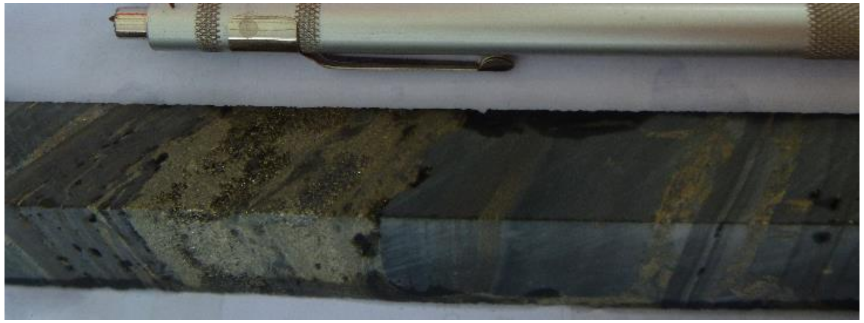	
10	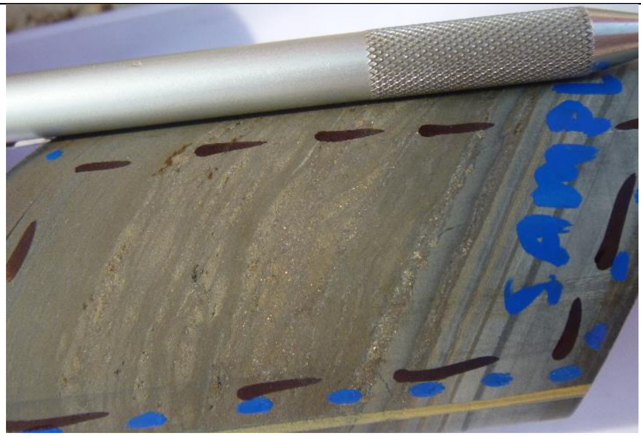 Full core Half core (wet+dry)	Inter bedded Fine and Coarse grained Pyrite within a region of pyritic enriched shale (Tray 147, @ 491.3m)

	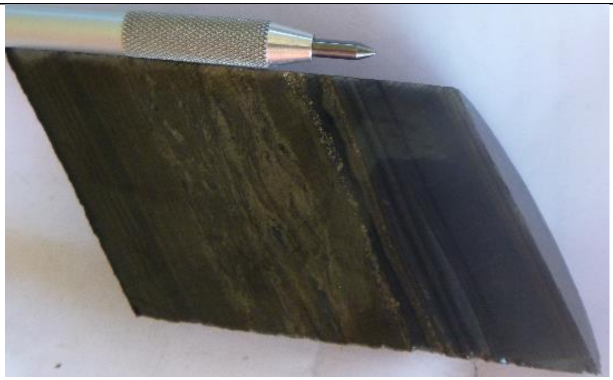 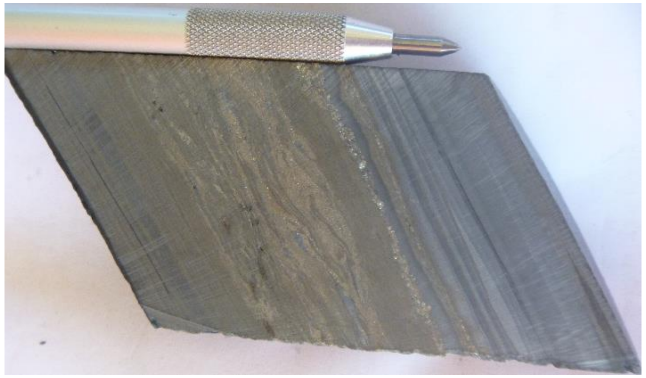 Quarter Core:	

<table>
<tr>
<td>11</td>
<td>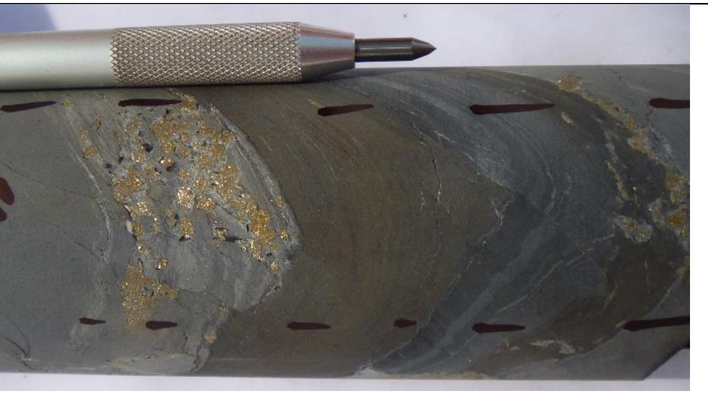
Full core

Half Core
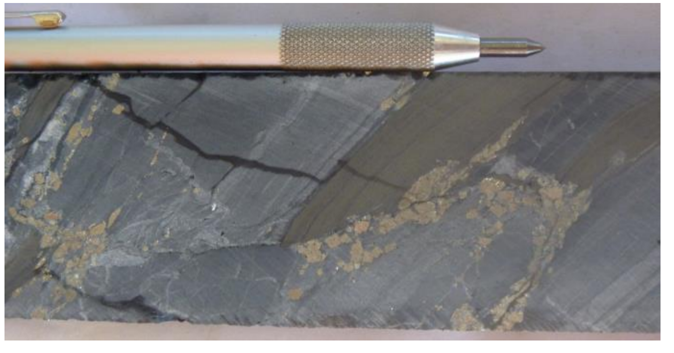</td>
<td>Fine and Coarse grianed pyrite, within stockwork zone of Dolomitic veins. See Coarse grain pyrite in Cubic crystal shapes and not following bedding foliation. (Tray 152 @ 512.8m)</td>
</tr>
</table>

12	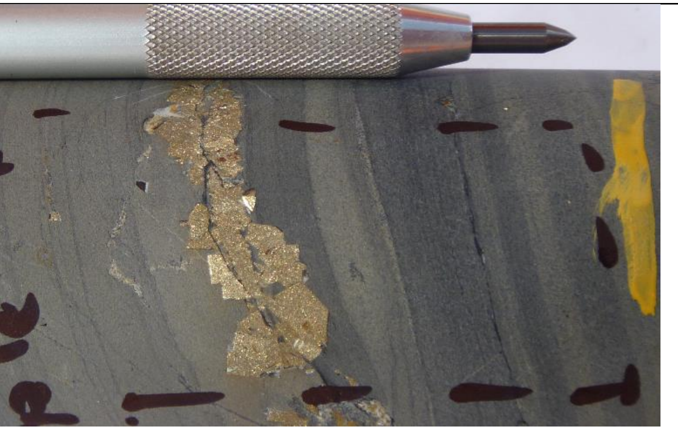 Full core Half core 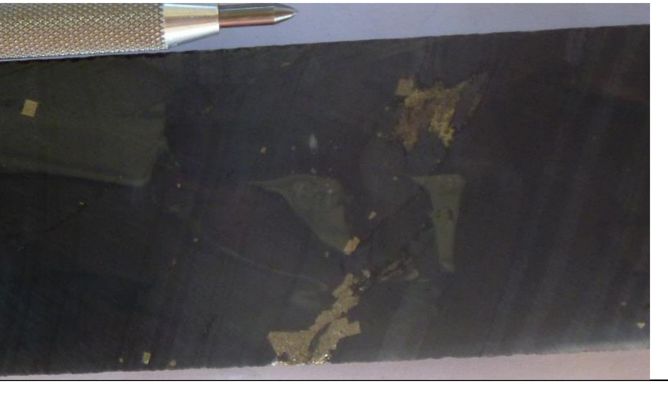	Coarse Grained Pyrite seen parallel to bedding and overprinting it. Chalcopyrite is noted to be present also. (Tray 156, @ 530m)

	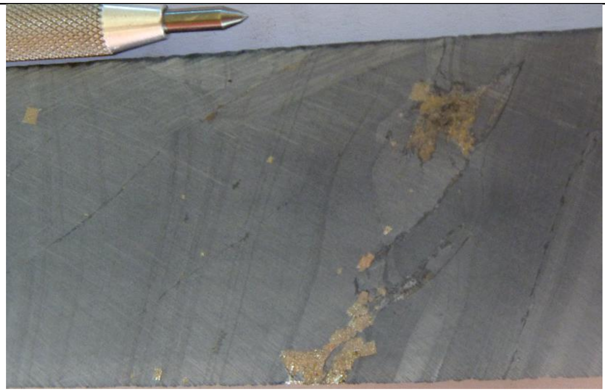	
13	 Full core Half core:	Fine gained pyrite beds, coarse grained and chalcopyrite overprinting. Found within bedded sulphide zone. Beds are slightly deformed; shearing? (tray 161, @ 549.2m)

	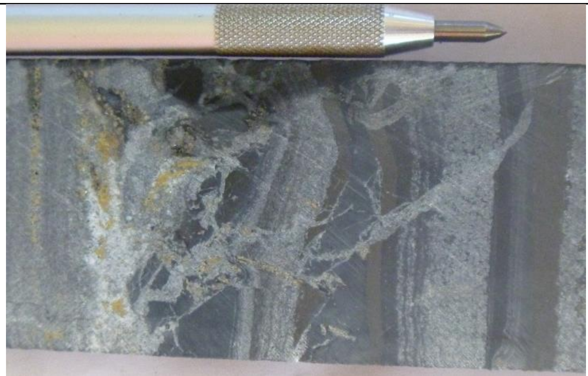	
14	 Full core Half core:	Coarse and fine grained pyrite bedded within shale. See coarse grained pyrite overprinting beds and shale. Potentially see coarse-grained pyrite replacing fine grained. Potentially see some chalcopyrite also. Sample collected near a shear zone. (Tray 165, @ 562.4m)

	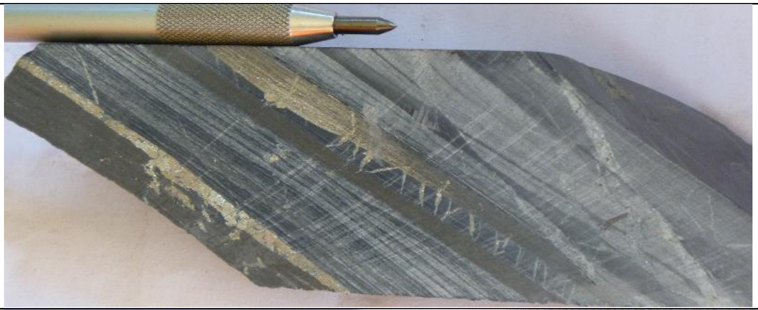	
15	 Full core Half core	Fine Grained pyrite, with coarse grained pyrite and +/- chalcopyrite within a semi brecciated/remint brecciated zone. (tray 170, @583.6m)

	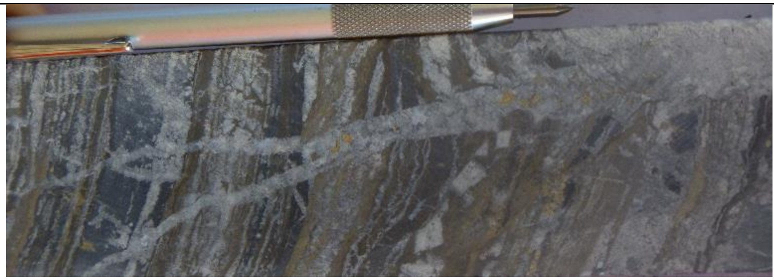	
16	 Full core Half core: 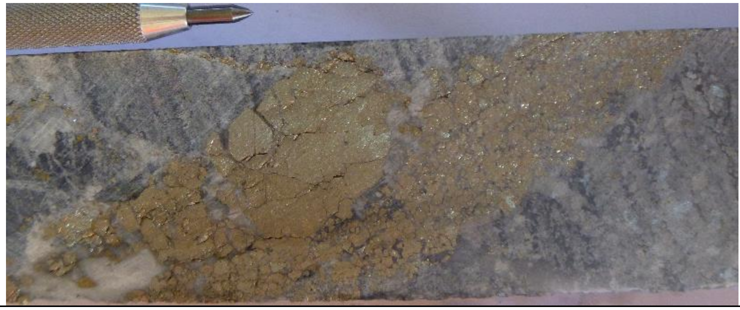	Coarse grained pyrite in recrystallized shale (transitional halo) (Tray 177 610.7m)

	Quarter Core: 	
17	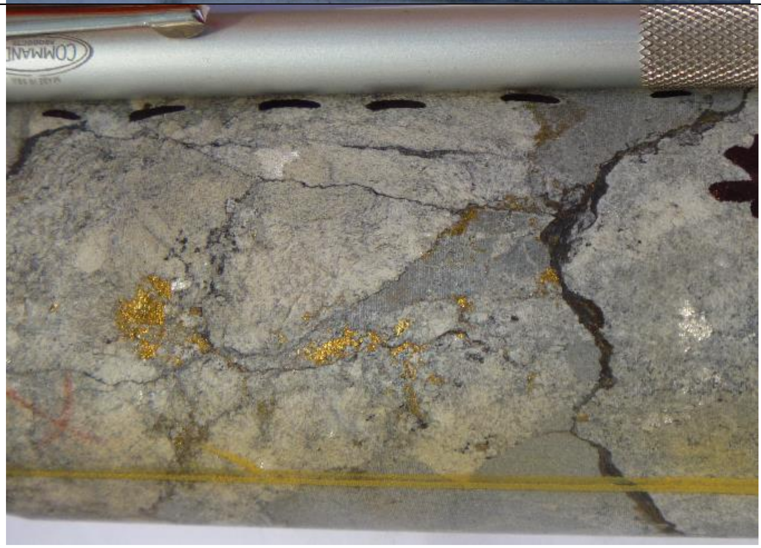 Full core Half core	Fine and coarse grained pyrite in brecciated zone. Still within shale lithology. Seeing chalcopyrite within zone also. (tray 182, @629.8m)

	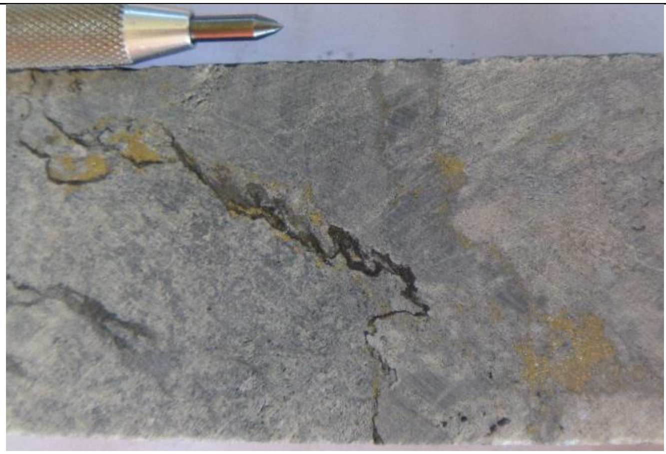 Quarter Core: 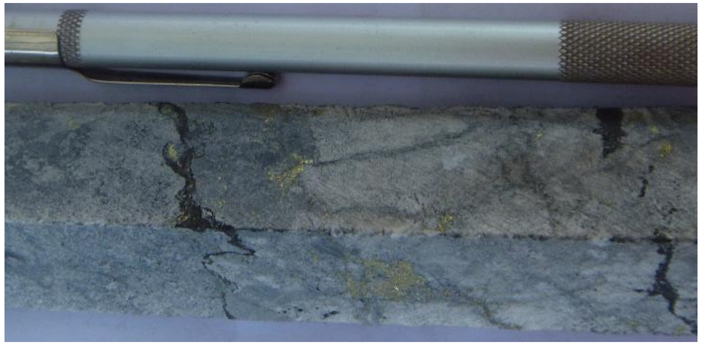	

	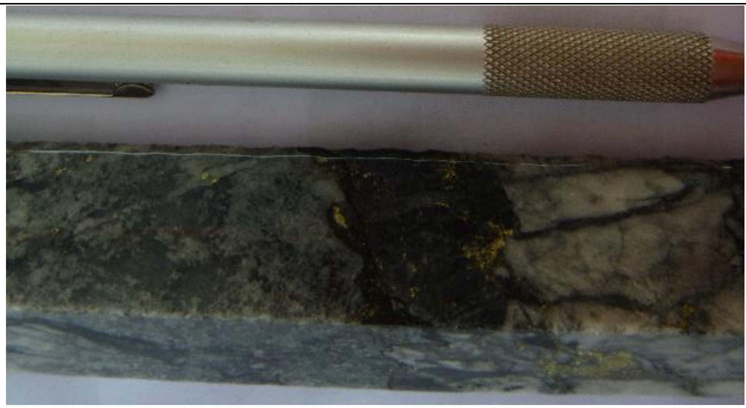	
18	 Full core Half core	Coarse and fine grained pyrite and chalcopyrite. Sample is the contacted between the brecciated zone and the shale. (tray 186, @650m)

	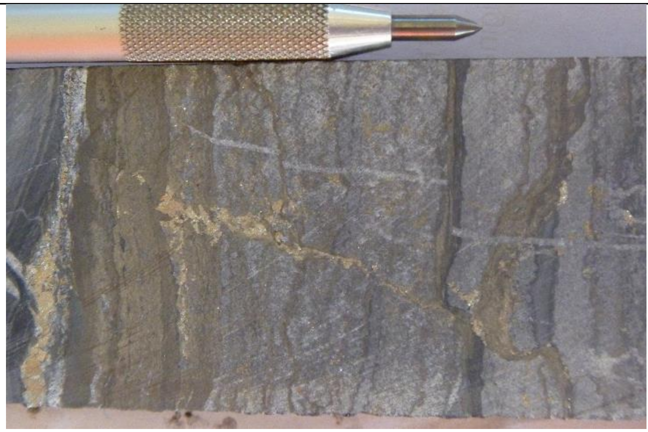 Quarter Core: 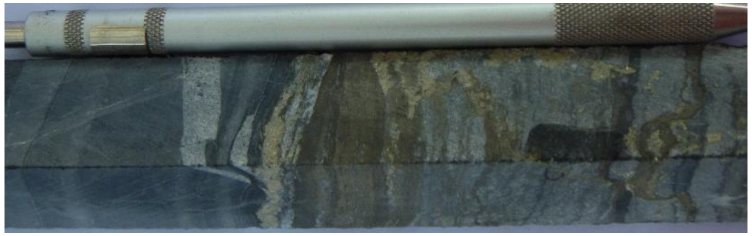	
19	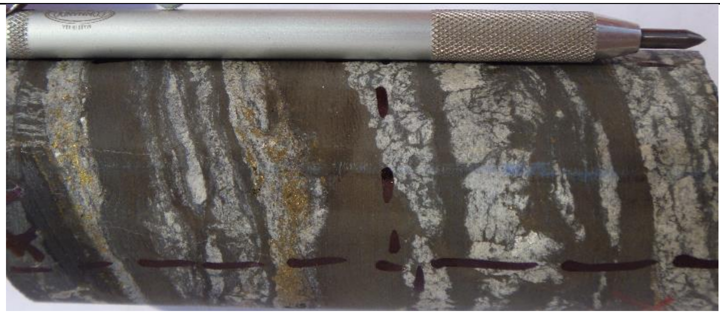 Full Core	Brecciated mass sulphide zone, within shale unit. Seeing fine and coarse grained pyrite, +/- chalcopyrite. (tray 187, @ 653.8m)

	Half Core 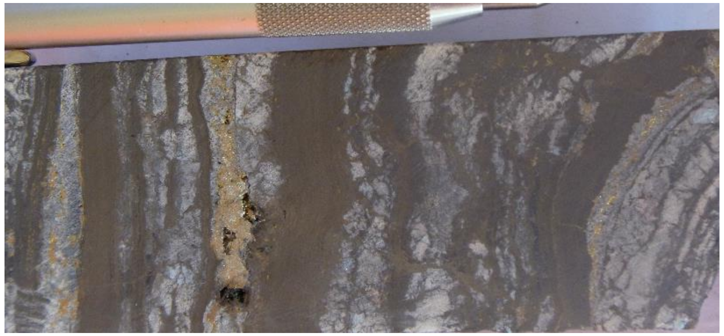 Quarter Core: 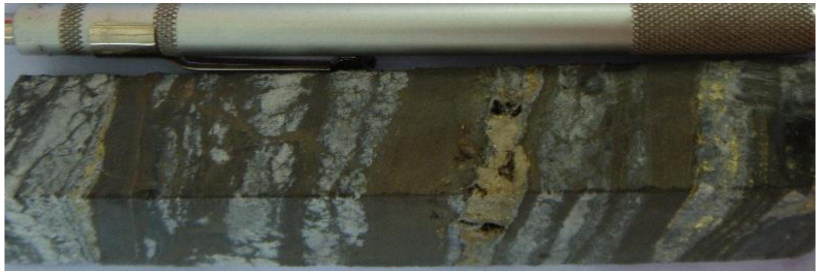	

<table>
<tr><td>20</td><td>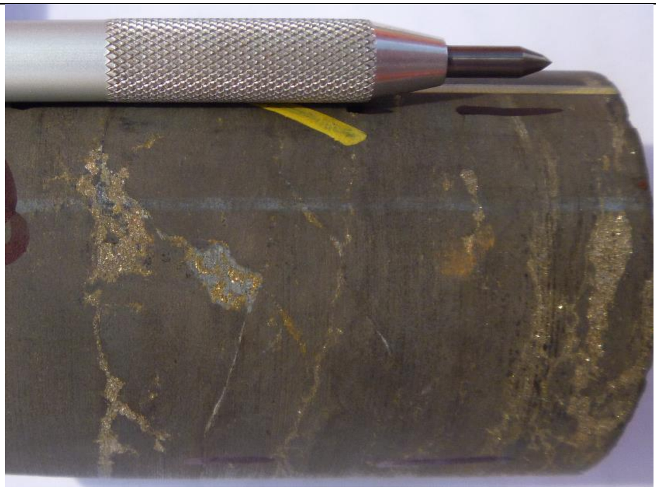
Full Core

Half Core
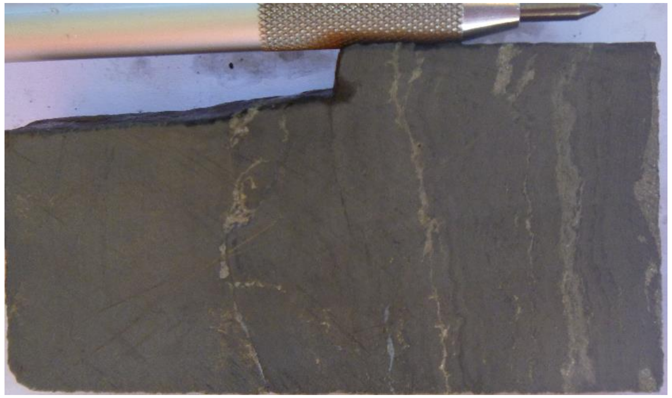

Quarter Core:</td><td>Massive fien grained pyrite zone, with coarse grained pyrite (Tray 188, @ 654.8)</td></tr>
</table>

	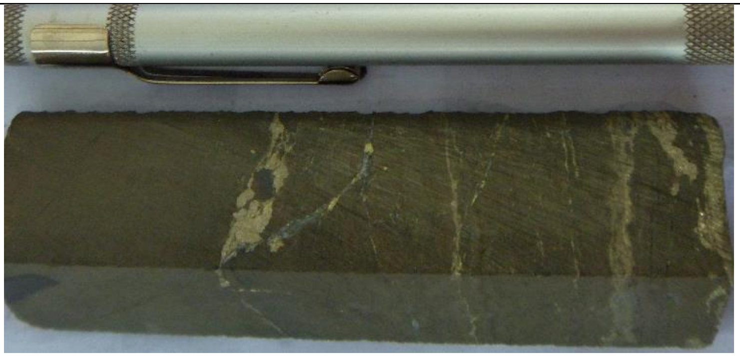	
21	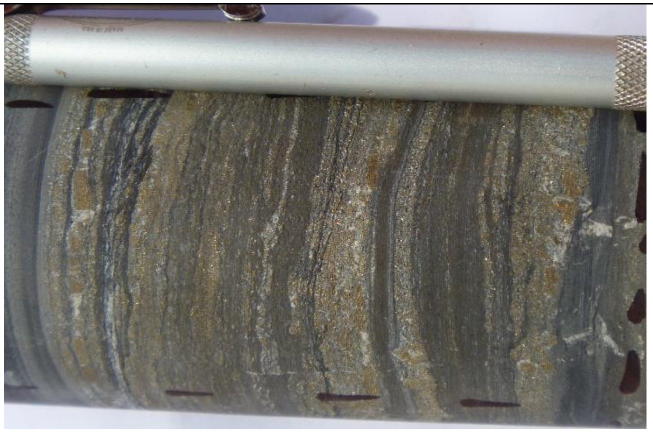 Full Core Half Core	Massive fine grained yrite zone with coarse grained pyrite within (tray 191, @ 669.2m)

<table>
<tr><td></td><td>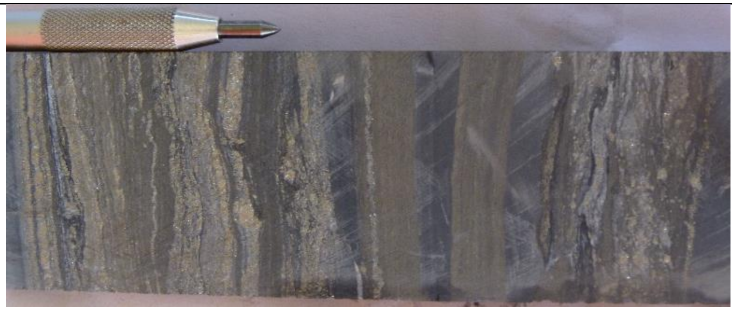
Quarter core:
</td><td></td></tr>
</table>

22	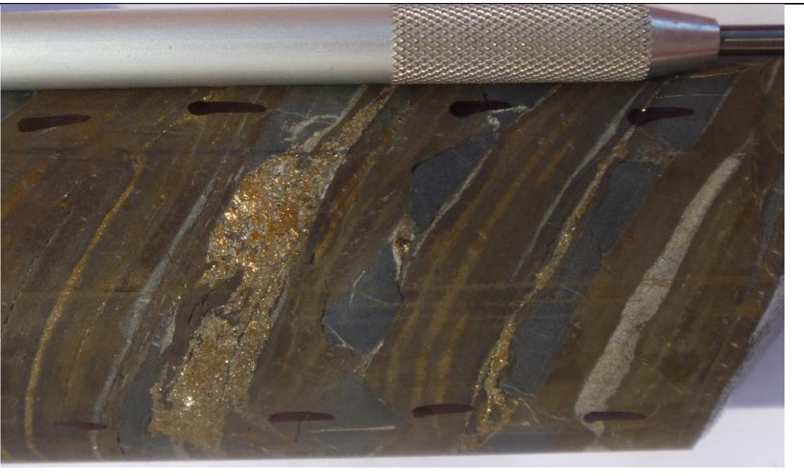 full core half core 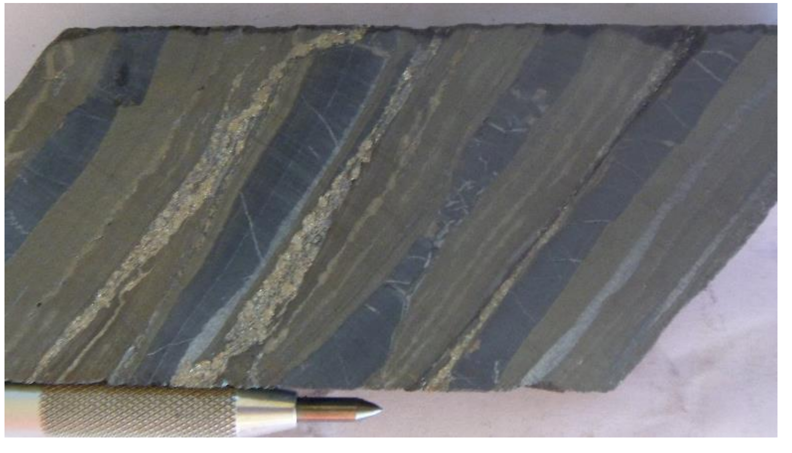 quarter core:	Within mass bedded sulphide zone, shows fine and coarse grained pyrite and shale inter-bedded relationship (tray 198, @ 695.4m)

	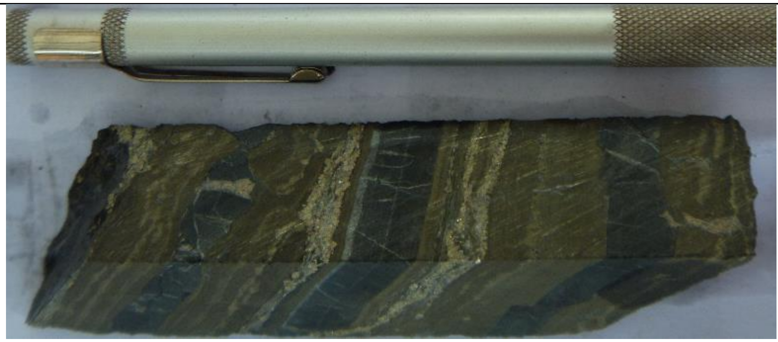	
23	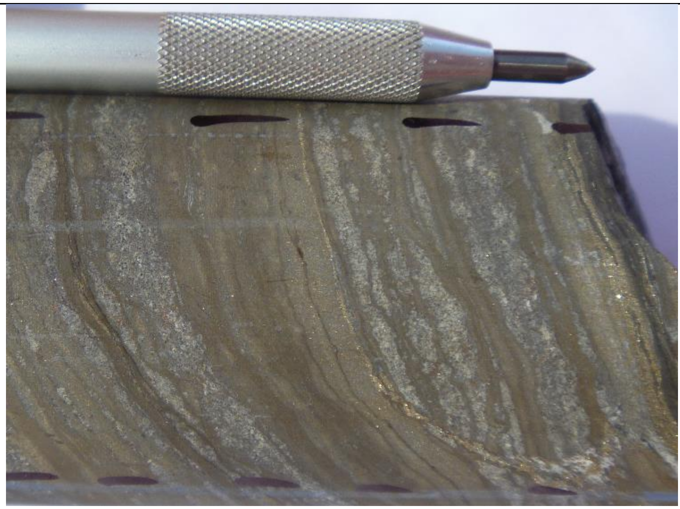 Full core Half core	End of sulphide mass zone and seeing fine and coarse-grained pyrite bedded parallel. Also seeing coarse grain pyrite over printing beds and fine-grained pyrite. (Tray 202, @ 712.9m)

	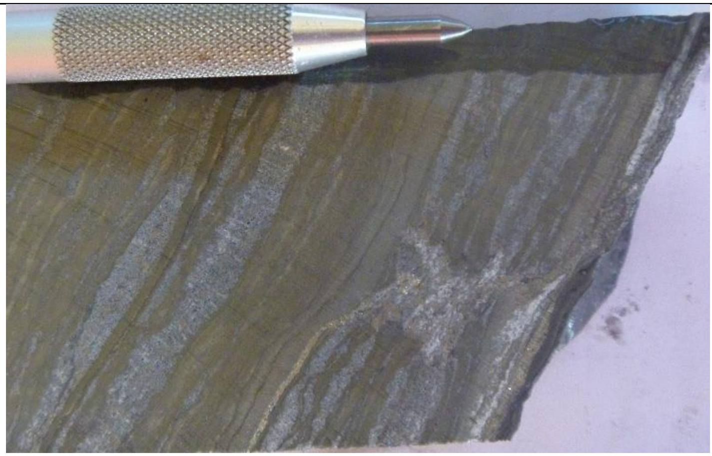 Quarter Core: 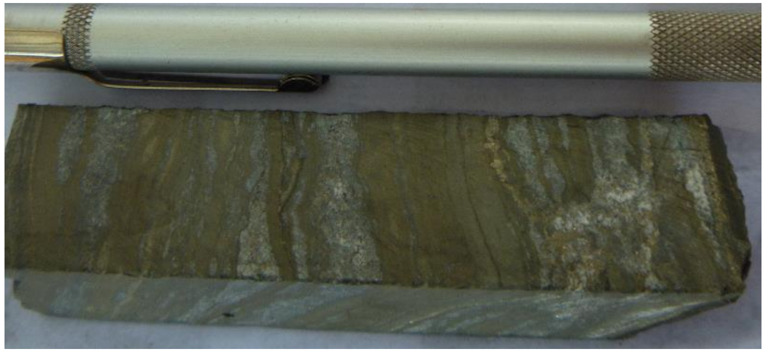	

<table>
<tr>
<td>24</td>
<td>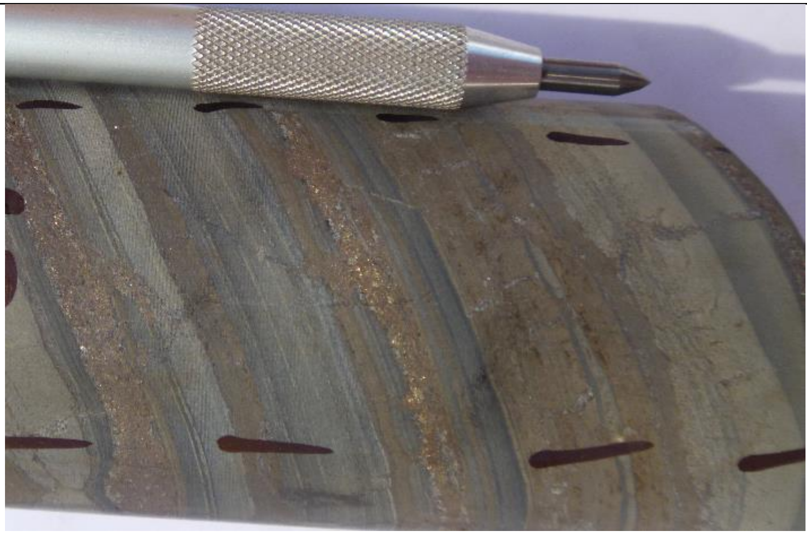
Full core

Half core:
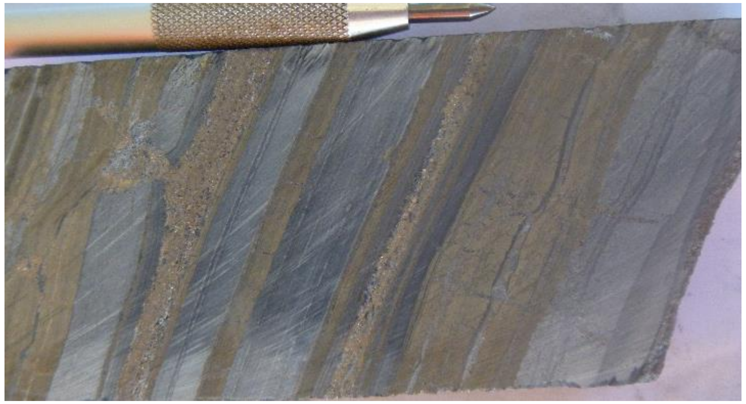

Quarter Core:</td>
<td>E.O.H, out of mass sulphide zone, and into a slightly enriched pyritic shale zone, which appears to be enriched in Pyrrhotite and Sphalerite, with fine grained pyrite.
(tray</td>
</tr>
</table>

	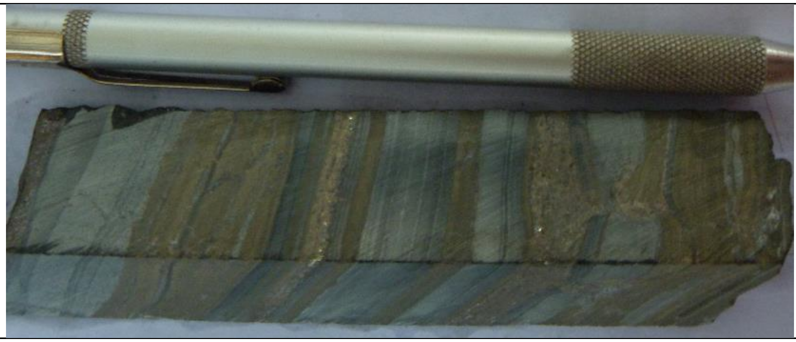	

9.4 APPENDIX D: PETRO RESULTS ALL 24 SAMPLES

Appendix D, details the petrological analysis conducted and determined for all 24 samples from the 0406ED2 transect. The Petrological analysis was conducted on samples, as per details in section 3.2 optical petrology.

Full Petrology analysis of all 24 samples.
Thesis Sample 01 (TS01): hosted in the Kennedy spear siltstone, consisting of quartz and quartz enriched carbonate. There appeared to be a distinctive foliation within the host rock. Large pyrite 2 crystals surrounded by carbonate overprinted this foliation with talc/quartz/carbonate vein. The veining appears to be a patchy and discontinuous. Some of the pyrite 2 grains appear to be slightly deformed/disseminated.

Thesis Sample 02 (TS02): hosted in the Kennedy Spear Siltstone. There is a distinct Pyrite and carbonate, quartz, and talc vein, with chalcopyrite appearing in some regions of the vein. The pyrite 2 and chalcopyrite is disseminated/deformed/ altered. The vein follows the foliation of the host rock.

Thesis Sample 03 (TS03): hosted in the Kennedy Spear Siltstone. Enriched in quartz, and carbonate with a distinct foliation. There is a Clear and distinct pyrite 2 vein, which follows the foliation of the Kennedy Spear Siltstone. It is noted that the centre of the vein appears to be more disseminated; rather than clear-cut cubic crystal edges, like the outside edges of the pyrite 2 veins. The identifiable pyrite 2 grains vary in size throughout the vein, from approximately 200μm to 800μm. Chlorite appears to be present in the disseminated centre of the pyrite 2 veins.

Thesis Sample 04 (TS04): this is sample is predominately Kennedy Spear Siltstone, but is seen to contain recrystallized carbonate enriched in quartz, with a distinct foliation consistent with the siltstone. This is the first sample seen with pyrite 1 (fine-grained pyrite), appearing near a vein of pyrite 2. The vein follows the foliation of the siltstone and similar to the vein seen in TS03 with the disseminated centre and clear cut cubic edges or pyrite 2 grains.

Thesis Sample 05 (TS05): Pyritic shale unit within the Urquhart Shale, predominantly pyrite 1 which is bedded and foliated. A brecciated vein is apparent within the sample, which contains pyrite 2 grains, within a quartz matrix. Some of the pyrite 2 grains appear to be quiet fragmented and contain numerous inclusions, such as chalcopyrite galena.

Thesis Sample 06 (TS06): host rock appears to be recrystallized carbonate. Pyrite 2 appears to be singular cubic crystals, with only a few present within the sample. The grains do consistently follow the foliation. There is some chalcopyrite present within the sample, which appears to overprint the foliation, but is fragmented. Talc, quartz and carbonate veins appear throughout the sample measuring from microns to centimetres, significant veining in the top right-hand corner of the sample, with small pyrite 2 within the veins.

Thesis Sample 07 (TS07): host rock is the pyritic shale member within the Urquhart Shale formation. Pyrite 1 is the dominate sulphide mineral with distinct textures that have both pyrite 1 and 2, with deformation events also. There is folding and ramping folds of pyrite 1 and 2 with shale inter-bedded and folded. This helps identify timing of deformation events... The pyrite 2 that is bedded and folded also appears to be smaller than the typical pyrite 2 grains seen in the MIM samples. There is also a distinct region of pyrite 1 and pyrite 2 where there is no folding. A vein is located in the bottom left corner of the slide. The vein is contains talc, carbonate and quartz, with pyrite 2 grains which are large and cubic. The vein is not deformed.

Thesis Sample 08 (TS08): sample is hosted in the Urquhart Shale, in the pyritic shale component, which contains pyrite 1 and pyrite 2 interbedded, predominately pyrite 2 within. Pyrite 1 appears to follow the foliation of the bedded shale. The pyrite 2 is the smaller variation of pyrite 2, 20-100µm, and also follows the foliation. There are some areas of larger pyrite 2 grains, occurring in veins with talc, carbonate and quartz

Thesis Sample 09 (TS09): hosted within the pyritic shale, which is pyrite 1 and pyrite 2 within the sample. Pyrite 2 is the dominant mineral within the sample. This is the smaller version of pyrite 2 appearing again, within the sample. There is pyrite 1 within veins of quartz, talc, and carbonate, which appears to be slightly deformed and overprinted by pyrite 2. Pyrite 1 holds the original foliation. The sample is mixed of pyrite 1 and pyrite 2, yet there are regions of solely pyrite 1 and solely pyrite 2 areas.

Thesis Sample 10 (TS10): hosted with the Urquhart shale, in the pyritic shale member. Contains both pyrite 1 and pyrite 2. There is a region in the sample, which is distinctively pyrite 1, is bedded and contains a foliation, consistent with the host rock and other samples. The remainder of the sample is inter-bedded pyrite 1 and pyrite 2. The reminder of the slide has high contents of pyrite 2, within veins, which are enriched in carbonate and quartz. _Both variations of pyrite 2 are present within this sample. The smaller pyrite 2, 20-100µm, occurs in masses of grains, similar to pyrite 1. The larger pyrite 2, is cubic in crystal shape, and appears to be over printing and can range up to 200 µm, within this sample.

Thesis Sample 11 (TS11): hosted within the brecciated shale unit within the Urquhart shale formation. The sample contains large amounts of carbonate and carbonate-talc veins, quartz, with pyrite 2 and chalcopyrite. Larger regions and crystals of carbonate occur within sample. The pyrite 2 within the sample is surrounded by talc, quartz and carbonate. Chalcopyrite is associated with pyrite 2, within areas of carbonate, talc and quartz enriched shale. There are small amounts of pyrite 1 present within the sample, associated with pyrite 2, talc and shale. The pyrite 2 overprints the shale and carbonate within the sample.

Thesis Sample 12 (TS12): hosted within quartz and carbonate rich shale unit,, within the Urquhart shale formation. There is a distinct foliation/bedding within the sample, which is overprinted by pyrite 2 in a vein of quartz and carbonate. The larger pyrite 2 grains are cubic, there are some pyrite 2 grains that appear in a cluster that is associated with quartz, carbonate and talc vein. There is chalcopyrite surrounding the pyrite 2 that appears in the cluster.

Thesis Sample 13 (TS13): hosted within the brecciated shale unit within the Urquhart shale formation. Small amounts of pyrite 1, bedded within the shale. Pyrite 2 occurs within the sample as cubic crystals, by overprinting the shale. The pyrite 1 which appears to follow the fracturing patterned within the sample of veins. There are large amounts of quartz and carbonate within the sample, presumably from the brecciating event. Chalcopyrite is also present in the quartz-enriched areas.

Thesis Sample 14 (TS14): hosted in dominantly bedded pyritic shale, with inter-bedded shale. Bedded pyrite 1 with pyrite 2 within quartz and carbonate veins. The veins follow the foliation that is present within the bedded and pyritic shale. The pyrite 2 present within the veins is more disseminated in the centre and more cubic on the edges. There are regions of pyritic shale is separated by shale with boarders of pyrite 2.

Thesis Sample 15 (TS15): hosted within severely brecciated pyritic shale unit within the Urquhart shale formation. The sample is dominated in pyrite 1 and pyrite 2 that has undergone mass brecciation. The sample is also dominant in quartz, and talc. The pyrite 1 is bedded in some areas, and broken up by quartz, talc and recrystallized carbonate. Pyrite 2 is hosted within veins and beds of pyrite 2.

Thesis Sample 16 (TS16): hosted within the intensely brecciated pyritic shale, with large pyrite 2 vein occurring within. The pyrite 2 is within a quartz vein. In section of the pyrite2, there are regions of deformation and stress, shown within the pyrite 2 grains. The pyrite 2 grains are quite large within this sample; some grains are greater than 200µm.

Thesis Sample 17 (TS17): sample is within the brecciated shale with pyritic vein. There is chalcopyrite and pyrite 2 are found within the sample. The dominant mineral assemblage is quartz and carbonate, with chalcopyrite and pyrite featuring as veins and clusters. The sample also contains recrystallized carbonate within the sample. The pyritic vein within the sample consists of large chalcopyrite and pyrite 2 grains. The shale is predominantly enriched in carbon.

Thesis Sample 20 (TS20): hosted within the pyritic shale unit within the Urquhart shale formation. The sample contains mass pyrite 1 contents, which is bedded and foliated. A vein of carbonate and quartz with chalcopyrite occurs along the vein at irregular intervals. Pyrite 2 is seen to be occurring at the bottom of the sample, with large cubic grains (>200µm). Pyrite 2 and chalcopyrite are found within a vein of quartz and carbonate. There are 2 distinct types of veins, which occur within the sample, the first follows the foliation of the pyritic shale and the second is seen to overprint and cross cut the foliation.

Thesis sample 21 (TS21): hosted within the brecciated and pyritic shale, this sample contains pyrite 1 and pyrite 2 inter-bedded with shale, which both follow the foliation. The middle region of the sample is highly brecciated, with the dominant mineral assemblage being quartz and carbonate enriched. The shale and pyritic shales are cross cut by veins containing talc and carbonate.

Thesis Sample 22 (TS22): Hosted within Urquhart shale, within a semi pyritic component. The sample is shale inter-bedded within pyritic shale. There is pyrite 1 throughout the bedded shale. Noticeably see the distinct pyritic bands. There is a pyrite 2 vein, which is enriched in carbonate and quartz. Again noticing two variations of the pyrite 2, along with pyrite 1 and carbonate within some veins.

Thesis Sample 23 (TS23): Hosted within the pyritic shale component of the Urquhart shale that is slightly brecciated. Pyrite 1 is the dominant mineral within the sample, with pyrite 2 occurring occasionally around pyrite 1 following the foliation. Potentially seeing recrystallized carbonate with pyrite 2 (small, not sully formed crystals – second variation of pyrite 2), with chalcopyrite also present. It is noted that there are significant amounts of pyrite 1 occurring with carbonate within the sample.

Thesis Sample 24 (TS24); Hosted within the pyritic shale component of the Urquhart shale. This sample contains strata-bound lead-zinc mineralisation. Clear bands of pyrite interbedded with shale occur periodically, with sphalerite and galena. Small amount of pyrite 2, smaller variations occurring along the bedded planes of pyrite 1.

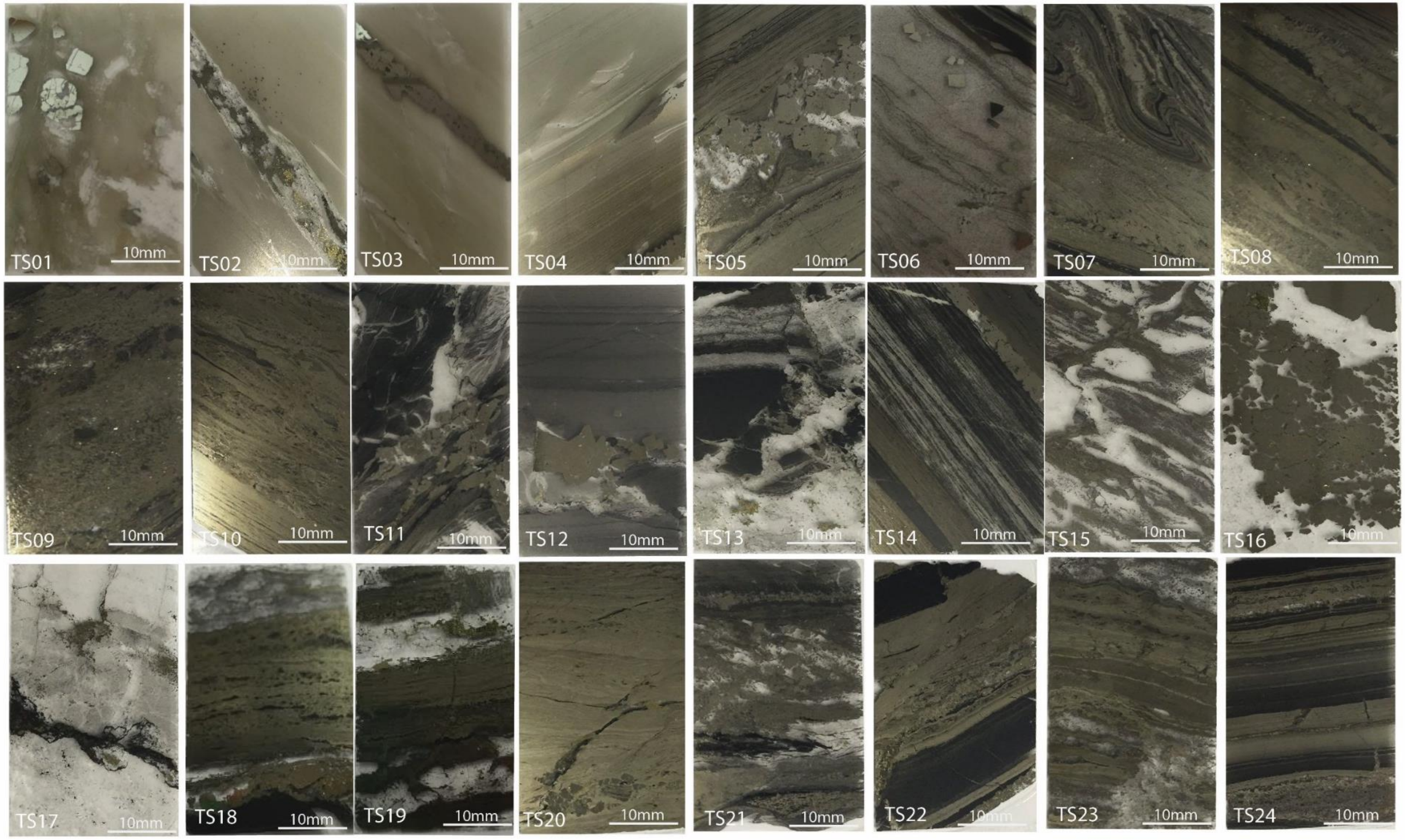

Appendix 9.4: Figure 25 displays the tin section images for the 24 samples collected (section 3.1) from the 0406ED2 transect, which were analysed by optical petrological (section 3.2) methods using the equipment's specified in section 3.2.

9.5 APPENDIX E: MASS_1 INFORMATION

Appendix E; details the information regarding the MASS_1 standard, which was supplied by Adelaide Microscopy, for analysis purposes during the LA-ICP-MS data collection.

United States Geological Survey

Certificate of Analysis

Polymetal sulfide, MASS-1

MASS-1 was prepared using a specially designed coprecipitation process utilizing Copper, Iron and Zinc solutions in combination with a Sodium Sulfide solution. A total of twenty five trace elements were added to the mixture prior to the precipitation step. The resulting precipitate was washed with deionized water, ground to <50 microns, dried and aliquots of the powder pressed into pellets. Samples of the dried powder were analyzed for its total element composition at the U.S. Geological Survey using a variety of analytical techniques. Micro-homogeneity was assessed using LA-ICPMS.

Preliminary values

Element	Wt, %	±
Cu	13.4	0.05
Fe	15.6	0.1
H_2O	13.6	
Na_2O	3.3	0.02
S	27.6	0.10
Zn	21.0	0.5

Element	µg/g	±
Ag	50	5
As	65	3
Ba	14	5
Cd	60	7
Co	60	10
Cr	65	11
Ga	64	11
Hg	57	3

Element	µg/g	±
Mn	280	80
Mo	59	9
Ni	97	15
Pb	68	7
Sb	60	9
Se	51	4
Sn	59	6
V	63	10
W	20	2

Information values

Bi	60
In	50

Ir	42
Te	15
Tl	50